Ph.D. Dissertation of Forest Environmental Science

Distribution and Adaptation of Mangroves with Different Aerial Root Types to Accretion and Erosion in Coastal Areas of Ca Mau, Vietnam

베트남 카마우 지역 퇴적지와 침식지에서 서로 다른 기근을 가진 맹그로브의 분포와 적응

August 2023

Graduate School of Agriculture and Life Sciences

Seoul National University

Forest Environmental Science Major

Nguyen Thuy My Linh

Distribution and Adaptation of Mangroves with Different Aerial Root types to Accretion and Erosion sites in Coastal Areas of Ca Mau, Vietnam

Under the supervision of Professor Pil Sun Park

Submitting a Ph.D. Dissertation of
Forest Environmental Science

August 2023

Graduate School of Agriculture and Life Sciences
Seoul National University
Forest Environmental Science Major

Nguyen Thuy My Linh

Confirming the Ph.D. Dissertation written by
Nguyen Thuy My Linh
August 2023

Chair: KIM, HYUN SEOK_____

Vice Chair: PARK, PIL SUN_____

Examiner: IM, SANGJUN_____

Examiner: KANG, HO SANG_____

Examiner: LEE, BORA_____

Abstract

Mangrove forests are a representative estuarine ecosystem and distributed in the inter-tidal region of the tropics and subtropics. Aerial roots are unique adaptive characteristics of mangrove trees to survive in poor oxygen conditions and support the role of mangroves in formation and stabilization of alluvial banks through sediment regulation. The study was conducted in the coastal area of Ca Mau, Vietnam, where a large area of natural mangrove forests remains. This study compared stand structure of mangroves with different aerial root types between accretion and erosion sites and distances from the shoreline to understand stand dynamics and specific-species distribution and adaptation characteristics of mangroves to different timescale or intensity of accretion and erosion.

Seven study sites were selected in natural mangrove stands of coastal protection mangrove forests. Each site experienced accretion or erosion processes at different intensity and timescales: new and slight accretion (site A1), long-term and strong accretion (site A2 and A3), new and slight erosion (site E1 and E2), long-term and strong erosion (site E3), and new and strong erosion (site E4). A total of 57 plots were established using transect line method. Three parallel transect lines with 100 m intervals were established from the edge of the closed canopy of a mangrove stand landwards at each study site. Each transect included three 20 m × 20 m plots that were separated by 30 m along the transect at seaward (0–50 m), intermediate (50–100 m), and landward (100–150 m) zones. Species, stem diameter, height and spatial distribution of trees larger than 6 cm DBH (diameter at breast height) were measured at each plot. Three subplots were established diagonally within each plot to measure species and height of seedlings and saplings. Three main aerial root types of stilt roots, pneumatophores and knee roots were invetigated. The number of primary stilt roots was counted and aboveground stilt root height was measured for overstory trees of *Rhizophora apiculata* BL. The number of pneumatophores of *Avicennia* spp. and knee roots of *Bruguiera* spp. was counted and dry biomass of all aboveground stilt roots, pneumatophore and knee roots were cut within 1-m^2 suplots. Elevation, soil pH, salinity, bulk density, moisture content and total organic carbon of soil were measured in the same 1-m^2 subplot. Vegetation, aerial roots and soil data were compared between between accretion and erosion sites.

The elevation, soil salinity, bulk density and soil moisture content significantly differed between accretion sites and erosion sites ($p < 0.05$). The elevation increased gradually from the sea to the land and positively correlated with soil salinity and soil bulk density and negatively correlated to soil moisture ($p < 0.05$).

Species richness of overstory was five and six at accretion and erosion sites, respectively, with only one species difference. *Excoecaria agallocha* L. is a hard substrate-adapted species, associated to higher elevation and soil bulk density and lower moisture content and was solely found in erosion sites. In understory layer, species richness was six and nine at accretion and erosion sites, respectively, showing more difference between accretion and erosion sties. Species richness in understory increased with timescale and intensity of erosion as highest species richness of understory was at site E3 and E4 that were long-term and strong erosion sites. Appearance of new invading species of *Ceriop tagal* (Perr.) C. B. Rob., *Lumnitezera racemose* Wild., *Bruguiera cylinica* (L.) Blume., and *Xylocarpus mekongensis* Piere in understory at long-term and strong erosion sites implied more inland-like substrate of these sites.

Regarding species composition, *Avicennia alba* BL. and *Rhizophora apiculata* BL. dominated the most at accretion and erosion sites, respectively. The distribution and adaptation characteristics of these two species, therefore, reflected the development of mangrove stands in different timescale and intensity of accretion and erosion.

At accretion sites, *A. alba* dominated overstory. A new and slight accretion site of site A1 was a mixed stand of *A. alba* and *R. apiculata*. Meanwhile, at a long-term and strong accretion of site A2, pure *A. alba* in seaward plots was changed to *R. apiculata* dominance from intermediate plots. Site A3 with a longer accretion time showed pure *A. alba* distributed in both seaward and intermediate plots, *A. alba* mixed with *Avicennia officinalis* L. in landward plots, and *R. apiculata* only appeared in understory layer. At all accretion sites, tree size of *A. alba*, mostly stem diameter, decreased from landward plots to seaward plots, illustrating the on-going expansion of this pioneer species to the sea, that was associated to accretion process of alluvial banks. *R. apiculata* was not as dominant as *A. alba* in understory, especially in seaward plots, but exhibited strong regeneration under *A. alba* stands, showing the natural succession at accretion sites. Both the density and biomass of pneumatophore roots at seaward plots were significantly higher at accretion sites than at erosion sites ($p < 0.01$), indicating that adaptive characteristics of pneumatophores of *A. alba* supported its dominance at accretion sites since.

At erosion sites, *R. apiculata* was dominant species in general. The dominance of *R. apiculata* in overstory occurred at sites E2 and E3, regardless of distance from the seashore. *A. alba* still appeared dominant in overstory layer in seaward plots at site E1 and both seaward and intermediate plots at site E4. Adaptive characteristics of pneumatophore of *A. alba* such as developing stilt roots and branched pneumatophores supported the tree from being washed away in newly or slightly eroded sites. However, *A. alba* showed poor regeneration potential when mixed with other species at erosion sites. The tree size of *R. apiculata* changed by timescale and

intensity of erosion. Stilt root biomass showed a negative relationship with the density and biomass of pneumatophores, corresponding to changes in dominance between *R. apiculata* and *A. alba* at erosion sites. Branched lateral roots that developed even above the branch separation point on *R. apiculata* improved the anchorage on unstable eroding mud to uphold the tree to confront strong waves and high tidal stress, supporting the tree's survival at erosion sites. Adaptive characteristics of stilt roots of *R. apiculata* supported its dominance at erosion sites.

The findings on mangrove species composition and stand structure by distance from the shoreline, intensity and timescale of accretion and erosion provided important information for the selection of suitable species for mangrove restoration in specific locations. *A. alba* could be used for coastal protection in accretion area. In erosion area, the *R. apiculata* could be applied as mangrove-based solutions. Temporary measures including net systems, fences or permeable barriers such as bamboo fences and brushwood dams could be used to protect seedlings from the impact of waves and tides and provide favorable conditions for the development of mangroves.

Keywords: *Rhizophora apiculata* BL., *Avicennia alba* BL., stand structure, stilt root, pneumatophores, knee roots

Student ID: 2015-30769

Table of contents

List of abbreviation and symbols

Aa	*Avicennia alba* BL. (Mấm trắng)
Am	*Avicennia marina* (Forssk.) Vierh. (Mấm biển, Mấm ổi)
Ao	*Avicennia officinalis* L. (Mấm đen)
A.s.l.	Above sea level
ARN	Assisted Natural Regeneration
A1	Accretion site A1
A2	Accretion site A2
A3	Accretion site A3
Bc	*Bruguiera cylinica* (L.) Blume. (Vẹt trụ, Vẹt hôi, Vẹt thăng)
BD	Soil Bulk Density
Bp	*Bruguiera parviflora* (Roxb.) W. ex Griff. (Vẹt tách)
Ct	*Ceriop tagal* (Perr.) C. B. Rob. (Dà vôi)
DARD	Department of Agriculture and Rural Department
DBH	Diameter at Breast Height
Ea	*Excoecaria agallocha* L. (Giá)
EMR	Ecological Mangrove Restoration
E1	Erosion site E1
E2	Erosion site E2
E3	Erosion site E3
E4	Erosion site E4
I	Intermediate plots
IV	Importance Value
L	Landward plots
Lr	*Lumnitezera racemose* Wild. (Cóc trắng)

MARD	Ministry of Agriculture and Rural Development
NP	National Park
NE	Northeast
NW	Northwest
Ra	*Rhizophora apiculata* BL. (Đước đôi)
S	Seaward plots
Sa	*Sonneratia alba* J. Smith (Bần trắng, Bần đắng)
SE	South East
TOC	Total Organic Carbon
Xm	*Xylocarpus mekongensis* Piere (Su Mekong)

List of tables

List of figures

List of publications

This doctoral dissertation consists of tables, figures and conents of following publications:

1. Linh Thuy My Nguyen, Hanh Thi Hoang, Han Van Ta and Pil Sun Park, 2020. Comparison of Mangrove Stand Development on Accretion and Erosion Sites in Ca Mau, Vietnam. Forests 2020, 11, 615. https://doi.org/10.3390/f11060615.

2. Linh Thuy My Nguyen, Hanh Thi Hoang, Euho Choi, Pil Sun Park 2023. Distribution of mangroves with different aerial root morphologies at accretion and erosion sites in Ca Mau Province, Vietnam. Estuarine, Coastal and Shelf Science 287, 5 July 2023, 108324. https://doi.org/10.1016/j.ecss.2023.108324.

Author's contribution

1. **Publication 1.** Comparison of Mangrove Stand Development on Accretion and Erosion Sites in Ca Mau, Vietnam.

   Linh Thuy My Nguyen and Pil Sun Park conceived and designed the study. Linh Thuy My Nguyen and Hanh Thi Hoang collected the data. Linh Thuy My Nguyen and Pil Sun Park analyzed the data and wrote the manuscript.

2. **Publication 2.** Distribution of mangroves with different aerial root morphologies at accretion and erosion sites in Ca Mau Province, Vietnam.

   Linh Thuy My Nguyen: Writing – original draft, Project administration, Methodology, Formal analysis, Data curation, Conceptualization.

Chapter 1. INTRODUCTION

1.1. Study background

Coastal areas are constantly changing by the complex interactions of geomorphological processes and biological processes by sediment exchanges over time (William et al. 1997; Rogers et al. 2006). The drivers contributed to the changes in geomorphology and sediment load such as oceanic currents, waves, winds, tidal oscillations, sea-level rise and anthropogenic agents (e.g., Gensac et al. 2019; Mujabar and Chandrasekar 2011; El Banna and Frihy 2009; Lefebvre et al. 2004; Nayak et al. 2010; Masselink et al. 2020; Cahoon and Tuner 1989) simultaneouslly work to erode or transport sediments away creating erosion (Stachew et al. 2021) or trap and deposit sediments creating accretion (Braat et al. 2019), consequently alter the coastal landscapes (Gensac et al. 2019). Accresive and erosive states transited also depending on the intertidal topography and particle sizes of fine sediment (Vousdoukas 2012; Dyer 1998).

In the aspect of biological process, biological agents (flora and fauna) combined with physical agents affecting the accretion and erosion by changing the mass or location of sediments, mostly in intertidal zone (e.g., Wood and Widdows 2002; Widdows et al. 2000; 2004; Alejandro 2001). Mangrove ecosystems were highly productive sources of organic matter and sediment sinks. Mangrove develop by interacting with sediment dynamics and shifting mudbanks, and control erosion or accretion along the shoreline (Plaziat et al. 2004; Nascimento 2013). By that way, estuary channels and mangroves on tidal flats import and retain sediments and the sedimentation process leads to a seaward expansion of new mangrove habitats (Asp et al. 2018). In other words, mangroves play a key role in formation, stabilization, and development of muddy banks (Carlton 1974; Rogers et al. 2005), and control the spatial and vertical distribution of nutrients and sediment grain size in estuaries (Krishna Prasad and Ramanathan 2008). The remote sensing data (aerial photographs and SPOT satellite images) over the last 50 years in French Guiana provided evidence that mangroves were markers of coastal dynamics which influenced by the combined action of accretion and erosion and those disturbances then determine the structure and composition of mangrove forests (Fromard et al. 1998 and Baltzer et al. 2004).

Mangrove forests are a representative estuarine ecosystem and distributed in the inter-tidal region of approximately 140,000 km^2 in the tropics and subtropics (Giri et al. 2011). This forest type is naturally adapted to ordinary estuarine processes (Lugo and Snedaker 1974), but sensitive to environmental changes caused by incidents (Alogi et al. 2008; Emma et al. 2016). The

colonization of mangroves is controlled by site specific conditions of salinity, pH, bulk density, flooding/inundation, light or shade, canopy gaps, elevation and sediment characteristics (e.g., Clarke and Allaway 1993; Sherman et al. 2000; Boto and Wellington 1984; Cardona and Botero 1998; McKee 1993; Ball 1998; Joshi and Ghose 2003). Mangroves demonstrated a zonation of species parallel to the shore and reflected succession patterns (Woodroffe 1992). Succession in mangroves is cyclic and leads to a series of cyclic stages. Any disruptive impacts on cyclic stages of mangrove succession will affect their development in an adaptive or vulnerable way (Lugo 1980). Numerous studies suggested that the vulnerability of mangroves during growth and succession processes can be used as a principal indicator of coastal disturbances (overviewed by Nitto et al. 2014). The responses of mangrove ecosystems to external forces result in zonal distribution, which could be classified as fringe forests, riverine forests, over-wash forests, basin forests, and dwarf forests processes (Lugo and Snedaker 1974). Mangrove species also adapt to coastal processes with their morphological or physiological characteristics, and show a species-specific spatial distribution when responding to accretion and erosion (Hesp 1991; Pham et al. 2019). The genus of *Avicennia* and *Rhizophora*, for example, are dominant species in mangrove forests; however, they differ in colonization and stand structural development, which is the *Avicennia* species is commonly dominant in fringe forest areas, while the *Rhizophora* species dominates more landward areas in basin and transition forests (Estrada et al. 2013; Fromard et al. 1998).

Aerial roots are also one of the unique adaptive characteristics of mangroves processes (Lugo and Snedaker 1974) and solely found in mangrove species that are distributed in intertidal zones with poor oxygen conditions. They have lenticels that provide the function of gas exchange by supplying oxygen to underground roots in oxygen-poor mud, thus, aerating below-ground roots and enabling mangroves to survive on anaerobic substrates (Srikanth et al. 2016). Aerial roots are classified into several types including stilt roots, pneumatophores, and knee roots (Dahdouh-Guebas et al. 2007; Ohira et al. 2013). The morphology of aerial roots may be adaptive characteristic to topographic and soil variations within the intertidal zone and reflects the ecological features of the tree and surrounding environment. For instance, the pneumatophore density of *A. marina* is positively correlated with mud content in soil (Saifullah and Elahi 1992) and significantly higher for places with longer inundation periods, suggesting its adaptation to anaerobic condition (Dahdouh-Guebas et al. 2007). *Avicennia germinans*, *Laguncularia racemosa*, and *R. mangle* also change main root axes, root length, root diameter, and lateral root density to avoid low oxygen stress in anaerobic soils (McKee 1996). The root system of red mangroves (*R. mangle*) has high plasticity such as variations in the number of lateral roots, aerial

roots, lenticels and many other morphological and anatomical properties to respond to the substrates environment (Gill and Tomlinson 1977).

Beside that, each type of aerial roots has its own abilities to trap and bind sediment, resulting in different rates of vertical accretion and elevation changes in soils (Krauss et al. 2003). Knee roots and pneumatophores promote deposition and prevent subsurface erosion more effectively than stilt roots (called as prop roots in cited article) (Chen et al. 2023). Surface vertical accretion rate was the highest in plank roots, followed by root knees and pneumatophores in Zhenzhu Bay, China (Du et al. 2021). The aerial root system also functions as an anchor to firmly stabilize the tree exposed to tides (Ong and Gong 2013).

However, a rise in sea-level attributable to climate change (Trincardi et al. 1994), tsunami damage (Choowong et al. 2007; Breanyn et al. 2009), dam construction (Malini and Rao 2004), sand mining, and shrimp farming (Saengsupavanich et al. 2009) have accelerated coastal erosion, thereby negatively affecting mangrove ecosystems (Alongi 2002). Human activities such as the conversion of mangroves to aquaculture or agriculture were identified as the primary cause of global mangrove loss from the period 1996–2010, and the greatest proportion of mangrove loss was observed in Southeast Asia (Thomas et al. 2017). In this context, mangrove restoration is extremely difficult and its success largely depends on the type of restoration and technical used (Jenny et al. 2021). Nature-based solutions achieving ecology mangrove restoration is considered to be cost-effective and ecology-effective but they have not been paid enough attention or lack of awareness. Attempts to restore mangroves, therefore, failed in many countries, mainly distributed to wrong selection of species and site conditions (Winterwerp et al. 2013).

In Vietnam, the area of mangroves was reported to be 408,500 ha in 1943. However, under the impact of chemical attack during the Second Indochina War, 124,000 ha of mangrove forests were destroyed from 1965 to 1970 (Hong and San 1993). Another range of causes consist of converting mangroves to agriculture and aquaculture, urbanization, sea level rise and alterations to sediment budgets as result of damming, particularly in the Mekong delta (Veettil et al. 2019; Phuong et al. 2020) leading to mangrove deforestation in Vietnam has continued with about 0.25% of the mangrove area lost per year from 2000 to 2012 (Hai et al. 2020). Apart from mangrove deforestation, mangrove degradation also has been an issue in Vietnam. Only 21% of the existing mangrove forests in Vietnam were natural forests while the remainder were re-planted (Hai et al. 2020). Although the above impacts have been persisting, many mangrove restoration efforts that have increased the area of mangroves in Vietnam to 194,806 hectares in 2019 (Phuong et al. 2020).

There has been state and non-government investment in mangrove reforestation and restoration projects over the last threee decades in Vietnam (Hai et al. 2020). These projects provided indicators of the causes of project failure or success. Much focus has been on the use of mono-species rather than restoring functioning mangrove ecosystems. Failures can be attributed to lack of understanding of reason for the loss of mangroves, poor site and species selection, and lack of incentives to engage local residents in the long-term management of restored areas (Hai et al. 2020).

The study was conducted in the coastal area of Ca Mau, Vietnam, where a large area of natural mangrove forests remains. Total mangrove area in Ca Mau as of 2020 is 1.7 thousand ha (of which, 23% is natural mangroves), accounted for 35.4% of total mangrove of the whole country (MARD 2020). This area has also been experiencing pronounced accretion and erosion. The process of shoreline erosion and accretion in Ca Mau province has occurred during various periods in 1903–2016. The accretion area increased by 877 ha and the erosional area increased by 140 ha from 2009 to 2017 in the study area (Hien 2017). Little erosion was detected in western Ca Mau province until the 20th century. However, erosion has been detected in the western areas of Ngoc Hien, Phu Tan and Tran Van Thoi districts since 2001, and the sediment loss rate has reached 15 m yr^{-1}. Nam Can and Ngoc Hien districts have experienced strong accretion processes (Hien 2017). A recent increase in erosional and accretion processes resulted in the loss of mangrove forests of 8,870 ha in estuarine and coastal regions in the last ten years (SIWRP 2013).

1.2. Purpose of study

The purpose of the study is to understand species-specific distribution and adaptation characteristics of mangroves with different aerial root types and mangrove stand dynamics to different timescale or intensity of accretion and erosion. This is an important scientific foundation for mangrove-based solutions of coastal protection in the study area.

The study questions:

i. What are differences in elevation and soil properties between accretion and erosion sites and among distances from the shoreline. And how are soil properties and elevation correlated?

ii. What are differences in the stand structure of mangroves between accretion and erosion sites and among distances from the shoreline?

iii. What are adaptive morphologies of different aerial root types supporting mangrove distribution and adaptation at accretion and erosion sites and among distances from the shoreline?

iv. How can the study's findings be applied in mangrove restoration in Ca Mau province?

The study hypothesis:

i. Elevation and soil properties differ between accretion and erosion sites and among distances from the shoreline and soil properties are positively or negatively correlated to the change in elevation.

ii. Stand structure of mangroves differs between accretion and erosion sites and among distances from the shoreline and is correlated to species-specific distribution and adaptation characteristics to timescale and intensity of accretion and erosion.

iii. Different aerial root types present adaptive morphologies which are correlated to mangrove distribution and adaptation at accretion and erosion sites and among distances from the shoreline.

iv. Insights into distribution and adaptation of mangrove with different aerial root types provide important information on species selection and target condition for mangrove-based solutions for coastal protection at accretion and erosion area.

The study:

i. compared the differences in elevation and soil properties between accretion and erosion sites and among distances from the shoreline and correlations between elevation and soil properties.

ii. compared the differences in stand structure of mangroves between accretion and erosion sites and among distances from the shoreline.

iii. investigated the adaptive morphologies of different aerial root types in correlations with mangrove distribution and adaptation at accretion and erosion sites and among distances from the shoreline.

iv. provided suggestions on mangrove-based solutions for coastal protection at accretion and erosion sites relied upon study findings.

The study content consists of four Chapters:

Chapter 2. LITERATURE REVIEW

2.1. Geomorphological and biological processes of coastal accretion and erosion

2.1.1. Geomorphological process

Coastal accretion and erosion caused by geomorphological processes are typically regulated by sediment exchanges over the time. A study conducted in the Sea Island Section of the Coastal Plain Physiographic Province showed that geomorphic cyles related to the nature of inlet flow and delta morphology effecting the bypassing of sediments and therefore determined the patterns of beach erosion and accretion in ebb deltas. Since ebb deltas is transected by a radially distributed pattern of channels, the flows of sediment across the inlets caused different disturbances to the sediment budget of the adjacent shoreline. As consequences, erosion was taken place along the inlet margin and accretion occurred at the distal ends of the spits by sediment transported from eroded positions (Oertel 1977).

A later study used multi-temporal/multi-resolution Landsat MSS and TM data to monitor the geomorphological changes along the coast of Karichi, Pakistan. Signicant changes in land accretion and erosion was observed in the Korangi-Phitti Creek area along Bundal and Buddo Islands over the 20 years period from 1987 to 1998 as resulted by the transport of sediment into the creeks from the erosion prone open coast beaches as well as through small rivers and inlets, and dispersed and deposited along the coast (Siddiqui and Maajid 2004).

Basically, erosive and accretive states transited depending on the intertidal topography, which was controlled by wave forcing, tidal modulation of the wave power at different levels of the beach and interactions between the existing beach cusp systems (Vousdoukas 2012). Besides, the fine sediment with different particle sizes determined the sediment distribution in estuaries through transporting or trapping, then creating accretion or erosion in estuaries (Dyer 1988).

The drivers contributing to the changes in geomorphology and sediment load such as oceanic currents, waves, winds, tidal oscillations, sea-level rise and anthropogenic agent were also explored in previous studies.

Winds, waves, tides and ocean currents continually work to erode, transport, and deposit sediment, altering coastal landscapes (Gensac et al. 2019). A study demonstrated a complex interaction of various natural (i.e., tides, wind, waves, currents, sea level, tectonics and storms) and humnan-induced coastal processes (i.e., construction of dam, buildings on beaches, harbours, mining of beach sand etc.), to coastal vulnerability and risks of southern coastal Tamil Nadu of India. The combined impacts of given drivers consequenced the variation of erosion and accretion along the coastline of study site (Mujabar and Chandrasekar 2011).

The natural processes of wave-induced longshore currents and sediment transport, along with man-made coastal protection structures denoted the erosion and accretion patterns observed in the northeastern coast of the Nil delta, Egypt. Accordingly, during the period of 1990 to 2000, accretion rate was recorded maximum 15 m year^{-1} within the embayment of Gamasa and in the shadow of Ras El Bar detached breakwater system, whereas erosion rate was approximately -14 m year^{-1} in the downdrift side of Damietta habor (El Banna and Frihy 2009).

A study quantified the rate of geomorphic changes at different time scales: 1951 - 2001 and 1999 – 2002 using various modes of erosion and the diversity of the eroded topography. The creation of a mudflat and the rate of erosion was demonstrated to be strongly related to the hydrodynamic perturbation off the mean alongshore coastal currents generated by river discharge and tidal outflow from the estuaries (oceanic dynamics) and the period of tidal immersion. The study indicated that the general direction of coastal oceanic dynamics was northwestwards and mudflat development always occurred southeast (updrift) of the river mouths. This nature consequently contributed to form a mudcape in their northwestward diversion and resulted erosional processes on the marine side off mudcapes, in a secondary outlet channel (Lefebvre et al. 2004).

Geomorphic processes in the Central West Coast of India were generated by monsoon. The beach showed accretion during postmonsoon and premonsoon intervals, and erosion during monsoon. As results, sedimentation in the estuary and dynamic changes leading to erosion and accretion was recorded in the northern side and southern side of the Venkatapur River mouth (Nayak et al. 2010).

In the context of climate change, relative sea-level rise indicated the impact on coastal geomorphology and coastal erosion in the coastline of the UK and Ireland. Nearshore was sensitive to extreme storms due to reduction of sediment accumulated by relative sea-level rise. Erosion and accretion occurred on the lower part profile and on the upper part of the nearshore, respectively, as natural response to sea-level rise in estuaries, barriers and tidal flats (Masselink et al. 2020). Sea level variations associated to erosion and accretion was also detected in the

coastal belt of Pakistan. Accordingly, the horizontal beach lost 110 mm year^{-1} caused by increasing in 1.1 mm year^{-1} of sea level (Khan et al. 2002).

An observation of man-made induced impact in a brackish Spartina patens marsh on Louisiana's Chenier plain showed that vertical accretion rates in natural and man-made canal waterway (3-4 mm year^{-1}) along a hydrologically restricted marsh region were significant lower than that along a nonhydrologically restricted natural waterway nearby (11 mm year^{-1}) (Cahoon and Tuner 1989).

2.1.2. Biological processes and role of mangroves

Similar to the geomorphological process, the impact principle of biological process affecting the accretion and erosion is to change the mass or location of sediments, mostly in intertidal zone. A study showed that biotic influences on transport of sediment within intertidal zone were significant and played a role in determining sediment budgets over tidal to monthly timescales (Wood and Widdows 2002). Thus, the biological agents (flora and fauna) and combination of physical agents controlling the process were much focuses in many previous studies.

The role of marine animals and benthic organisms in biological processes has received a great deal of research attention in relation to sedimentation and resulted in accretion and erosion. Sediment erodability and accretion rate in the Humber estuary, UK was quantified in relation to changes in the balance between bilogical and physical processes of sediment "stabilisation" and "destabilisation" related to current velocities and density of natural benthic community (i.e., the clam, namely *Macoma balthica* and algal). In the case of well developed benthic alga firms and low densities of bioturbating clams, there were a significant sediment accretion on the intertidal mudflat, but little accretion on the upper salt marsh. Conversely, significant erosion was recorded due to the higher densities of *M. balthica*. There were greater sediment accretion on the upper salt marsh as a consequence of enhanced erosion of the mudflat and re-suspension of sediment and vice versa (Widdows et al. 2000).

An overview article showed different physical and biological processes including tidal currents, air exposure, bio-stabilisation, biodeposition and bioturbation contributed to sedimendation, erosion and mixing of the Molenplaat tidal flat in the Westerschelde (SW Netherlands). The changes in sediment dynamics was associated with a shift from a tidal flat dominated by benthic diatoms and a low biomass of bioturbating clams (*Macoma balthica*), to a

more erodable sediment with a lower microphytobenthos density and a higher biomass of *M. balthica* (Widdow et al. 2004). Another type of benthic clam, namely *Meretrix meretrix* Linnaeus was analyzed the effects on bed erodibility and sediment erosion-accretion processes in an intertidal flat. The critical shear stress for erosion and the mangnitudes of bed-level change also revealed the large effected of *M. meretrix* (Shi et al. 2019).

Erosion-accretion dynamics in sandy beaches on the coast of central Chile related to the relationship between species richness of macroinvertebrates and sediment grain size. Accordingly, grain size became coarser, erosion-accretion dynamics more intense, and swash frequency and velocity increase as morpho- dynamic conditions change from dissipative to reflective extremes, involved different bio-logical processes or species (Alejandro 2001). The natural benthic community structure and sediment properties, and the abundance of key intertidal species were also used to quantify the erodability of undisturbed intertidal sediments (Widdows and Brinsley 2002).

The role of biological process on sediment flocculation process and sediment concentration was studied at Rudong, Jiangsu, China. As results, excretion of exopolymer particles provided by clam enhanced the flocculation process of cohensive sediment under combined stress of wave and current. Severe erosion events in aqualculture areas, therefore, were detected less than in the bare tidal flats (Li et al. 2021).

Biological processes in aspect of plant, a study indicated the contribution of root production and root mass accumulation of marshes and mangroves (i.e., fringe, basin, scrub, and dwarf forest types and a restored forest) and benthic mat formation to vertical accretion and elevation change in Calibbean Region. Surface growth of turf-forming algae, microbial mats, or accumulation of leaf litter and detritus also made significant contributions to vertical accretion (McKee 2011).

Geologist indicated the links between the ecology of mangrove communities and their sedimentary setting. They considered mangrove ecosystems as highly productive sources of organic matter and sediment sinks, characterized by long-term import of sediment and in accelerating the rate of mud accretion. Mangrove roots and pneumatophores were reviewed as efficient sediment trappers and effectively slowed water movement and fine roots of mangrove played an important role as sediment binders (Woodroffe 1992).

Based on remote sensing data (aerial photographs and SPOT satellite images) over the last 50 years and field surveys in French Guiana, Fromard et al. (1998) and Baltzer et al. (2004) stated that mangroves as markers of coastal dynamics which influenced by the combined action of accretion and erosion.

The role of mangroves in coastal and estuarine sedimentary accretion in Southeast Asia was synthesised and analyzed. The authors mentioned a distinctive mechanism of mangroves in trapping sediment and accelerating land-building processes in tide-dominated coastal and estuarine environments. The efficiency of sediment trapping by mangroves was species specific and the complex hydrodynamic and salinity conditions, accumulation rates of both organic and inorganic sediments, primary surface elevation, and hydroperiod influence sediment retention mechanism within mangrove ecosystems. Abundant terrigenous sediment supply could form dynamic mud banks and the complex aerial root system of mangroves may lead to accretion of sediment by weakening the tidal velocity (Chaudhuri et al. 2019).

Mangrove forests develop by interacting with sediment dynamics and shifting mudbanks, controlling erosion or accretion along the shoreline (Plaziat et al. 2004; Nascimento 2013). By that way, estuary channels and mangroves on tidal flats import and retain sediments and the sedimentation process leads to a seaward expansion of new mangrove habitats (Asp et al. 2018). In other words, mangroves play a key role in formation, stabilization, and development of muddy banks (e.g., Carlton 1974; Rogers et al. 2005; Keita Furrukawa et al. 1996, 1997), and control the spatial and vertical distribution of nutrients and sediment grain size in estuaries (Krishna Prasad and Ramanathan 2008).

According the early review paper of Carlton (1974), in Atlantic and Caribbean Sea, the trapping by mangroves of sediments and other marine debris resulting in the formation of new land was earliest studied by Curtis and McIntosh (1951). The most extensive research on that role of land-building by mangrove as a stabilizer was presented by Davis (1938, 1939). Ten miles (16 km) inland from present mangrove swamps built-up based on alluvial clays of mangroves were suggested by Carter (1959). This review paper also summarized the function of genus *Avicennia* and *Rhizophora* in reclaiming soils, catching drift and lodging humus.

A study in the Guianese coast indicated the combined action of accretion and erosion shifted mud banks towards northwest determined the structure and composition of mangrove forests and implied the adaptation characteristics of mangroves. The natural processes of coastline changes (i.e., net accretion from 1951-1966 and erosion from 1966-1991) showed a relation to replenishment of mangrove forests recorded over the period 1951 – 1999. A combined model of mangrove forest development model, forest gap dynamics and sedimentological dynamics was created (Figure 1).

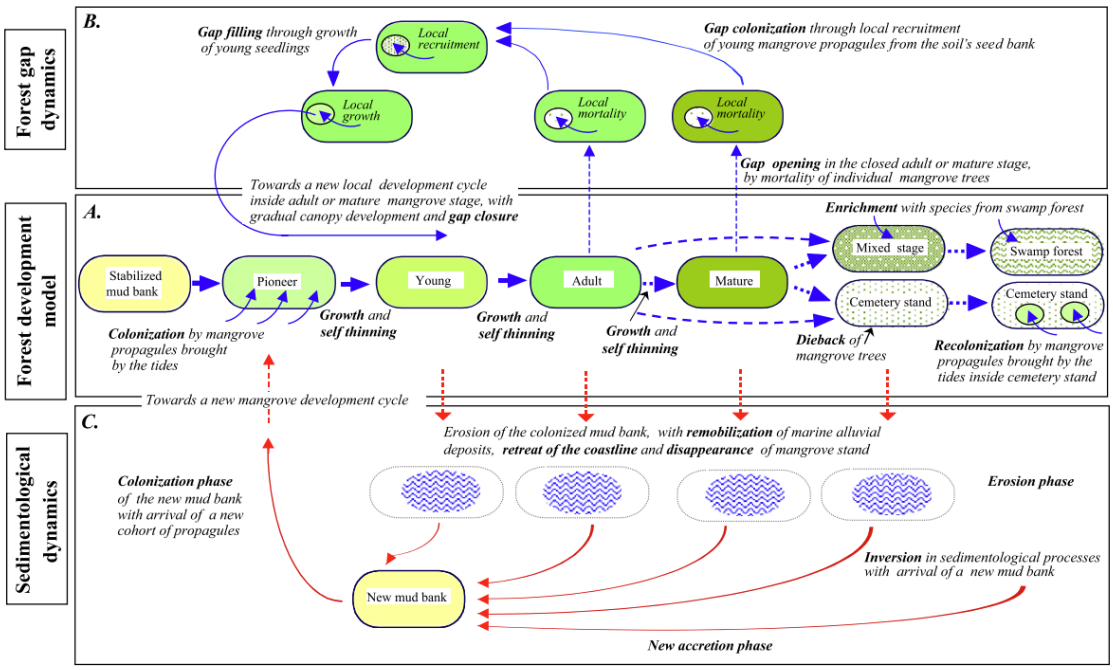

Figure 1. A new combined model of Guianese mangrove dynamics. (A): Forest development model, mainly based on growth and self-thinning processes. (B): Forest gaps dynamics, brought about by local decaying and death of individual mangrove trees. (C): Sedimentological dynamics, the major driving force in French Guiana as in the entire coastal area under Amazonian influence. (use origin figure in Fromard et al. 2004, Fig. 5, p. 276).

2.2. Mangrove distribution and adaptation

2.2.1. Mangrove distribution

Mangroves distribution reflects their habitats and functional ecology and are classified by sixe categories: i) Overwash mangroves: generally composed of *Rhizophora*, completely overwashed, and not characterized by litter accumulation; ii) Fringe mangrove: a *Rhizophora* – dominated littoral fringe inundated by daily tides, but litter accumulation; iii) Riverine mangrove: tall, productive *Rhizophora* – dominated mangrove stands flanking a river channel receiving nutrient – rich freshwater flushing; iv) Basin mangrove: typically mixed, or *Avicennia* – dominated characteristic of interior areas of mangrove forests; v) Scrub mangrove: a dawrfed stand especially of *Rhizophora* < 1.5 m tall, often in nutrient-poor areas; vi) Hammock mangrove: a special form of basin mangrove found in the Everglades, forming small islands of mangrove

over mangrove-derived peat which infills a depression in the underlying limestone substrate. (overviewed by Woodroffe 1992).

Avicennia and *Rhizophora* are dominant species in mangrove forests; however, they differ in colonization and stand structural development. The *Avicennia* species is commonly dominant in fringe forest areas, while the *Rhizophora* species dominates more landward areas in basin and transition forests (Estrada et al. 2013; Fromard 1998). Overview the distribution conditions of mangrove forests and species-specific distribution conditions are summarized in the Table 1 and Table 2 below.

Mangroves demonstrated a zonation of species parallel to the shore and reflected succession. According to a study on mangroves in Florida (USA), the seawardmost zone was *Rhizophora mangle* as pioneer, attributing it a role in the shoreline progradation, the succesive zones of mature *Rhizophora*, *Avicennia* with salt marsh species and *Conocarpus* to be seral stages in the sequence of replacement. In similar zoned mangroves in Jamaica, the viviparous nature of mangrove propagules were particularly well-adapted to dispersal and in shallow-water supporting for the notion that mangroves "claim land from the sea". Zonation of mangrove species and pattern of distribution reflected ecophysiological response to environmental factors, of which, central zones of the mangrove may represent a climax community. (overviewed by Woodroffe 1992).

A mixed forest of *Rhizophora* and *Laguncularia racemosa* had developed toward a *Rhizophora* dominated stand in intertidal areas, while *Laguncularia* dominated in areas above the mean high water elevation, responding to salinization in Biscayne Bay, North Miami, Florida (Ball 1980).

Mangrove succession in the Cananéia-Iguape coastal system, São Paulo, Brazil were exhibited a successional colonization pattern of mangrove and correlated to changes in depositional environments (Figure 2): (i) the propagation zone was an exposed bank, colonized by *Spartina alterniflora*; (i) *S. alterniflora* was replaced by *Laguncularia racemosa* as propagation took place; (iii) *Avicennia schaueriana* replaced *Laguncularia racemosa* as the substrate consolidated (Cunha-Lignon et al. 2009).

Table 1. Soil characteristics of mangrove forests in northern Australia, Carribean Coast of Colombia, south-west Florida, southern Japan, and western Sundarbans, India.

Location	Soil characteristics	Sources
Mangrove forests in Northern Australia	- pH: 6.2 – 7.0 - Salinity and soil bulk density varied by elevation: + Salinity: 30 - 34‰ (elevation < 1.4 m); 30 - 50‰ (elevation 0.8 – 1.4 m); 34 - 37‰ (0.6 – 1.4 m) + Soil BD: 0.38 $g.cm^{-3}$ (elevation 1.2 – 1.4 m); 0.45 $g.cm^{-3}$ (elevation < 1.4 m) - Organic matter: *ca.* 30% of dry weight	Boto and Wellington 1984
Mangrove forests in the Caribbean Coast of Colombia	- pH: 5.8 – 6.85 - Salinity varied by topographic: 19.8 – 53.5‰ (uneven topography); 40.2 - 103‰ (low topographic level, almost completely dead mangroves); 34.4 – 93.1‰ (more inland, narrow belt of poor developed mangrove trees) - Soil bulk density: 0.176 $g.cm^{-3}$ (inland) - 0.742 $g.cm^{-3}$ - Organic matter: 14.26% - 57.05% (inland)	Cardona and Botero 1998
Mangrove forests at Rookery Bay in south-west Florida (USA)	- pH: 6.7 - 7.0 - Salinity varied by zone: 33 - 38‰ (fringe zone); 50‰ (basin-mixed zone); 42‰ (basin-monospecific zone)	McKee 1993

Location	Soil characteristics	Sources
Mangrove forests along the Adelaide River floodplain, northern Australia	- Salinity varied by soil depth: 7 - 219‰ (30 cm soil depth, the highest soil salinities occurring in very dry soil) - Soil moisture: 10% (more mineral sediments, inundation during late dry season) – 70% (highly organic sediments, regularly flooded by the tides)	Ball 1998
Mangrove forests in southern Japan	- pH: 8.2 – 8.4 - Salinity: 32 - 34‰	Wakushima et al. 1994
Mangrove forests at Lothian Island of the western Sundarbans, India	- pH: 7.0 – 7.9 - Salinity: 13 – 31.2‰	Joshi and Ghose 2003

Table 2. Distribution characteristics of *Rhizophora* spp., *Avicennia alba, Avicennia officinalis, Avicennia marina, Sonneratia alba, Bruguiera* spp., *Lumnizera racemosa, Ceriops* spp., *Excoecaria agallocha*

Species	Specific conditions of distribution			
	Elevation	Inundation	Soil pH	Soil salinity
Rhizophora spp.	0.6 – 1.4 m (80 - 300 m distance from the coast) (Boto and Wellington 1984); seedlings survived at elevation higher than 0.4 m (Kitaya et al. 2002)	High tolerant (seedlings) (higher *Avicennia* pioneer species) (Kitaya et al. 2002)	Dominant with pH: 6.7 - 7.0 (the most at 6.7) - more tolerant in acidic condition (McKee 1993)	34 - 37‰ (Boto and Wellington, 1984); 30 - 50‰ (the most at 33 - 38‰) (McKee 1993)
Avicennia alba	More concentrated near the coast (Joshi and Ghose 2003)	Regular diurnal inundation (Joshi and Ghose 2003)		Optimal: 17.7 – 20.9‰ (Joshi and Shose 2003)
Avicennia officinalis	More concentrated at landward site (Joshi and Ghose 2003); seedlings survived at elevation higher than 0.4 m (Kitaya et al. 2002)	Tolerant species (seedlings) (Kitaya et al. 2002)		Wide range, optimal: 13.0 – 31.25‰ (Joshi and Ghose 2003)
Avicennia marina	Seaward zone (Wakushima et al. 1994); Regardless distance from the coast (Joshi and	Regular diurnal inundation (Joshi and Ghose 2003)	Varied (Joshi and Ghose, 2003); high pH -	Wide range, optimal: 18.4 – 20.9‰ (Joshi and Ghose 2003);

Species	Specific conditions of distribution			
	Elevation	Inundation	Soil pH	Soil salinity
	Ghose 2003); most foreshore species (Pi et al. 2009)		neutral to weakly alkaline (Wakushima et al. 1994)	high salinity (Wakushima et al. 1994)
Sonneratia alba	Seaward zone (Wakushima et al. 1994); seedlings survived at the lowest elevation of 0 – 0.2 m (Kitaya et al. 2002)	Very high tolerant (seedlings), higher than *A. officinalis* and *R. apiculata* (Kitaya et al. 2002)	high pH - neutral to weakly alkaline (Wakushima et al. 1994)	High salinity (Wakushima et al. 1994)
Bruguiera spp.		Weak tolerant (seedlings) (Kitaya et al. 2002); wide range of pH (Wakushima et al. 1994)	Limited range of salinity (Wakushimaet al. 1994)	
Lumnizera racemosa	Uneven topography (Cardona and Botero 1998); Basin-mixed zone: 20 - < 65 m inland (McKee 1993); landward zone (Wakushima et al. 1994); landward species (Pi. et al. 2009)	Conspicuous water flow during major rainy season and high tide (Cardona and Botero 1998)	6.7 (McKee 1993); wide range (Wakushima et al. 1994)	19.8-53.5‰ (Cardona and Botero 1998); 50‰ (McKee 1993); medium salinity (Wakushima et al. 1994)

Species	Specific conditions of distribution			
	Elevation	Inundation	Soil pH	Soil salinity
Ceriops spp.	0.8 – 1.4 m, 80 – 220 m inland, high elevated site (Boto and Wellington 1984); seedlings survived at elevation higher than 1.4 m (Kitaya et al. 2002); Away from the coast (Joshi and Ghose 2003)	Weak tolerant (seedlings) (Kitaya et al. 2002)		30 - 50‰ (Boto 1984); restricted to low salinity (Joshi and Ghose 2003)
Excoecaria agallocha	Away from the coast (Joshi and Ghose 2003); landward species (Pi et al. 2009)			Restricted to low salinity (Joshi and Ghose 2003)

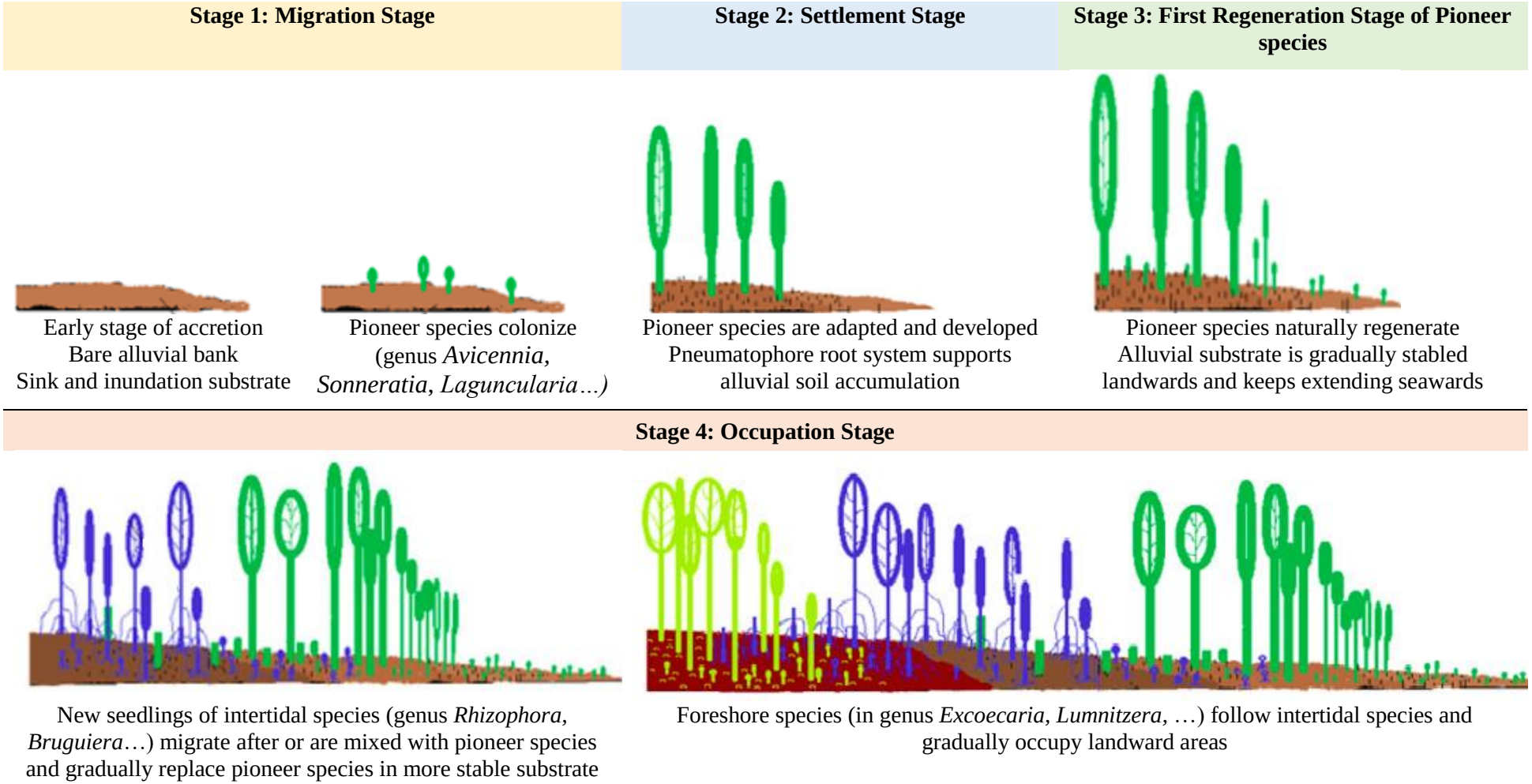

Figure 2. Illustration of mangrove succession strategy (drawn by the author based on literature overview).

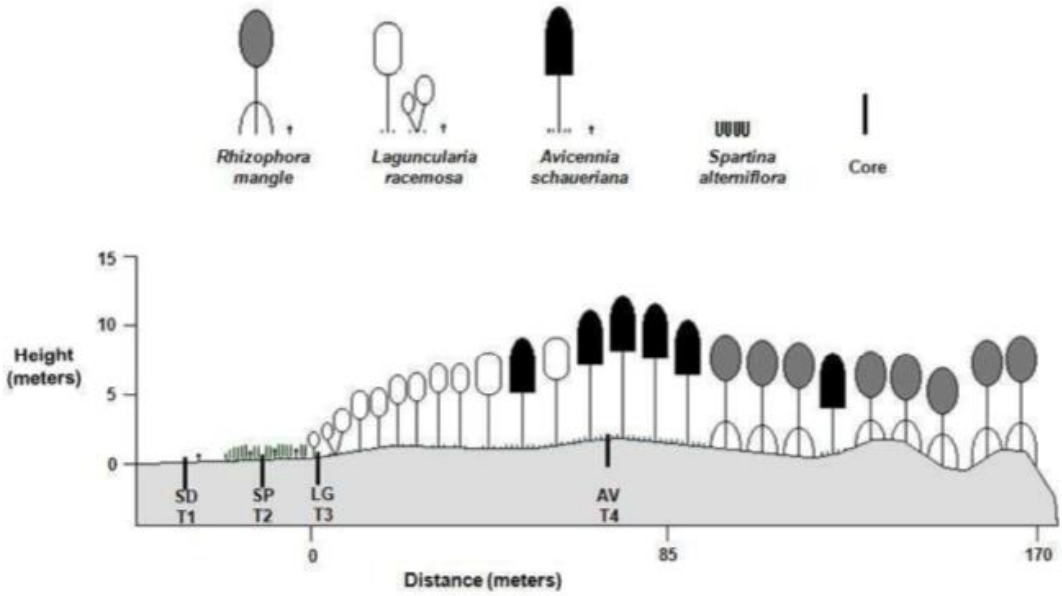

Figure 3. Colonization pattern of mangrove and correlated to changes in depositional environments in the Cananéia-Iguape coastal system, São Paulo, Brazil (use origin figure in Cunha-Lignon et al. 2009, Fig. 2, p. 164).

Mangroves are primarily regenerated from viviparous propagules, which are dispersed land—or sea—wards by tidal amplitude, waves, or even hurricanes (Baldwin et al. 2001). Succession in mangroves is cyclic and leads to a series of cyclic stages. Changes in each cyclic stage are controled by one or several external factors (Lugo 1980). Any disruptive impacts on natural succession of mangroves will affect their development in an adaptive or vulnerable way. Understanding their succession, therefore, is critially important in studies on mangroves to indentify the factors that regulate their distribution and adaptation. Based on the literature overview, in normal natural growing condition, four stages of mangrove succession could be illustrated in Figure 2. Accordingly, mangrove succession strategy is classified as 4 stages and characterized as follows: Pioneer species (i.e., genus *Avicennia*, *Sonneratia*, *Laguncularia*) is the first species to colonize on sink and inundation bare alluvial bank (Stage 1 – Migration Stage). Pioneer species are adapted and developed (Stage 2 – Settlement Stage), becomes mature and naturally regenerate (Stage 3 – First Regeneration Stage of Pioneer species). Development of pioneer species with pneumatophores root system supports alluvial soils to accumulate and be gradually stabled landwards and keep extending seawards from Stage 1 to Stage 3. Suitable substrate facilitates new seedlings of intertidal species (genus *Rhizophora*, *Bruguiera*…) to migrate after or are mixed with pioneer

species and gradually replace pioneer species in more stable substrate. Foreshore species (in genus *Excoecaria, Lumnitzera,* …) follow intertidal species and gradually occupy landward areas (Stage 4 – Occupation Stage).

2.2.2. Mangrove adaptation

Mangrove ecosystems are responsive to estuarial processes such as drainage, channelization, siltation, hurricanes, and thermal loading, which are related to its tolerance to flood, salinity, and temperature. It is naturally adapted to ordinary estuarine processes (Lugo and Snedaker 1974), but sensitive to environmental changes caused by artificial incidents (Alongi 2008; Emma et al. 2016).

Mangrove species adapt to coastal processes with their morphological or physiological characteristics, and show a species-specific spatial distribution when responding to accretion and erosion (Hesp 1991; Pham et al. 2019; Linh et al. 2023).

The individual tree shows complex adaptation to environmental conditions and on larger scales leading to local variations of the forest tructure. Additional disturbances are driving forces for the vegetation structure. They influence the ecosystem composition and structure across different spatial and functional scales. Mangrove forests, therefore, develop zonation as well as mosaic patterns with different cohorts of different succession stages with distinct canopy height patchiness. (overviwed by Vogt 2012).

Mangrove adaptation related to species-specific adaptation to environmental extremes: *Avicennia Germinans* will form monocultures and succeed itself under extreme conditions of low winter temperature or high soil salinity. *Rhizophora mangle* will do the same under conditions of high tidal energy, in deep ocean water, and/or low soil salinities. *Laguncularia racemosa* will grow alone when the water table is too deep for other mangrove species (overviewed by Lugo 1980).

The colonization of mangroves is controlled by site specific conditions of salinity, light, canopy gaps, forestry canopy, and sediment characteristics (Clarke and Allaway 1993). On the other hand, each mangrove species has its own tolerance to environmental factors such as salinity, flooding, or shade, which results in species zonation in mangrove forests (Sherman et al. 2000). *Avicennia marina* and *A. officinalis* are distributed in a wide range of soil salinities, while *Ceriops decandra*, and *Excoecaria agallocha* are restricted to low salinity areas (Joshi and Ghose 2003). *Lumnitzera racemosa* colonize in soil with a wide range of pH and medium salinity (Wakushima et al. 1994). *Sonneratia alba*, *R. apiculata*, *A. officinalis*, and *C. tagal* are more tolerant to higher

tidal inundations than *Bruguiera cylindrica* and *Xylocarpus granatum* during the seedling stage (Kitaya et al. 2002). *A. marina* is more tolerant to waterlogged soil than *B. gymnorrhiza*, *E. agallocha*, and *L. racemosa* are considered to be one of the most foreshore species (Pi et al. 2009). *Rhizophora mangle* indicated the ability of adaptation in post-hurricane conditions in the Indian River Lagoon in Florida (USA). The seedlings and saplings of *Rhizophora mangle* dominated the area after hurricane whereas *Laguncularia racemosa* and *Avicennia Germinans* showed low densities (Vogt 2012).

Forest dynamics influenced by natural disturbance regimes are described by successional stages between pioneer, young and mature mangrove processes (Fromard et al. 1998). Sucession was used to compare between mangrove in a restored mangrove site and a natural mangrove forest in terms of species richness, species colonization, vegetation cover, stand structure and so on (Proffitt and Devlin 2005).

Mangroves were identified as a key element in reducing the erosion rate by providing a protective barrier along the shoreline (Hochard et al. 2019). Mangrove roots controlled sediment movement and stabilize the soil beneath them (Woodroffe et al. 2016). Although some parts of the coastline with reasonably well-developed mangrove stands show erosion, indicating that mangroves may not be enough to provide complete protection against erosion in all situations, the rate of erosion would have been much faster without them (GIZ 2014). Moreover, mangrove forests provide a wide range of ecosystem services, including habitats for mangrove fauna (Ma et al. 2022), climate change mitigation (Duarte et al. 2013), and a high soil carbon sequestration capacity (Kida and Fujitake 2020).

Based on remote sensing data (aerial photographs and SPOT satellite images) over the last 50 years and field surveys in French Guiana, Fromard et al. (1998) and Baltzer et al. (2004) stated that mangroves as markers of coastal dynamics which influenced by the combined action of accretion and erosion. These disturbances then determine the structure and composition of mangrove forests and only this forest type adapted to this environment variation.

2.3. Aerial roots of mangroves

Aerial roots are one of the unique adaptive characteristics of mangroves processes (Lugo and Snedaker 1974) and solely found in mangrove species that are distributed in intertidal zones with poor oxygen conditions. Aerial roots in mangroves have lenticels that provide the function of gas exchange by supplying oxygen to underground roots in oxygen-poor mud, thus, aerating

below-ground roots and enabling mangroves to survive on anaerobic substrates (Srikanth et al. 2016). Thus, the morphology of aerial roots may be adaptive characteristic to topographic and soil variations within the intertidal zone and reflects the ecological features of the tree and surrounding environment.

In mature mangrove trees, complex root systems develop to facilitate the survival in specific substrate conditions. They have called in different names based on morphological characteristics. In general, aerial roots, mentioned above-ground roots, are classified into several types including stilt roots, pneumatophores, and knee roots (Dahdouh-Guebas et al. 2007; Ohira et al. 2013).

Stilt roots are commonly found in *Rhizophora* (Rhizophoracaea) (Kandasamy and Bingham 2001). Stilt roots in *Rhizophora* are also called prop roots, which descended from both trunk and branches, provided a stable support system. Submerged prop roots or stilt roots help to anchor the plant in place and collect water-born silt and debris to build soil beneath it. (overviewed by Srikanth et al. 2016). Pneumatophores are evolved in at least five mangrove families and genera but typically in *Avicennia* (Acanthaceae), *Sonneratia* (Sonneratiaceae) and *Laguncularia* (Combretaceae). They arise vertically from cable roots; abundant lenticels and aerenchyma may account for up to 70% of root volume to facilitate continuous oxygen diffusion. (Kandasamy and Bingham 2001; overviewed by Srikanth et al. 2016). Knee roots are common morphology of *Bruguiera* roots (Kandasamy and Bingham 2001; Du et al. 2021).

The pneumatophore density of *A. marina* is positively correlated with mud content in soil (Saifullah and Elahi 1992) and significantly higher for places with longer inundation periods, suggesting its adaptation to anaerobic condition (Dahdouh-Guebas et al. 2007). *Avicennia germinans*, *Laguncularia racemosa*, and *R. mangle* also change main root axes, root length, root diameter, and lateral root density to avoid low oxygen stress in anaerobic soils (McKee 1996). The morphology of aerial roots of *Rhizophora* spp. correlates with the basal area, height, and crown cover of trees (Méndez-Alonzo et al. 2015). The root system of *R. mangle* has high plasticity that renders it to adapt to changing environments (Gill and Tomlinson 1977).

Sonneratia spp. growths well in both saltwater and freshwater environments, both submerged and non-submerged dute to its root adaptation characteristics. *Sonneratia* spp. developed specialized pneumatophores for oxygen supply in the coastal region but did not develop that type of roots and any specialized roots as it was acclimatized in aerated soil. (overviewed by Srikanth et al. 2016).

Mangroves play an important role in coastal erosion and protection by regulating sediment accumulation with their aerial root systems (Spenceley 1977; Bird 1986; Kazemi et al. 2021).

Each type of aerial roots has its own abilities to trap and bind sediment, resulting in different rates of vertical accretion and elevation changes in soils (Krauss et al. 2003). Knee roots and pneumatophores promote deposition and prevent subsurface erosion more effectively than stilt roots (Chen et al. 2023). Surface vertical accretion rate was the highest in plank roots, followed by knee roots and pneumatophores in Zhenzhu Bay, China (Du et al. 2021). The aerial root system also functions as an anchor to firmly stabilize the tree exposed to tides (Ong and Gong 2013).

In Micronesian mangrove forests, stilt roots of *Rhizophora* spp. (called as prop roots in the cited article) facilitated vertical accretion (11.0 mm year^{-1}) more than pneumatophores of *Sonneratia alba* or bare soil controls (mean 8.3 mm year^{-1}). Sediment elevation, on the other hand, increased at an average rate of only 1.3 mm year^{-1} across all root types, with rate differences by root type, ranging from -0.2 to 3.4 mm year^{-1}, being detected within river basins. This investigation demonstrated that stilt roots can assist in the settling of suspended sediments from estuarine waters, yet their structures were not as successful as pneumatophores in maintaining sediment elevation over 2.5 years. As root densities increase over time, an increase in turbulence-induced erosion and in shallow subsidence as organic peat layers form is expected in Micronesian mangrove forests (Krauss et al. 2003).

The differences in the surface vertical accretion of sediment among aerial root types (*Avicennia marina* with pneumatorphores, *Bruguiera gymnorhiza* with root knees, and *Kandelia candel* with plank roots) were also investigated in Zhenzhu Bay of Beibu Gulf, China. As results, the highest accretion rate was detected in plank roots (1.51 cm year^{-1}), followed by root knees (1.05 cm year^{-1}) and pneumatophores (0.63 cm year^{-1}) (Du et al. 2021).

2.4. Mangrove restoration for coastline protection

Mangroves are important for shoreline stabilization. They provide protection against erosion, hurricanes and tsunamis, which can heavy impact on human life and infrastructure. The aboveground part reduces water velocities and turbulences and the stabilizing root system decreases eroding processes. (overviewed by Vogt 2012).

The coastal marsh is normally maintained under the balance between accretion and erosion processes (Reed 1990). However, sea-level rise due to climate change (Trincardi et al. 1994), tsunami damage (Choowong et al. 2007; Breanyn et al. 2009), dam construction (Malini and Rao 2004), sand mining, and shrimp farming (Saengsupavanich et al. 2009) have accelerated coastal erosion, thereby negatively affecting mangrove ecosystems (Alongi 2002). Human activities such

as the conversion of mangroves to aquaculture or agriculture were identified as the primary cause of global mangrove loss from the period 1996–2010, and the greatest proportion of mangrove loss was observed in Southeast Asia (Thomas et al. 2017). In this context, mangrove restoration is extremely difficult and its success largely depended on the type of restoration and the technical used (Jenny et al. 2021).

The ecology approach to mangrove restoration is considered to be a cost-effective solution and has been applied in many projects. One review paper indicated that "mangrove restoration projects should be to actively promote a return to the natural assemblage structure and function (within the bounds of natural variation) that is self-sustaining" (Ursula and Geoffrey 1998).

In addition, specific restoration methods and strategies should match the prevailing geomorphic settings (low tidal range, organic settings; minerogenic settings), which are strongly incorporated to the suspended sediment supply and tidal range (Thorsten and Daniel 2015). Significant effects on habitat connectivity indicated the the critical importance of identifying suitable areas for species-specific in mangrove restoration, case study in the Large Xiamen Bay in southeast China (Jie et al. 2022).

Winterwerp et al. (2013) provided a comprehensive review on mangrove rehabilitation attempts across the tropics. The large-scale rehabilitation attempts in Bangladesh have received much attention. Over 120,000 ha of mangroves was successfully planted since 1966, mainly on newly accreted land. Two species of mangrove, *Sonneratia apetala* and *Avicennia officinalis*, dominated the mangrove plantations, usually as monospecific stands. In spite of the success in Bangladesh, most attempts to restore mangroves failed completely in many countries. In West-Bengal, India, for instance, only 1.5% success rate of mangroves planted between 1989 and 1995.

In the Philippines, over the past two decades, more than 44,000 ha, mostly non-mangrove mudflats, sandflats and seagrass beds had been planted with mangroves, using almost exclusively the genus *Rhizophora*. In these areas, seedlings experienced high levels of mortality and the few that survived had displayed dismally stunted growth relative to the corresponding growth performance of individuals thriving at the high intertidal position and natural mangrove sites. Many reasons of failure in mangrove rehabilitation projects in Philippines were lack of awareness, complexity of interactions between natural system, social system, and human values, lack of community involvement and so on. In terms of ecology aspect, inappropriate species and sites leading to low survival rate at 10 – 20% were two of main reasons. The favoured but unsuitable *Rhizophora* are planted in sandy substrates of exposed coastlines instead of the natural colonizers *Avicennia* and *Sonneratia*. The filipinos researchers also eoncouraged multi-species mangrove

reforestation instead of dependence on monospecies stands of *Rhizophora* spp., which can be prone to pest attacks. (overviewed by Winterwerp et al. 2013; Garcia et al. 2014).

In Thailand, a massive 5-year mangrove-replanting program was launched by the Thai Government during 1991 – 1996, targeting to replant 40,000 ha. This programmed cannot be evaluated as successful, except in a few cases in Southern Thailand where a community-based management approach was followed. (overviewed by Winterwerp et al. 2013).

In China, many efforts have been made to rehabilitate mangrove forests. However, only 57% of successful rate was evaluated. Even in Fujian and Zhejiang provinces, survival rates of rehabilitated mangrove stands were reported as low as 1.3% - 31%. The unsuccessful rehabilitation of mangroves in China was also mainly attributed to wrong selection of species, unfavorable climate and site conditions. (overviewed by Winterwerp et al. 2013).

Various of authors have emphasized the failure in appropriate hydrological regimes (depth, duration and frequency, and of tidal flooding) in restoration sites caused low success rates, along with insisting on planting of non-pioneer species that lack specific biological traits related to inundation tolerance and rapid rooting. (overviewed by Winterwerp et al. 2013).

Based on literature review, Lewis III (2009) suggested three main concerns of specific site selection for mangrove restoration:

i) Investigate the areas of damaged mangroves showing secondary succession or recovery from a previous damage event.

ii) The time frame since the damage event needs to be known in order to answer the key question, which is, “does this site need management to support further recovery, or accelerate recovery, or is it likely to recover over time by itself without intervention?

iii) “Propagule limitation” to define a condition in which natural recovery is slowed or stalled due to a lack of natural mangrove propagules being available to volunteer at a damage site. Propagule limitation may be caused by a large loss of adult trees capable of producing propagules or by hydrologic restrictions or blockages (i.e., dikes), which prevent natural waterborne transport of mangrove propagules to a restoration site. If a damaged forest is going to recover on its own within an acceptable time frame, any attempt to introduce propagules or plant propagules or plant nursery grown mangroves is likely to be a waste of time and money.

Lewis III (2009) also provided six critical stpes to achieve ecological mangrove restoration (EMR) which were compiled from training courses in the USA, Nigeria, Indonesia, Thailand, Vietnam, Sri Lanka, and India as follows:

1. Understand the autecology (individual species ecology) of the mangrove species at the site, in particular the patterns of reproduction, propagule distribution, and successful seedling establishment.
2. Understand the normal hydrologic patterns that control the distribution and successful establishment and growth of targeted mangrove species.
3. Assess the modifications of the previous mangrove environment that occurred that currently prevent natural secondary succession.
4. Select appropriate mangrove restoration sites through application of Steps 1–3 above that are both likely to succeed in restoring a sustainable mangrove forest ecosystem, and are cost-effective given the available funds and manpower to carry out the projects, including adequate monitoring of their progress towards meeting quantitative goals established prior to restoration. This step includes resolving land ownership/use issues necessary for ensuring long-term access to and conservation of the site.
5. Design the restoration program at appropriate sites selected in Step 4 above to initially restore the appropriate hydrology and utilize natural volunteer mangrove propagule recruitment for plant establishment.
6. Only utilize actual planting of propagules, collected seedlings, or cultivated seedlings after determining through Steps 1–5 above that natural recruitment will not provide the quantity of successfully established seedlings, rate of stabilization, or rate of growth of saplings established as quantitative goals for the restoration project.

Babak and Roslan 2011 conducted a study on mangrove restoration without planting in Sungai Haji Dorani, on the west coast of Peninsular Malaysia. In order to take advantage of natural regeneration to restore the degraded shoreline exposed on the west coast of Peninsular Malaysia, a detached breakwater was built to prevent the ongoing erosion, promote sediment deposition and thus facilitate naturally recruitment of seedlings or progagues available from adjacent stands. The beakwater presence provided favorable conditions attracting mangrove recruits, facilitating reestablishment and natural recovery of the mangrove ecosystem without planting.

Nowsaday, variety of nature-based solutions of coastline protection were implemented as an alternative to hard infrastructure sea dams such as mangrove planting and permeable barriers (e.g., bamboo fences, brushwood dams etc.). This application was successfully applied in Guyana, Indonesia, Suriname, Thailand and Vietnam (Figure 4). The basic philosophy behind the

construction of permeable dams was the rehabilitation of mangrove habitat by restoring the net sediment balance (overviewed by Winterwerp et al. 2020).

Figure 4. Successful application of permeable dams for mangrove restoration in Guyana (a, b), Indonesia (c), Suriname (d, e), Thailand (f, g, h) and Vietnam (i, j). (use origin figures in Winterwerp et al. 2020, Fig. 7 – p. 6; Fig. 8 – p. 6; Fig. 11 – p. 7; Fig. 13 – p. 8; Fig. 14 – p. 9; Fig. 16 – p. 9).

2.5. Studies on mangroves in Vietnam

2.5.1. Distribution and composition of mangroves in Vietnam

Hong and San (1993) provided a comprehensive overview on mangrove forests in Vietnam. Before the second Indochina war (1962-1971), mangrove forests in Vietnam covered an area of about 400,000 ha, mainly found in the South (250,000 ha), of which approximately 200,000 ha were in Ca Mau peninsula. It was estimated that 149.982 ha of mangroves at Ca Mau were primary forests at that period. After two Indochin wars, the quantity and quality and composition of mangroves were changed greatly. The use of herbicides and napalm during the war (1962-1971) resulted in the destruction of nearly 40% of the mangrove forests in southern Vietnam. In other areas, mangroves were exploited as natural resources or replaced by agricultural and shrimp farms. Since 1983, there were 252,200 ha of remaining mangrove forests composed mainly of secondary growth, plantations and bushes, while natural forests occupy only a small area.

In Vietnam, there are 69 mangrove species found in the south and 34 species in the north. Seeds and propagules are carried by ocean currents to Vietnam and further north by southwest monsoon during the summer, but with the change in the direction of the current, some species did not reach the northern coast. This is reason why many species abundant in the south, such as *Sonneratia alba, S. ovata, Ceriops tagal, C. decandra, Rhizophora apiculata, R. mucrotana, Bruguiera cylindrica, B. parviflora, Avicennia alba, A. officinalis* and *Nypa fruiticans,* are absent in the north. The low winter temperature and cold water also restricted condition for them to survive in the north. (overviewed by Hong and San 1993).

The mangrove forests in Vietnam have been divided into 4 zones and 12 subzones (Figure 5, Hai et al. 2020) with common species distribution characterized as follows Hong (1984, 1991):

Zone I: Noth-east coast: *Rhizophora stylosa, Bruguiera gymorrhiza, Kandelia candel, Aegiceras corniculatum, Myrioporum bontioides, Scaevola hainanensis.*

Zone II: Northern delta: *Sonneratia caseolaris, Kandelia candel, Aegicaras corniculatum, Acanthus ilicifolius*.

Zone III: Central coast : *Sonneratia caseolaris, Rhizophora stylosa, R. mucronata, R. apiculata, Avicennia marina, A. officinalis, Bruguiera gymnorhiza, B. sexangula, Kandelia*

candel, Acanthus ilicifolius, Cyperus malaccensis, Aegiceras corniculatum, Acrostichum aureum, Clerodendron inerme, Excoecaria agallocha, Hibiscus tiliaceus, Thespesia polulnea, Lumitzera racemosa, Pandanus tonkinensis, Cerbera manghas, Xylocarpus granatum, X. obovatum, Nypa fruticans, Phoenix paludosa, Scyphiphora hydrophyllacea.

Zone IV: Southern delta (the coast of southern Vietnam): *Sonneratia alba, S. caseolaris, Rhizophora apiculata, R. mucronata, Avicennia alba, A. officinalis, A. marina, Bruguiera parviflora, B. sexangula, Kandelia candel, Xylocarpus granatum, X. obovatus, Ceriops tagal, Aegiceras corniculatum, Lumitzera racemosa, Excoecaria agallocha, Phoenix paludosa, Ceriops tagal, C. decandra, Acrostichum aureum, Scyphiphora hydrophyllacea, Heritiera littoralis, Flagellaria indica, Nypa fruticans, Cryptocoryne ciliata, C. malaccensis, Acanthus ebracteatus, A. ilicifolius, Derris trifoliata, Acrostichum aureum, Hibiscus tiliaceaus, Thespesia populnea.*

Zone IV provides the most favourable environmental conditions for mangrove development. Every year, this zone receives alluvium and fresh water from the Cuu Long and Dong Nai river systems. Additionally, it has been less impacted by storms than other three zones. With many sunny days and high radiation, zone IV supports the highest rates of growth of mangrove species and has nearly 80% of the total mangrove area in Vietnam (MARD 2014; Hai et al. 2020).

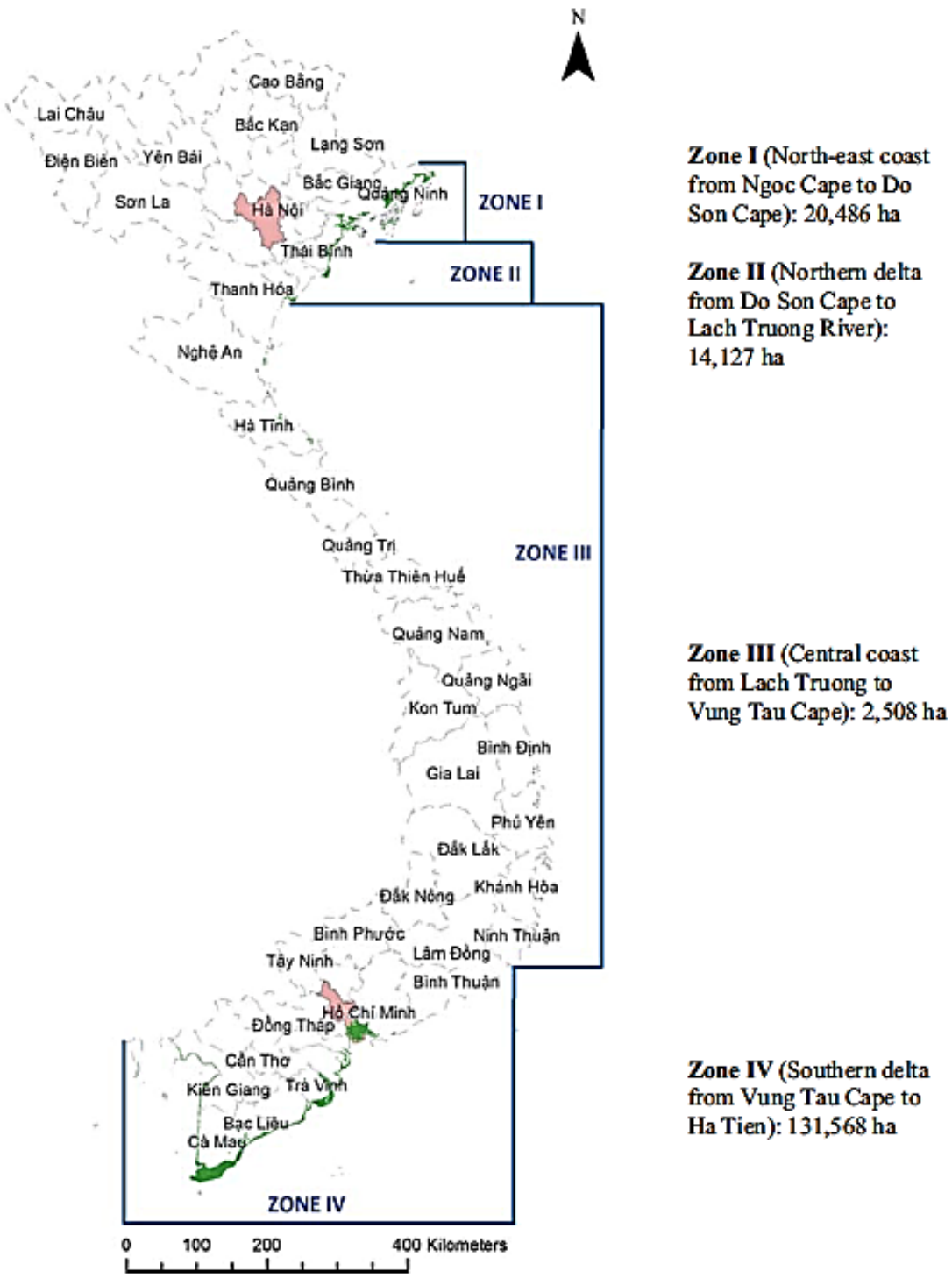

Figure 5. Distribution of mangroves in Vietnam in 2013 (use origin figure in Hai et al. 2020: Fig. 1, p. 18).

2.5.2. Succession of mangroves in Vietnam

Typical primary succession process of mangrove in Vietnam was summarized by Hong, and San (1993) (Figure 6). The regenerative process of secondary succession is best illustrated

by observing the stretches of forests at Ca Mau peninsula. The process of regeneration took place as follows (Hong and San 1993):

(1) *Avicennia alba* regenerated on land previously occupied by *Rhizophora* forest. The seeds of *A. alba* were brought by tidal water from adjacent areas. The clearing of dead trees for use as firewood also aided the regeneration. *A. alba* grows rapidly and after 10 years can reach a height of 8 – 10 cm. *Ceriops decandra* can be found beneath the canopy. If forest is not disturbed, *Rhizophora* growing on the edges of the mudflat, will replace in 10-15 years.

(2) A community of *Rhizophora-Bruguiera sexangula* regenerated on the mudflats along the rivers and canal banks flooded by tide. The seed source was abundant and *Rhizophora* forests could regenerate. *B. sexangula* or *Xylocarpus granatum* may also be found in this area. Only when the land is highly elevated, can *Lumnitzera littoralis* and *Xylocarpus* establish themselves.

(3) A community of *Ceriops decandra-Lumnitzera racemosa* is regenerating on land flooded by high tide. The denuded flats of firm mud-clay along canals and those further inland are unsuitable for the regeneration of *Rhizophora*. If the land continues to be elevated, after some time *Ceriops* can be eventually replaced by *Excoecaria*.

(4) There is some regeneration of *Phoenix padulosa* on rarely-flooded land. After the forest of *Rhizophora* and *Bruguiera* was destroyed, the land has degenerated. The seeds of *Phoenix padulosa* established themselves in the denuded flats. In low-lying areas, where the flats are flooded, scattered *A. alba*, *A. marina* and *Ceriops tagal* are found.

(5) The former community of *Rhizophora-Avicennia alba* on land flooded by high tide was cut down for firewood. The regenerated succession is complex: euryhaline liane species such as *Sarcobolus globosus*, *Gymnanthera nitida* and some other species like *Lumnitzera racemosa*, *Dolichandrone spathacea* and *A. marina* invaded these areas, but *A. officinalis* remains dominant. If left undisturbed, the species diversity will eventually decrease due to the closing of the *Avicennia* canopy and the liane species will be reduced in number.

(6) *Sonneratia caseolaris* forests used to grow in muddy swamps along brackish water rivers.

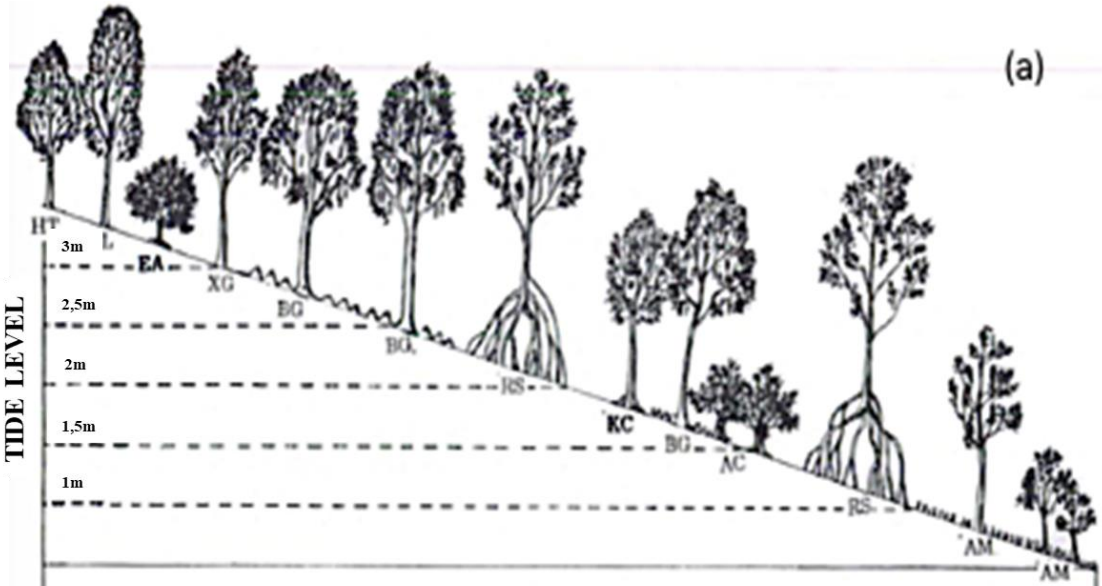

SUCCESSION STAGES			
Xylocarpus granatum Excoecaria agallocha Heriteara littoralis Hibiscus tiliceus	Bruguiera gymnorrhiza (dominant) Rhizophora stylosa (scattered)	Rhizophora stylosa Kandelia candel Bruguiera gymnorrhiza Kandelia candel Aegiceras corniculatum Avicennia marina	Avicennia marina (Pioneer)

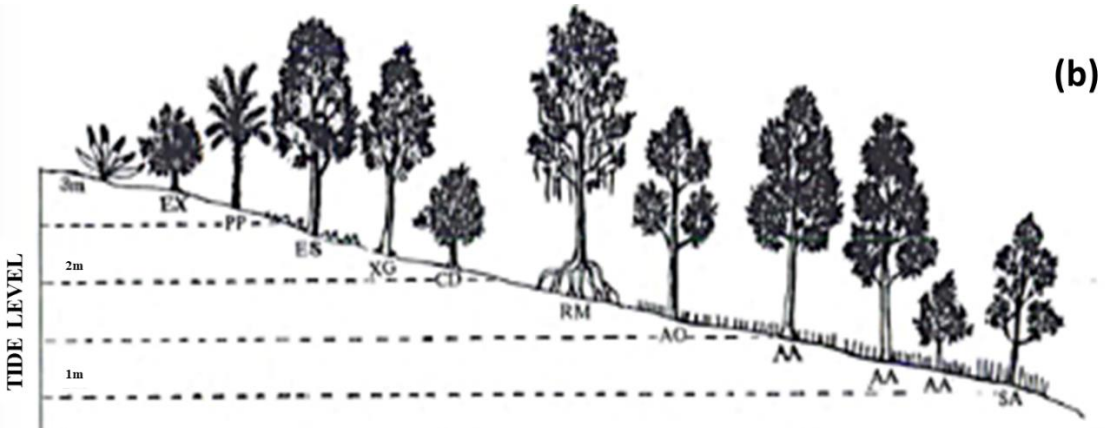

SUCCESSION STAGES			
Phoenix paludosa Excoecaris agallocha Acrostichum aureum Finlaysonia maritima	Rhizophora mucrotana Ceriops decandra Xylocarpus granatum Bruguiera sexangula (mixed community)	Avicennia alba (dominant) Avicennia officinalis	Sonneratia alba Avicennia alba (pioneer)

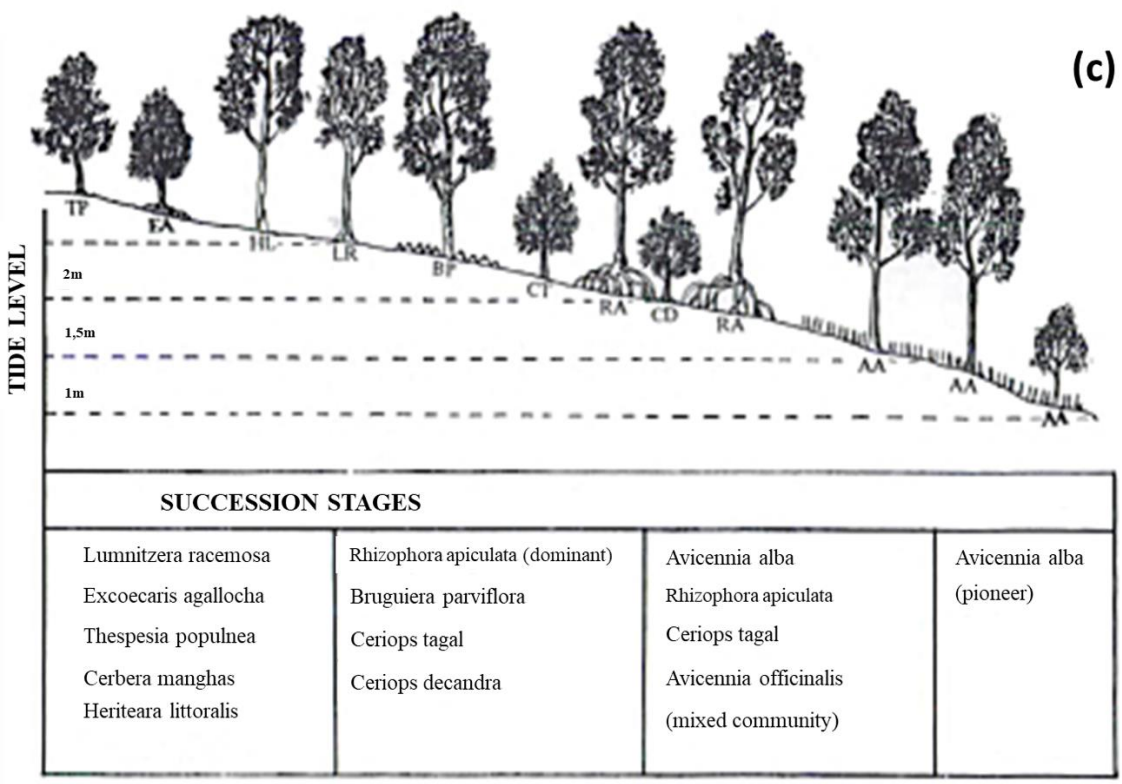

Figure 6. Primary succession of mangrove in Vietnam. (a) Primary succession of mangroves in the northeast coast Vietnam; (b) Primary succession of mangroves at Ba Lai estuary, Ben Tre province (Mekong Delta); (c) Primary succession of mangroves at Ca Mau peninsula (Mekong Delta). (cited from Hong and San 1993).

2.5.3. Ecology Mangrove Restoration in Vietnam

In Vietnam, the area of mangroves was reported to be 408,500 ha in 1943. However, under the impact of chemical attack during the Second Indochina War, 124,000 ha of mangrove forests were destroyed from 1965 to 1970 (Hong and San 1993). Another range of causes consist of converting mangroves to agriculture and aquaculture, urbanization, sea level rise and alterations to sediment budgets as result of damming, particularly in the Mekong delta (Veettil et al. 2019; Phuong et al. 2020) leading to mangrove deforestation in Vietnam has continued with about 0.25% of the mangrove area lost per year from 2000 to 2012 (Hai et al. 2020). Apart from mangrove deforestation, mangrove degradation also has been an issue in Vietnam. Only 21% of the existing mangrove forests in Vietnam were natural forests while the remainder were re-planted (Hai et al. 2020). Although the above impacts have been persisting, many mangrove restoration

efforts that have increased the area of mangroves in Vietnam to 194,806 hectares in 2019 (Phuong et al. 2020).

Over the last threee decades there has been considerable (c. 200,000 ha) state and non-government investment in mangrove reforestation and restoration projects in Vietnam (Hai et al. 2020). In the post-war period (1975 – 1980), mangrove restoration projects and programs were mostly implemented in zone IV to recover destroyed mangrove forests after the Second Indochina War. However, due to poor silvicultural techniques applied, projects failed in many places. From 1981 to 1990, mangrove restoration continued to be concentrated in zone IV, mostly Stated-funded. Since 1990, the government started a large mangrove reforestation program to replant 52,000 ha of mangroves. From 2011 to 2020, under the National Target Program, the Forest Protection and Development Plan and other related programs, 113 projects were implemented targeting restoration efforts accross 48,096 ha. Apart from State-funded projects, mangroves in Vietnam also have been restored with support from international organizations. From 1990 to date, the total restored mangrove area from these projects is 43,750 ha and in the next 5 year, a further 19,000 ha of mangroves are expected to be restored. (overviewed by Hai et al. 2020).

The main objectives have been coastal protection and stabilization and production of forest products, with fisheries, climate mitigation, and adaptation and ecosystem restoration as minor objectives. These have had reportedly varied success in terms of long-term survival rates. Much focus has been on the use of mono-species rather than restoring functioning mangrove ecosystems. These projects provided indicators of the causes of project failure or success. Failures can be attributed to lack of understanding of reason for the loss of mangroves, poor site and species selection, and lack of incentives to engage local residents in the long-term management of restored areas (Hai et al. 2020).

In aspect of ecology approach, some notable successful restoration programmes in Can Gio Mangrove Biosphere Reserve, the Ca Mau Peninsula, the Kien Giang Biosphere Reserve and the Red River Delta were overviewed by Veettil et al. (2019) as follows:

(1) Can Gio Mangrove Biosphere Reserve: Mangrove restoration in Can Gio has been acknowledge as a success due to favourable hydrological and geomorphological conditions and the fact that the planted species have mixed with naturally regenerated species. The key species used for mangrove restoration was *Rhizophora apiculata*. Other species planted include *Nypa fruticans*, *Ceriops tagal* and *Rhizophora mucronata*.

(2) Ca Mau Peninsula: Several mangrove rehabilitation projects funded by foreign agencies were established in Ca Mau in the 1990s and the World Bank Coastal Wetlands Protection and

Development Programme planted about 25,262 ha of mangroves in Ca Mau. There were also several naturally regenerated mangrove areas near shrimp ponds in the Ca Mau Peninsula consisting mainly of *Avicennia* spp. and *Rhizophora* spp.. Reforested areas were mainly planted with *Rhizophora* spp., which is predominantly responsible for the net increase in mangrove area in Ca Mau between 1992 and 2004. In order to protect different mangrove species in Ca Mau, Mui Ca Mau National Park was established on the south-western tip of the peninsula in 2003. Some mangrove areas of Ca Mau Peninsula were designated as a UNESCO International Biosphere Reserve in 2009 and this was designated as a Ramsar site in 2013.

(3) Kien Giang Biosphere Reserve: The key pressures on Kien Giang mangroves is coastal erosion due to the particular low-lying geomorpholohy and ocean currents induced by strong winds. The mangrove restoration project in the Vam Ray region of Kien Giang used different types of Melaleuca fences resulted in the gradual expansion of mangrove areas. The use of Melaleuca fences together with reforested mangroves for efficient coastal protection.

(4) Red River Delta and adjacent mangroves: Mangrove restoration in Red River Delta was started by the Red Cross in the 1990s as a method for shore protection against storms. A Japanese NGO named ACTMANG (Action for Mangrove Reforestation) started mangrove planting projects in three districts (Thai Thuy, Tien Lang and Tinh Gio) and a total of 1100 ha was planted. The main species planted in these regions were *Kandelia candel* and *Sonneratia caseolaris*.

However, the combined effects of anthropogenic factors and acclerated climate change causing sea level rise, coastal disasters, changes in currents, wind direction etc., the impacts of coastal erosion and accretion has become more complex, challenging mangrove rehabilitation.

Chapter 3. METHODS

3.1. Study area

3.1.1. Geographical and topographic conditions

The study was conducted at seven study sites in the coastal area of Ca Mau, the southernmost area of Vietnam and located in Mekong Delta region. This area is surrounded by the Gulf of Thailand to the west and the East Sea to the south and east (Figure 7). The terrain is relatively flat and low with the average elevation is from 0.5 m to 1.5 m from the sea level. The topography is fragmented by the complex system of rivers and canals. (DARD Ca Mau 2019).

3.1.2. Climate

Ca Mau is located in the intertropical region of the Northern Hemisphere and has the climate characteristics of the Mekong Delta, which has tropical monsoon and fairly mild and distinct wet and dry seasons.

The weather data of Ca Mau for 30 years from 1991 to 2021 is summarized in the Table 3. The annual mean temperature in Ca Mau is 26.7°C. The hottest month of the year is April, with a monthly mean temperature of 28.2°C. December is the coldest month of the year with the mean monthly temperature of 25.7°C. The variation in annual temperature is around 2.6°C.

The annual precipitation is 2465 mm. The driest month is February, with 22 mm of monthly precipitation. In October, the precipitation reaches its peak, with an average of 413 mm. The difference in precipitation between the driest month and the wettest month is 391 mm. The month with the highest relative humidity is October (87%). The month with the lowest relative humidity is February (71%). The month with the fewest rainy days is February (3 days). In Ca Mau, the sun shines for an average of 2978.24 hours per year. That comes out to 97.92 hours of sunshine each month.

Table 3. Monthly mean, minimum, and maximum temperature (℃), humidity (%) and sun hours, monthly precipitation (mm) and rainy days in Ca Mau for 30 years from 1991 to 2021.

	January	**February**	**March**	**April**	**May**	**June**	**July**	**August**	**September**	**October**	**November**	**December**
Monthly mean Temperature (ºC)	25.7	26.6	27.7	28.2	27.8	27.1	26.7	26.7	26.4	26.1	26	25.7
Minimum Temperature (ºC)	22.5	23	24.2	24.9	25.3	25	24.7	24.7	24.4	23.9	23.5	22.8
Maximum Temperature (ºC)	29.9	31.6	32.6	32.7	31.5	30.4	29.9	29.8	29.7	29.8	29.7	29.4
Precipitation (mm)	37	22	64	126	266	287	300	295	338	413	216	101
Humidity (%)	75	71	72	76	82	85	86	85	86	87	85	79
Rainy days (day)	5	3	7	12	19	20	21	21	20	21	16	10
Average sun hours (hours)	7.9	8.1	8.4	8.7	8.5	8.5	8.3	8.2	7.9	7.6	7.8	7.9

(Data source: Climate-data.org: https://en.climate-data.org/asia/vietnam/ca-mau-province/ca-mau-4244/#temperature-graph)

There are two main directions of winds year around year in Ca Mau: Southwest monsoons from June to September and Northeast monsoon from November to April. Generally, winds to the East coast will turn clockwise on the coast of the Gulf of Thailand in the Northeast monsoon season. The wind speed on the coast of the Gulf of Thailand is less than on the east coast. The average wind speed at the west coast is 3.6 m s^{-1} in the northeast and 3.4 m/s in the southwest monsoon. In the East Coast, the average wind speed is about 4.5 m s^{-1} during the Northeast monsoon and is 3.5 m s^{-1} the southwest monsoon. During the storms, wind speeds can range from 15 to 20 m s^{-1}. (DARD Ca Mau 2019).

3.1.3. Hydrogeography and marine conditions

3.1.3.1. Sea and river network

Ca Mau has a coast length of over 254 km, accounting for one third of the coastline of the Mekong Delta and is equal to 7.8% of the coastline of the whole country. This area has many estuaries open to the sea such as Ganh Hao, Bo De, Ong Doc, Ong Trang, Bay Hap, Khanh Hoi, etc. and an interlaced web system of rivers and canals, including many large rivers, deep water, leading alluvial accretion into the soil such as Tam Giang, Ganh Hao, Bay Hap, Song Doc, Dam Doi, Cai Tau, Trem Trem etc. Total area of water surface is 15,756 ha, accounting for 3.02% of the natural area of the province. (DARD Ca Mau 2019).

3.1.3.2. Wind and oceanic currents

During the dry season, the cold and saltwater flow from the north to coincide with the northeast monsoon, which approaches the eastern coast of Ca Mau, with an average speed of 0.4 – 0.9 m s^{-1} (DARD Ca Mau 2019). In this period, sea currents could cause severe erosion of areas absent of the wind and face the unprotected winds and transfer mud and sand to the south. During the rainy season, the southwest monsoon pushes the cold water outward from the shore, facilitating the water slides bearing alluvium of the Mekong River to the south. The total flow in the coastal area of Ca Mau province shows (DARD Ca Mau 2019): In the dry season (northeastern wind): The currents along the east coast flow southward at an average speed of about 40 – 90 cm s^{-1} and can reach 150 cm s^{-1}, provide main source of sediment on the beach. During the southwest monsoon season, the currents are in the opposite

direction – moving counterclockwise. The average speed is about 40 – 50 cm s^{-1}. The alluvium flows from this period are less. (DARD Ca Mau 2019).

3.1.3.3. Tide regime on the East Sea and the Gulf of Thailand

The tide is irregular semi-diurnal on the East Sea. The tide changes 4 times (2 times of high tide and 2 times of low tide) in each day. The actual data show that the largest tidal volume in the Mekong River mouth, which is 3.7 m in the high tide period, 2.7 m in the low tide period, decreasing toward the Ca Mau province. Tidal regime at high tide of 3.2 m in Ganh Hao gate; 3.0 m in Bo De gate and 2.2 m in Dat Mui area. Big tides reduce rapidly at Bay Hap to 1.1 m. On the Gulf of Thailand, the tide is irregular diurnal (the tide changes twice a day). The tidal currents rate reached 1.2 – 1.5 m s^{-1} on the East Sea and 0.5 – 0.8 m s^{-1} on the Gulf of Thailand. (DARD Ca Mau 2019).

At high tide of the East Sea, eroded sediments are carried into rivers and canals. When this tide meets the high tide of the Gulf of Thailand, it causes “interferential tidal waves”, rarely found elsewhere in the world. Under these conditions, the water literally stops flowing and sediments are accumulated at a much higher rate than at any other place. (Hong and Sam 1993).

3.1.4. Soil

There are five main soil categories in Ca Mau (DARD of Ca Mau 2019):

- Sandy soil: Cover an area of 671 ha, distributed in Ngoc Hien district.
- Saline soil: Cover an area of 212,877 ha (39.95% of the natural area), distributed in many areas in Dam Doi, Phu Tan, Tran Van Thoi.
- Acid sulfate soil: Cover an area of 279,928 ha (52.53% of the natural area), distributed mainly in U Minh, Tran Van Thoi, Ngoc Hien and Nam Can districts.
- Peat soil: Cover an area of 8,903 ha, distributed mainly in Melaleuca forest (indigo forests) area (U Minh Ha National park). However, after the fire of Melauleuca forest in 1982 and 2002, the area of thick peat layer was reduced so much, there are only about 5,000 ha.
- Mudflat soil: Cover and area of 12,193 ha, mainly distributed in the southwest of Ngoc Hien, Nam Can and Phu Tan districts.

3.1.5. Forest types

There are three main forest types in the province: (i) mangrove forests in Ngoc Hien, Nam Can, Dam Doi, and Phu Tan districts; (ii) Melalaeuca forests (indigo forests) in areas with brackish water in the districts of U Minh, Tran Van Thoi, and Thoi Binh; and (iii) inland forests in Hon Khoai, Hon Chuoi, and Hon Da Bac.

Natural mangrove forests are largely existed in this area. Total mangrove area in Ca Mau as of 2020 is 1.7 thousand ha (of which, 23% is natural mangroves), accounted for 35.4% of total mangrove of the whole country (MARD 2020). A total of 22 mangrove species have been discovered in Ca Mau province with dominant species of *Rhizophora apiculata*, *Avicennia alba*, *A. officinalis*, *A. marina* and *Bruguiera parviflora*.

This is one of the important sites of Vietnam's national biodiversity conservation program. Mui Ca Mau National Park (of Ngoc Hien and Nam Can districts) with an area of 41,861 ha, of which forest and mangrove forests area is 15,262 ha, is a natural mangrove ecosystem (estuarine ecosystem). U Minh Ha National Park (of U Minh and Tran Van Thoi districts) with an area of 8,527 ha, is the ecosystem of alum Melaleuca forests (indigo forests). Both national parks have high values of biodiversity, natural landscape, and environment and have been recognized by UNESCO as World Biosphere Reserve. (DARD Ca Mau 2019).

The secondary succession of mangroves in Ca Mau is considered typical for the Mekong Delta region and the regenerative process of secondary succession of mangroves is best illustrated by observing the stretches of forests in this area (Hong and San 1993). Because of the above characteristics, natural mangrove stands (coastal protection forests) are selected as the study subjects. It is considered that the natural distribution patterns and adaptation of natural mangrove stands should reflect the natural responses to coastal disturbances better than plantation forests.

Ca Mau province belongs to the low-lying delta in the southwest of the Mekong Delta. Under the influence of the northeast monsoon, the water currents carry fine-grained sedimentary materials from the upstream of the Mekong River system to create coastal alluvial flats suitable for the development of mangroves in the province. The ecological conditions are also favourable for the extensive development of mangroves (Hong and San 1993). In addition, Ca Mau is near the Indonesia and Malaysian archipelagoes, the places of origin for mangrove species. Due to warm streams and

south-west winds which carry saplings and seedlings to this area, together with the tropical monsoon climate, the composistion is rich and the tree sizes are the largest in the country (Hong and San 1993).

3.1.6. High tide and wind disturbances

High tides combined by wind, whirlwind, hurricane and salinity intrusion often occur in most coastal provinces of the Mekong Delta. Whirlwind occurs abnormally, blowing off houses, trees, and agricultural crops such as young rice and vegetables. High tides together with northeast winds usually occur once every 5-7 years, causing sea level rises, plus heavy rains to overflow embankments in the fields, causing significant damages to agricultural and aquaculture production. The summary results of the damages in Nam Can and Ngoc Hien districts show (DARD Ca Mau 2019):

- From 2010 to 2014:

▪ Ngoc Hien District: High tides on 18 and 19 October 2012 with the highest water level in history damaged 200 ha of land and 234 households.

▪ Nam Can District: The most affected communes were Dat Moi, Ham Rong, Tam Giang Dong, Lam Hai, Hiep Tung, and Nam Can town. Due to high tides, waters broke some embankments of shrimp ponds along the rivers (188 m); overflew over 1,000 m; the total area of shrimp farming was damaged over 11,000 ha, estimated the damage of nearly 2 billion.

- 2015: The tide rised unusually, particularly in the first months of the year (Lunar New Year) and at the end of the year as of November (maximum tide level in Nam Can on 14 February 2015 and 28 November 2015 were 1.65 m and 1.66 m, respectively). High tides combined with northeast winds to overflow the embankments, breaking them causing heavy damage to two districts of Nam Can and Ngoc Hien, in which:

▪ Nam Can District: On 11 February 2015, there were 20 broken embankments of about 559.5 m (including 299.5 m of bank break), affecting 86 ha of aquaculture land, causing damage of 1,350 million VND. On 28 November 2015, 11 overflown sections of about 599.3 m were broken (including 47 m of the embankment), affecting 9.1 ha of aquaculture land, causing damage of 70 million VND.

▪ Ngoc Hien District: 27 overflown sections of about 11,616 m were broken at both times (in which the embankment broke 206 m), affecting 303 ha of aquaculture, causing damage to 1,850 million VND.

- 2016: According to the water level monitoring in Nam Can, the maximum tide level on 8 February 2016 was 1.65 m and on 16 November 2016 was 1.69 m, the water has overflowed, breaking embankments causing severe damages to the two districts, of which:

▪ Nam Can District: On 8 February 2016, there were 16 broken overflow sections with about 429.5 m (including 104 m of concrete roads, 87.5 m of the embankment) affecting 86 ha of aquaculture land, causing damage of 2,096 million VND. On 16 November 2015; there were 11 overflow sections of about 599 m broken (of which the embankment break of 47 m), affecting 9.1 ha of aquaculture and lost 70 million VND.

▪ Ngoc Hien district: Both times had 32 overflow breaks of about 7.285 m (in which the embankment break of 205 m, affecting 172 ha of aquaculture and lost 1.728 million VND.

3.1.7. Coastal accretion and erosion

Ca Mau province is bordering the East Sea in the East, South and West. Under the influence of the northeast monsoon, the coastal currents carry fine-grained sedimentary materials from the upstream of the Mekong River system to create coastal alluvial flats suitable for the development of mangroves and coastal aquatic products in Ca Mau province. However, climate change has caused sea level rise, abnormal regimes of tide, wind and water currents, and loss or degradation of mangroves. In addition, hydropower dam construction and operation (keeping and discharging water) impacts the sediment budgets and sediment movement mechanism in Ca Mau province, altered erosion or accretion rates. The presence of dams may periodically increase or decrease water volume and sediment transport to the mangrove ecosystems depending on the region. Along the upper-middle and lowermost area reaching the Mekong River, the sediment flux was estimated to decline in the post-dam period of the Chinese dams, was estimated by Lu and Siew (2006).

The province has experienced an increase in both accretion and erosional areas in recent years (Tu et al. 2019; Bui and Bui 2020). Erosion and accretion, respectively, were mainly recorded at the East Sea (mean erosion rate of 33.24 m yr^{-1}) and the Gulf of Thailand an average accretion rate of 40.65 m yr^{-1}) from 1953 to 2011 (Thi et al. 2014). Since 2001, erosion was also detected in the western areas (coast of the Gulf of Thailand) of Ngoc Hien, Dat Mui commune, Phu Tan and Tran Van Thoi, and the sediment loss rate reached 15 m yr^{-1}, while Nam Can and Ngoc Hien have experienced strong accretion processes. From 2009 – 2017, the accretion area increased by 877 ha and the erosional area increased

by 140 ha in the province (Hien 2017). The shoreline changes reflected erosion and accretion processes occurred during different periods from 1903–2015 in the province were also mapped by Central Steering Committee for Disaster Prevention (2022) for monitoring and warning high risk of erosion or landslide areas (Figure 8). A recent increase in erosional and accretion processes resulted in the loss of mangrove forests of 8,870 ha in estuarine and coastal regions in the last ten years (SIWRP 2013).

3.2. Study sites

Seven study sites that met the following requirements were selected to conduct field survey:

i) Natural mangrove stands that have been protected as coastal protection mangrove forests;

ii) Representative sites for erosion or accretion

- Time scale (2017 as base year): New acrretion/erosion: The process has occurred less than or equal to 20 years; Long-term accretion/erosion: The process has occurred over 20 years.

- Intentisity of accretion or erosion: Slight: Shoreline change by accretion/erosion ≤ 20 m yr^{-1}; Strong: Shoreline change by accretion and erosion > 20 m yr^{-1}.

The time scales and intensity of accretion or erosion in the seven sites were: New and slight accretion (site A1); Long-term and strong accretion (site A2 and A3); New and slight erosion (site E1 and E2); Long-term and strong erosion (site E3); and New and strong erosion (site E4). Specific information of each site is described in Table 4 and their distribution is shown in Figure 7 and 8.

Table 4. Accretion or erosion processes in the study sites.

Site	Location	Accretion/erosion formed	Shoreline change by accretion (+) / erosion (-) (m yr^{-1})	Time scale/intensity
A1	Seaward side of Con Ngoai Ong Trang Island: NW bank, Cua Lon Estuary	Since 1980s	(+7.38) ± 7.61 (1992-2011) (*)	New and slight accretion site
A2	Seaward side of Con Trong Ong Trang Island: NW bank, Cua Lon Estuary	Since 1960s	(+48.69) ±3.01 (1979-2011) (*)	Long-term and strong accretion site
A3	Mui Ca Mau NP, at the boder between Gulf of Thailand and East Sea	Before 1953	(+44.74) ± 26.76 (1953-2011) (*)	Long-term and strong accretion site
E1	SE bank of Con Ngoai Ong Trang Island, Cua Lon Estuary	Since 2014	NA	New and slight erosion site
E2	SE bank of Con Trong Ong Trang Island, Cua Lon Estuary	Before 2004	NA	New and slight erosion site
E3	Mui Ca Mau NP, behind the sea dam	1940-1985	-40.8 (1998-2002) (**)	Long-term and strong erosion site
E4	Coastline of Gulf of Thailand, in front of sea dam	After 1998	(-10.28) ± 2.64 (1953-2011) (*)	New and strong erosion site

Data souce: Adapted from Linh et al. 2020; 2023; *Thi et al. 2014; **Lap and Oanh 2012. NA means Not Available data recorded.

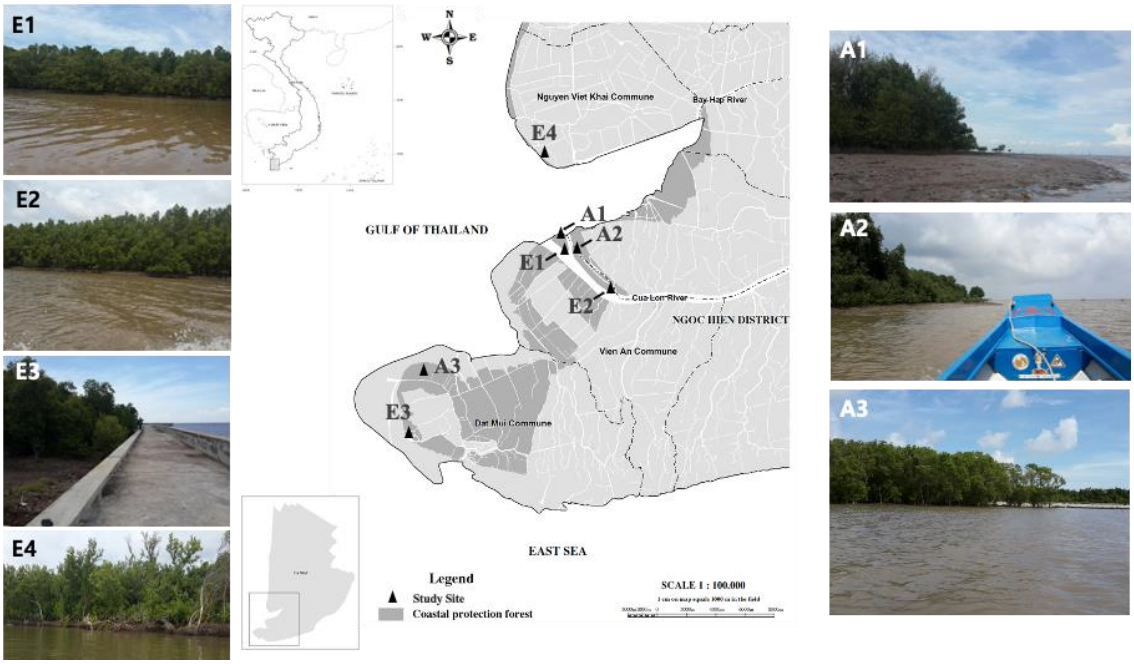

Figure 7. Map and photos of the study study sites in Ca Mau Province, Vietnam. Sites A1, A2, and A3 are accretion sites, and E1, E2, E3 and E4 are erosion sites.

Two accretion sites (A1 and A2) and two erosion sites (E1 and E2) are located on the northwest and southeast banks, respectively, of the Cua Lon Estuary in Nam Can (Figures 7 and 8). Of which, A1 and E1 were on Con Ngoai Ong Trang Island, and A2 and E2 were on Con Trong Ong Trang Island. Accretion and erosion have occurred in opposition between the two banks in the Cua Lon Estuary, in which, northwestern bank is accreted seawards, whereas erosion processes have occurred on southeastern banks on both Con Ngoai Ong Trang and Con Trong Ong Trang islands. Erosion on the SE bank (sites E1 and E2) was previously of little concern because the process of accretion and erosion between the two banks was balanced seasonally (rainy season and dry season). However, since 2004 for Con Trong Ong Trang and 2014 for Con Ngoai Ong Trang, a fine sediment budgets supplied to this area was reduced, together with changes in wind and water currents, causing erosion processes greater than accretion process in the SE banks regardless of the season (i.e., sediments input were less than sediments output). Shoreline was shrinking at both sites E1 and E2, of which the shoreline shrinking at site E2 was more clear, possibly due to longer time scale (Figure 8). No data on intensity of erosion was available for E1 and E2, however, actual observations and images of shoreline changes showed that the erosion processes had occurred for less than 20 years and intensity of erosion was not severe, thus E1 and E2 were considered new and slight erosion sites.

Site A3 and E3 were both loaced in Mui Ca Mau National Park. Accretion site A3 was located at the northwestern end of Mui Ca Mau NP, which was the border between the Gulf of Thailand and the East Sea and erosion site E3 was located in the southwestern part of Mui Ca Mau NP. The tide is irregular semi-diurnal on the East Sea and irregular diurnal on the Gulf of Thailand. At high tide of the East Sea, when this tide meets the high tide of the Gulf of Thailand, it causes “interferential tidal waves”, rarely found elsewhere in the world, together with northeast monsoon in dry season and southwest monsoon in raining season, sediments carried from southeast to northwest area and from Mekong River system to the south have been strongly accoumulated in site A3 for a long time. For erosion site A3, the increase in speed of the northeast monsoon when approaching the southeast coast of Ca Mau and without any protection of sea dam as nowsaday, sea currents caused severe erosion in this area. A concreted sea dam was built in 2011 to protect coastline erosion in site E3. The sea dam construction took place for many years, the part of the dyke passing through Mui Ca Mau NP was only really completed in 2016. Therefore, the erosion process has not been significantly limited in this area.

Erosion site E4 is located at Phu Tan district, coastline of Gulf of Thailand. This area has only experienced strong costal erosion since 1998. The main reason is due to sea level rise combined with high tide and strong flows of southwest winds in the rainy season, occurring at the same time. This area only has a very thin strip of natural mangrove forest, but plays a critical role in protecting the sea dyke right behind.

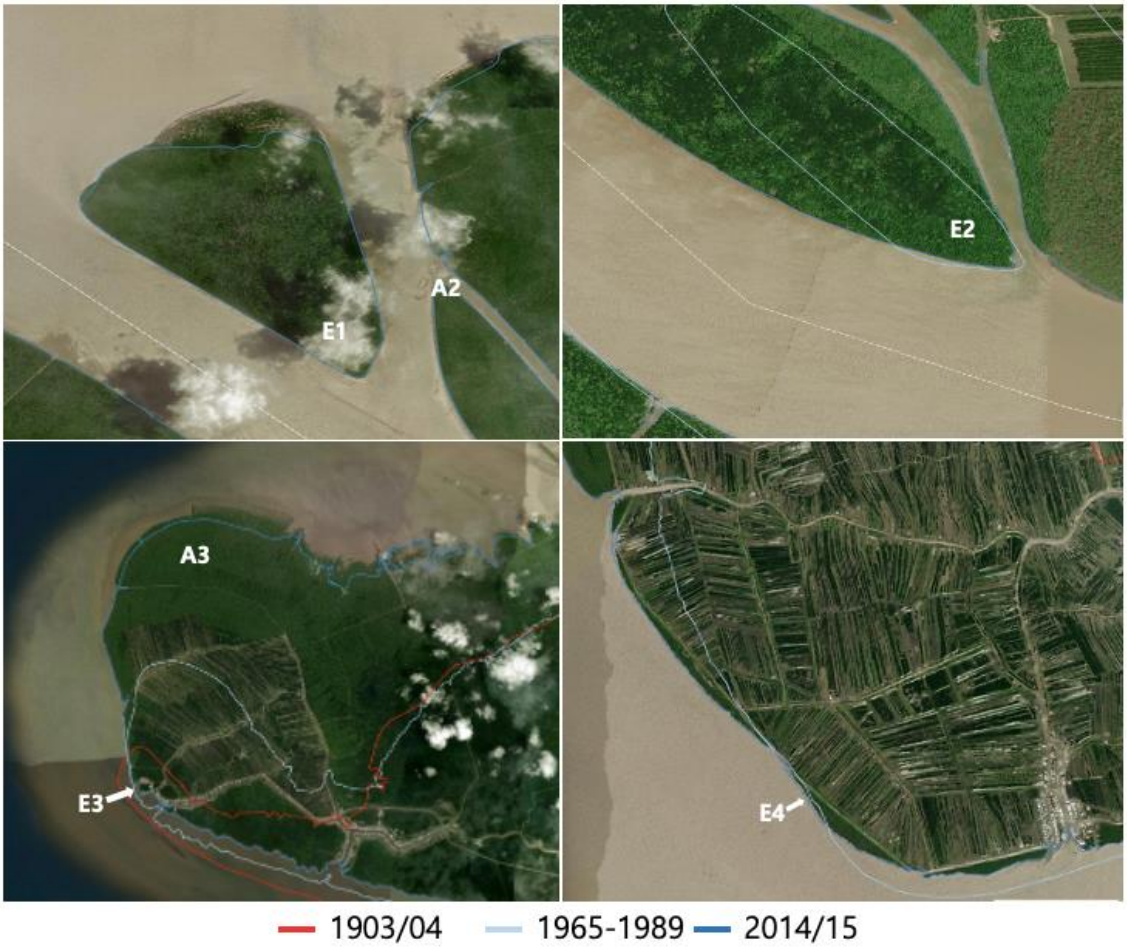

Figure 8. Map showing shoreline changes by accretion and erosion in different periods between 1903 and 2016 in the study sites. Sites A1, A2, and A3 are accretion sites, and E1, E2, E3 and E4 are erosion sites. (Source: Central Steering Committee for Disaster Prevention, 2022; URL: http://satlo.vndss.com/#11/8.7782/104.9335/c0).

3.3. Plot establishment and tree measurement

Three transect lines were installed inland from the starting edge of the closed canopy in the mangrove stand, perpendicular to the shoreline at each study site (Figure 9). Transect lines were parallel to each other and 100 m apart. Three 20 m x 20 m plots were established 30 m apart along the transect line from the seaward plot (S) through the intermediate (I) to landward plot (L) (Figure 9a).

Site E3 and E4 were located in two representative locations of strong erosion with natural mangroves existed and the mangrove stands were separated from the mainland by canals and creeks close behind. Although the remaining forest bands were narrow, research still had to be conducted to examine the distribution and adaptation characteristics of mangroves here. Hence, only two 20 m x 20

m plots (seaward and intermediate) of each transect line were designed for site E3 and site E4 (Figure 9b). A total of 57 plots of 7 sites were used for the measurement.

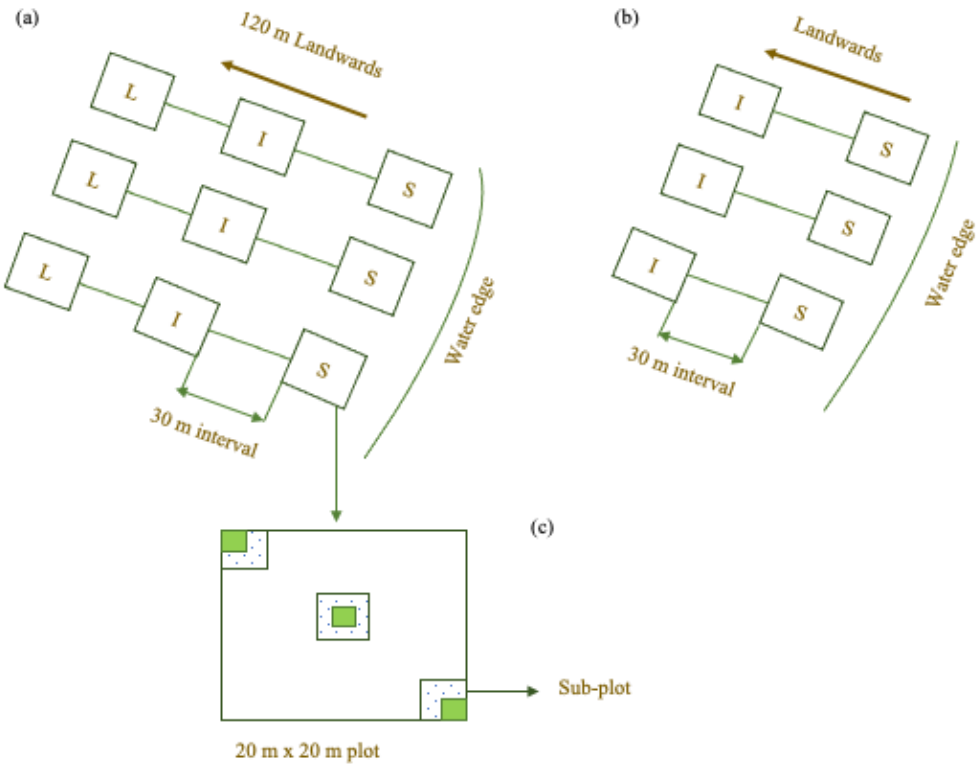

Figure 9. Diagram of plot and sub-plot design. (a) Plot design of site A1, A2, A3, E1 and E2. (b) Plot design of site E3 and E4. (c) Sub-plot design of each 400 m^2 plot.

The geographic coordinates of each plot were recorded at the starting point of the plot using a GPS receiver accurate to within 5 to 10 meters (GPSMap 76CSx, Garmin, Olathe, Kansas, USA). GPS location of plots was imported in Google Earth Pro to check. Some plots detected too far from the shoreline to the sea or too more inland were relocated. Latitude and Longitude of each plot verified by Google Earth Pro was shown in Appendix 2.

Mangrove trees with DBH (diameter at breast height) ≥ 6 cm were considered overstory trees. Species name, stem DBH, and height were recorded for all trees with DBH ≥ 6 cm within a 20 m x 20 m plot.

- The DBH was measured at 1.3 m above the ground. For *Rhizophora apiculata* with a root height exceeding 1.3 m above the ground, DBH was measured at 20 cm upper point of the highest stilt root (Ohira et al. 2013).

- Height was measured from the soil surface to the top of tree, using a vertex laser hypsometer or Blume-Leiss equipment.

- X, Y coordinate of individual trees was measured: X – distance to horizontal axis of plot (m) and Y – distance to vertical axis of plot (m).

3.4. Understory tree measurement

Understory trees mentioned seedlings and saplings. Mangrove trees with a height ≥ 50 cm and DBH < 6 cm were considered saplings, and mangroves with a height < 50 cm were considered seedlings (Tan 2008; Linh et al. 2020).

Three subplots were established diagonally within a 400-m^2 plot (Figure 9c). A total of 171 subplots were used for measuring saplings and seedlings. Almost plots used 2m x 2m subplots. Some plots 1m x 1m and 10m x 10m subplots due to lack of agreement on implementation methods among survey groups. This is a methodological limitation of the study. To deal with it, the investigation data of suplots were analyzed to ensure the correct area of investigated subplot. Number of trees by species and tree height of all seedlings and saplings were measured in investigated subplots and estimated per one hecta (density ha^{-1}).

3.5. Aerial root measurement

3.5.1. Aerial root types

Aerial root systems is one of unique characteristics that enables mangroves to survive in mangrove swampt habitat. Aerial roots have different names and different morphologies depending on specific species and living conditions. In study sites, three main aerial root types were detected: stilt roots, pneumatophores, and knee roots. The identification morphology of these roots are as follows:

Stilt roots normally arise from basal nodes in the main stem and grow downward to the soil. Stilt roots were found mostly in *Rhizophora* (Figure 10a, 10b). This type of root is also known as prop roots with the role as anchor and respiratory support because it contains lenticels on the roots.

Avicennia and *Bruguiera* could develop additional stilt roots in a few cases, especially when they were in danger of losing their anchorage. Some *Avicennia* were found to develop stilt roots at erosion

sites in the study area (Figure 10i, 10m). Some stilt roots did not reach the soil surface, hanging in the air. We defined those roots as aerial stilt roots in this study. *Rhizophora apiculata* developed aerial stilt roots from the upper part of the stem above the point of branch separation at erosion sites (Figure 10j). These aerial stilt roots were emerged from lateral roots for extra support for respiration to survive on tide-washed, soft and anaerobic substrates that hindered the exchange of dissolved oxygen in the soil (Gill and Tomlinson 1977).

Figure 10. Photographs of aerial root types at the study sites. Stilt roots (a, b) and knee roots (c) of *Rhizophora apiculata*. Pencil-like pneumatophore roots of Avicennia sp. (d, e) and cone-like pneumatophore roots of Sonneratia spp. (f). Knee roots of *Bruguiera* spp. (g, h, i). Aerial stilt roots of *Rhizophora apiculata* (j) and Avicennia sp. (i, m) at an erosion site. Branched pneumatophore roots of Avicennia spp. (k) at an erosion site.

Pneumatophores vertically arise from the horizontal roots under the soil surface. Among the mangroves with pneumatophores at the study sites, *Avicennia* had pencil-like pneumatophores that are called pencil roots (Figure 10d, 10e). *Avicennia* species prefers growing in oxygen-poor sediments supported by pencil-like pneumatophores with numerous lenticels that enable gas exchange directly above the surface (Hogarth 2015). Another pneumatophores was cone-like pneumatophores detected in *Sonneratia* (Figure 10f). *Sonneratia alba* showed limited distribution on narrow banks or was sparsely distributed along the riverside at the study sites.

Pneumatophores were usually not branched, but nevertheless, branched pneumatophores were found at erosion sites (Figure 10k). A branched pencil root was defined as a pencil root with a secondary root developed from the main root.

Knee roots grow vertically from the horizontal roots just below the soil surface and immediately loop downward, which resembles a bent knee. The knee roots were typical aerial root types of *Bruguiera* (Figure 10g, 10h, 10i). Some of the stilt roots of *R. apiculata* occasionally developed knee roots (Figure 10c).

3.5.2. Measurement of stilt roots

The number of primary stilt roots of *Rhizophora apiculata* were counted for all trees with DBH ≥ 6 cm within 400 m^2 plots. We counted the number of primary roots that were the main roots that grew

from the trunk for each tree (Ohira et al. 2013) and measured the highest point (m) of stilt root attachment on the trunk from the ground (aboveground stilt root height hereafter) in a 400 m^2 plot.

Three 1m^2 subplots were established in each plot (Figure 9c). All stilt roots above the surface in the 1 m^2 subplot were cut and transported to the laboratory for measuring root dry mass. Roots were oven-dried at 70°C until the weight was constant and root biomass was estimated.

3.5.3. Measurement of pneumatophores and knee roots

Pencil-like pneumatophores were found under *Avicennia alba, Avicennia marina* and *Avicennia officinals* at the study sites. The roots of *A. marina* usually appeared larger, and the diameter was similar between the ground and root top, resulting in a tube-like shape. In contrast, the roots of *A. alba* appeared smaller than those of *A. marina*, and the diameter decreased as height increased to the root top, similar to a pencil shape. However, their roots were too similar to distinguish separately on the mud floor. Therefore, we treated them as pneumatophores of *Avicennia*.

Each plot included three 1 m x 1 m subplots for root measurement (Figure 9c). The same 1 m^2 subplots that were used for stilt root dry mass estimation were used for pneumatophore and knee root measurement. We counted the number of roots and estimated the density of roots over the ground for all pneumatophores and knee roots. All pneumatophore and knee roots above the surface within 1 m^2 m subplots were also cut, collected and transported to the laboratory for measuring root dry mass. In this study, we only considered aboveground root biomasses. Roots were separated by root type and species and dried at 70°C until the root weight reached a constant value and root biomass was estimated.

3.6. Soil sampling and measurement

The elevation of each plot was recorded from the field, at the seaward starting point of the plot using a GPS receiver accurate to within 5 to 10 meters (GPSMap 76CSx, Garmin, Olathe, Kansas, USA). GPS location of plots was imported to Google Earth Pro to check. Some plots were recorded too far from the shoreline either seaward or landward due to GPS errors, thus GPS locations were modified using Google Earth Pro (Appendix 2).

Using the subplots for root measurement, a total of 171 soil samples (3 plots x 3 subplots x 3 replications for 5 sites and 2 plots x 3 subplots x 3 replications for 2 sites) were collected from late April to early May 2017 during the transition period between the rainy and dry seasons. Previous studies in

Ca Mau showed that soil pH and salinity are subject to seasonal variations (Khiem 2012; Thao 2017). Soils were sampled at a 20 cm depth at the center of each subplot and transported to the laboratory of Ca Mau Technical Center of Standards Metrology and Quality for measuring soil moisture, soil bulk density, and total organic carbon. Soil pH and salinity were directly measured in the field at each subplot using a portable pH meter (HI-8314, Hanna Instruments, Cluj-Napoca, Romania) and a refractometer (U-10, Horiba, Kyoto, Japan), respectively. The depth of 20 cm was considered since there was the most variation in mangrove soil and it could reflect the impacts of accretion and erosion over time (Sukristijono 1994).

Soil samples for soil bulk density and soil moisture content were collected using 100 cm^3 volume metal containers. Soil samples were oven-dried at 105°C until the weight was constant, and the soil bulk density and soil moisture content were calculated. The total soil organic carbon content (TOC, %) was estimated using TCVN 8941:2011 (National standard of Vietnam) based on the Walkley Black method (MOST 2011; FAO 2020).

3.7. Data Analysis

3.7.1. Relationship between elevation and soil properties

The relationship between elevation and soil properties were analyzed using Spearman's rho. Shapiro-Wilk normality was used for normality test and some of variables were normally distributed, thus non-parametric correlation analysis was used. SPSS platform (v. 25, IBM SPSS Inc. Chicago, IL, USA, 2017) were used for the analysis. Significance was set at $p < 0.05$.

3.7.2. Mangrove stand structure

3.7.2.1. Overstory trees

Species richness, density (number of trees per hectare), species composition, DBH distribution, height distribution and spatial distribution of trees were compared between accretion (A1, A2, A3) and erosion (E1, E2, E3, E4) sites and among seaward, intermediate and landward plots.

Species richness was counted as the total number of different species. Species composition of each plot was examined using the importance value (IV, %) which is the sum of relative density, relative coverage, and relative frequency of a species (Curtis and McIntosh 1951). Coverage was calculated using stem basal area at 1.3 m.

The histogram of the number of trees by DBH classes, species, plots and sites were made for DBH distribtuion. DBH was classified as 8 classes: I: 6-10 cm; II: 10-15 cm; III: 15-20 cm; IV: 20-25 cm; V: 25-30 cm; VI: 30-35 cm; VII: 35-40 cm; VIII: ≥ 40 cm (5 cm intervals). The N-H distribution of height trees was analyzed using the histogram of the number of trees by height classes, species, plots and sites. Height was classified as 5 classes: I: < 3 m; II: 3-5 m; III: 5-7 m; IV: 7-9 m; V: > 9 m (2 m intervals).

Spatial distribution were shown using *ggplot* function in R (R version 3.4.4 and Rstudio version 1.1.442). Point spatial distribution used X, Y coordinate (X – distance to horizontal axis of plot, Y – distance to vertical axis of plot) to simulate distribution of individual trees by species on forest floor by point markers. Aggregation levels determined distribution patterns: Random, Aggregated, or Regular (Mariem 2021):

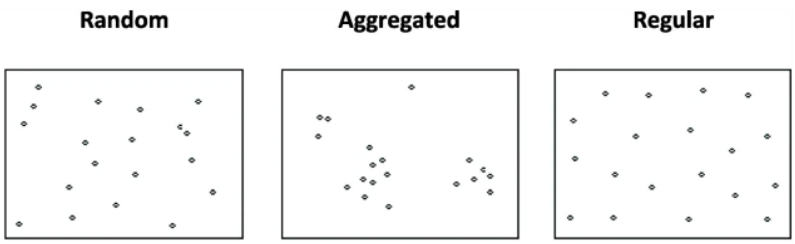

3.7.2.2. Understory tree

Species richness, species composition, density (number of stems per hectare), height distribution and number of trees higher than mean height of understory trees were compared between accretion and erosion sites and among seaward, intermediate and landward plots.

Species composition of seedlings and saplings for each plot was examined using composition coefficient (k_i):

$$k_i = \frac{n_i}{\mathrm{m}} x10$$

In which: k_i: Composition coefficient of species i

n_i: Number of individuals of species i

3.7.2.3. Aerial root analysis

Differences in root density and biomass among plots at accretion and erosion sites tested using one-way ANOVA and Schéffe test for post hoc comparisons. Two-way ANOVA was used to compare the number of primary roots per tree and the highest root height of stilt roots, density and biomass of pneumatophore roots, and biomass of knee roots among seaward, intermediate and landward plots and sites. Schéffe test was conducted for post hoc comparisons. Significance was set at $p < 0.05$. The Spearman's rho correlation was used to analyze the relationship among density and biomass of root types, elevation and soil characteristics. Data was analyzed in SPSS platform (v. 25, IBM SPSS Inc. Chicago, IL, USA, 2017).

Chapter 4. RESULTS AND DISCUSSION

4.1. Elevation and soil properties at accretion and erosion sites

4.1.1. Elevation at accretion and erosion sites

At accretion sites, mean elevation was -2.89±0.63 m asl and gradually increased from seaward to landward as-3.0±0.71 m in seaward plots, -2.89±0.60 m in intermediate plots, and -2.78±067 m in landward plots. The elevation significantly changed among seaward, intermediate and landward plots ($p < 0.05$).

Mean elevation at erosion sites was 2.43±3.80 m, significantly higher than that at accretion sites ($p < 0.05$). The change in elevation showed significance between intermediate plots and landward plots only ($p < 0.05$). It slightly increased from seaward plots (1.5±3.26 m) to intermediate plots (2.33±3.78 m) and dramatically went up to landward plots (4.5±4.68 m). The standard deviations of elevation values at erosion sites was very high, reflecting a large variation between specific sites (Figure 11b), might be affected by different disturbances of erosion process.

Mean elevation at all accretion sites (A1, A2, A3) was lower than sea level. Site A2, a new and slight accretion site, showed the most clearly the significance in elevation increase to landward plots (Figure 11a). In contrast, except site E1, mean elevation at all erosion sites (E2, E3, E4) was above sea level (Figure 11a).

Elevation has strong correlation with flooding and tidal amplitude (i.e., negative correlation) leading to variation in physic-chemical conditions then effecting the distribution patterns of mangrove species (Boto and Wellington 1984; McKee 1996; Kitaya et al. 2002).

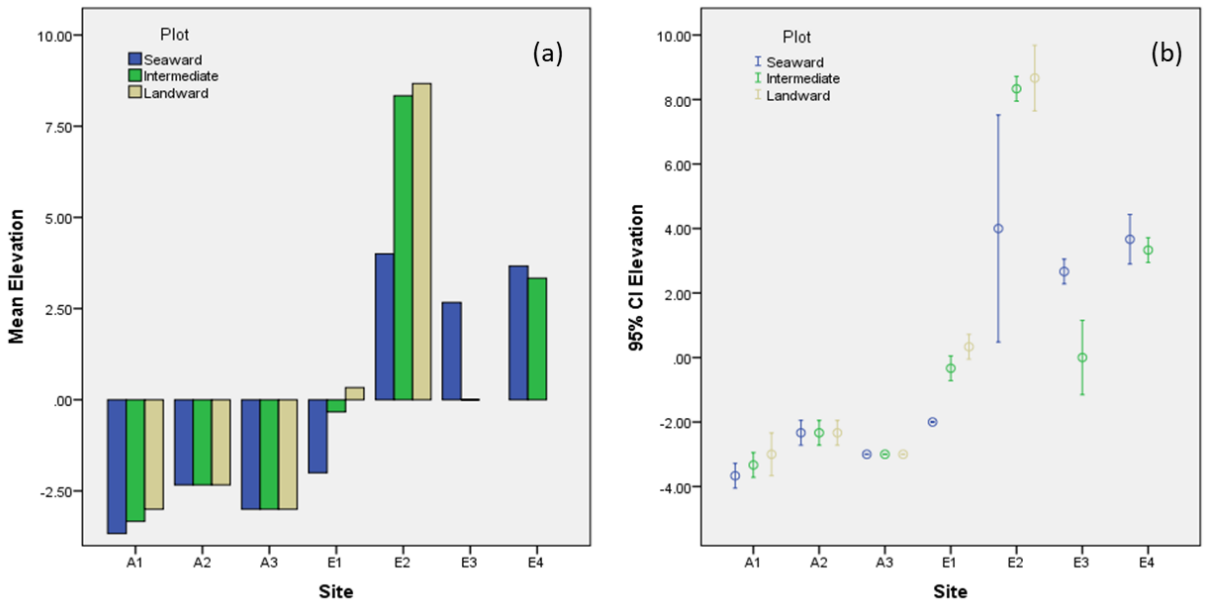

Figure 11. Mean elevation (m) (a) and standard deviation of mean elevation (b) in seaward, intermediate and landward plots at accretion (A1, A2, and A3) and erosion (E1, E2, E3 and E4) sites.

Site E1 had below sea level elevation in seaward and intermediate plots and above sea level elevation in landward plots. The trend of increasing elevation landwards at erosion sites was seen most clearly at site E1 and E2, both new and slight erosion sites. Site E3, a long-term and strong erosion site, had a sudden drop in elevation when entering the intermediate position. possibly due to the phenomenon of coastline erosion being gradually improved, supported by a concrete sea dyke and need more time to affect the interior. Elevation at site E4, a new and strong erosion site was almost similar between seaward and intermediate plots.

4.1.2. Soil properties at accretion and erosion sites

Apart from climate (temperature, rainfall, storms), hydrology (tides, currents, sea level), geomorphology (sediments, catchment size, slope), soil is a critical factor in mangrove study and therefore have received much research attention. Soil salinity and soil nutrient was indicated as important external factors impacting succession of mangroves (Lugo 1980). Basic soil properties consisting of particle size distribution, bulk density, total carbon, extractable Nitrogen and Phosphorus, soil redox potential, pH and salinity were examined in relation to mangrove forests in Northern Australia (Boto and Wellington 1984). Salinity, soil chemistry properties and nutrient content were identified as natural-induced disturbances on mangrove structure, function and distribution at zonal scale (Alongi 2002). In

short, majority of previous studies preferred focusing on evaluating important physic-chemical conditions affecting mangrove seedling or propagule establishment and survival. The typical factors were consider the most such as salinity, pH, bulk density, nutrient, total carbon and soil redox (e.g., Lugo 1980; Boto and Wellington 1984; Alongi 2002; McKee 1996; Delgado et al. 2001; Krauss et al. 2008).

Majority of soil studies in Ca Mau province were conducted at Con Trong Ong Trang (Ngoc 2011, Thao 2017) and Con Ngoai Ong Trang (Tan 2008). Soil properties impacting mangrove establishment, distribution and structure were studied including salinity, pH, bulk density, organic matter, soil texture, soil maturity, and Eh (Tan 2008; Ngoc 2011; Thao 2017).

Soil pH, salinity, bulk density, total organic carbon and moisture in the study sites were illustrated using box plots in Figure 12. Soil in both accretion and erosion sites was characterized as alkaline soil. Mean pH at accretion sites was 6.86±0.27, higher than mean pH at erosion sites (6.76±0.33) but did not show significance ($p > 0.05$). Soil pH also not significant changed between seaward (mean 6.84±0.25), intermediate (mean 6.76±0.22) and landward plots (mean 7.01±0.29) at accretion sites ($p > 0.05$). Soil at erosion sites had a significant increase from seaward (mean 6.74±0.37) to intermediate (mean 6.71±0.32) ($p < 0.05$) and a slight increase landwards (mean 6.87±0.28). Soil pH looked similar among all sites regardless of accretion and erosion sites, except site E4, a new and strong erosion site (Figure 12a). Site E4 had a lower pH value than other sites.

Soil pH resulted from the study is slightly lower than some other studies, however, it is still in a normal range of distribution condition of mangrove forests. Soil pH in mangrove distribution area was estimated 6.2 – 7.0 in Northern Australia (Boto and Wellington 1984), 5.8 – 6.85 in the Caribbean Coast of Colombia (Cardona and Botero 1998), 6.7 – 7.0 at Rookery Bay in South-west Florida (USA) (McKee 1993), 7.0 – 7.9 at Lothian Island of the western Sundarbans, India (Joshi and Ghose 2003), or much higher soil pH with mangrove forest distributed found in Southern Japan (Wakushima et al. 1994). In comparison to previous studies conducted at the same study sites, average soil pH was estimated as 6.89 by Ngoc (2011), 7.25 by Thao (2017) and 7.1 by Tan (2008). Soil pH got the highest at the beginning muddy bank then decreases at the middle area and increase again at longer distance area due to fall in number of inundated days (Thao 2017; Khiem 2012; Tan 2008).

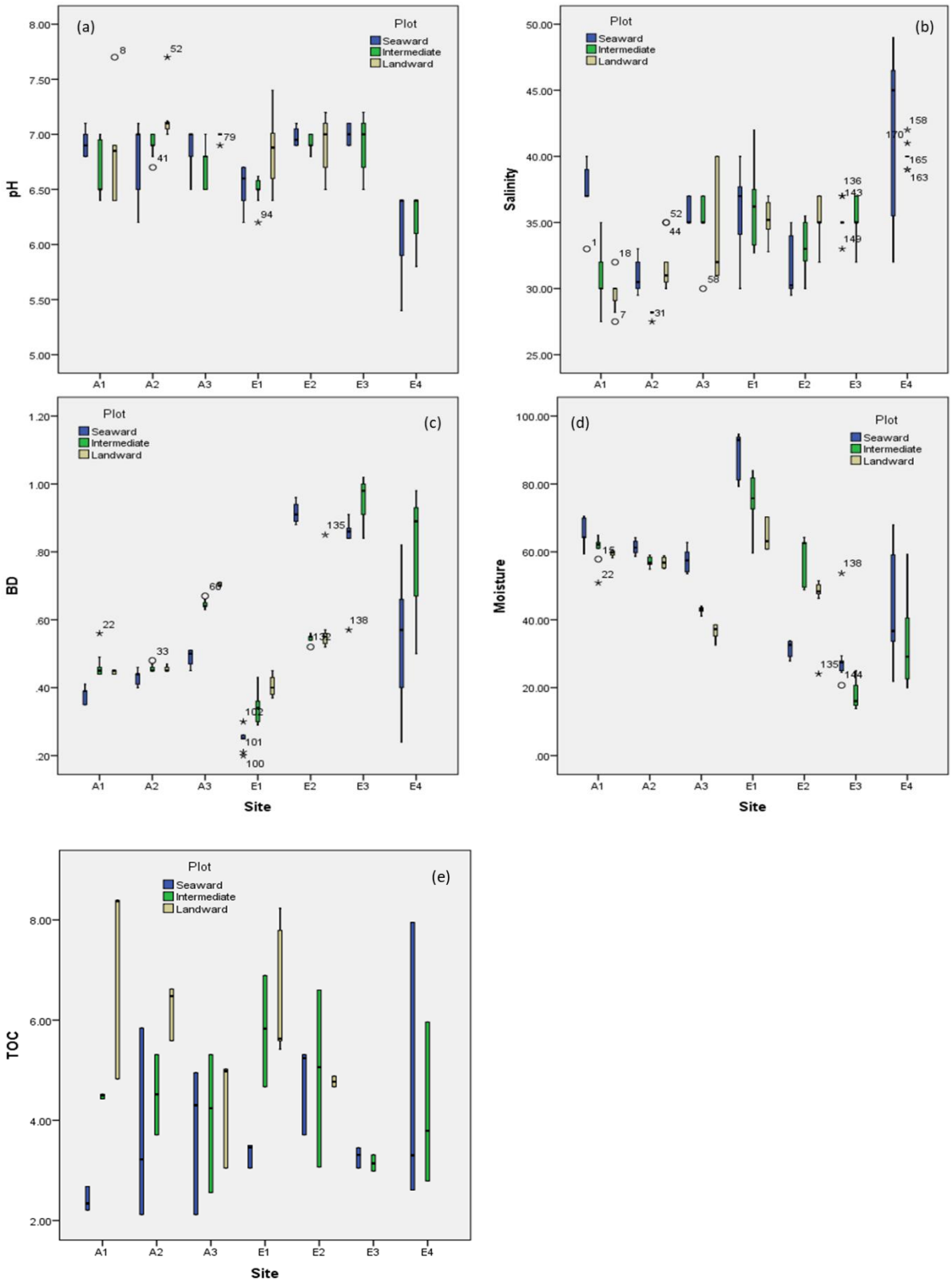

Figure 12. Soil properties from field measurements. Box plots of (a) soil pH, (b) soil salinity (‰), (c) soil bulk density (BD, g cm^{-3}), (d) soil moisture (%), (e) soil total organic carbon content (TOC, %) in seaward, intermediate and landward plots at accretion (A1, A2, and A3) and erosion (E1, E2, E3 and E4) sites.

Almost mangrove species has an optimum pH range which relating the community structure and species distribution of Sundarbans mangroves in India (Joshi and Ghose 2003). Soil pH may be influenced by plant activities (e.g., leaf shoot appearance and root exudates) which was indicated less variable (6.2 – 6.6) during high activity period of plant (Boto and Wellington 1984). A little bit different results of soil pH were also reported by (Joshi and Ghose 2003) for Sundarbans mangroves in India (i.e., the average soil pH was slightly alkaline ranging from 7.05 to 7.89). Also following Joshi and Ghose (2003), there is no clear change uniform in soil pH along the distance from the tidal coast.

Soil salinity at accretion sites (mean 32.78±3.63 ‰) was significantly lower than that at erosion sites (mean 36.06±3.84 ‰) ($p < 0.05$). The significant variation of salinity occurred from seaward to intermediate regardless accretion and erosion sites ($p < 0.05$) but in opposite trend (i.e., decreased from mean 34.70±3.13 ‰ at accretion seaward plots to mean 31.34±3.52 ‰ in intermediate plots but increased from 36.14±5.13 ‰ at erosion seaward plots to mean 36.30±3.22 ‰ in intermediate plots). This property slightly different in landward plots in both accretion and erosion sites (i.e., mean 32.55±3.44 ‰ in accretion landward plots and mean 35.42±1.49 ‰ in erosion landward plots). In contrast to soil pH, the soil salinity at site E4 looked much higher than the other sites (Figure 12b).

Soil salinity is commonly seen going with pH as an important couple factor of soil conditions in mangrove wetland. They were assessed determining species distribution by zones which divided into seaward zone, meso zone and landward zone through affecting salinity and pH species tolerances (Wakushima et al. 1994). Also relied upon tolerance of mangrove species to salt stress, species response along gradients of soil salinity and nutrient over time was simulated (Chen and Twilley 2002). However, if soil pH did not show much variation, soil salinity in mangrove distributed condition presented a wide range of value in other studies. It was from 30 – 50 ‰ in Northern Australia (Boto and Wellington 1984) and the same at Rookery Bay in South-west Florida (USA) (McKee 1993), 19.8 – 40.2 ‰ in the Caribbean Coast of Colombia (Cardona and Botero 1998), 32 – 34% in Southern Japan (Wakushima et al. 1994), and 13 – 31.2 ‰ at Lothian Island of the western Sundarbans, India (Joshi and Ghose 2003). In general, soil salinity resulted by the study indicated a normal value compared to other study.

This result slightly differred in variation tendency of soil salinity by distance to the sea which was gradual rise illustrated in previous studies (Thao 2017; Khiem 2012; Tan 2008; and Joshi and Ghose 2003) (i.e., initial increase of soil salinity was seen with increasing distance and decrease then). It could be explained due to differences in position of soil sampling and soil condition at specific intensity and time scale of accretion and erosion process.

Soil bulk density at accretion sites (mean 0.4965±0.103 g cm^{-3}) showed a significant lower value than that at erosion sites (mean 0.6138±0.255 g cm^{-3}). This property also significantly varied between seaward, intermediate and landward plots regardless accretion and erosion sites ($p < 0.05$). At accretion sites, soil bulk density gradually increased associated with the increase in elevation reflecting the gradual stable substrate from seaward plots toward landward plots (i.e., increased from mean 0.4322±0.05 g cm^{-3} in seaward plots to mean 0.5220±0.091 g cm^{-3} in intermediate plots to mean 0.5354±0.122 g cm^{-3} in landward plots). Mean value of soil bulk density also significantly increased from seaward plots to intermediate plots but significanly decreased in landward plots (i.e., increased from mean 0.6331±0.289 g cm^{-3} in seaward plots to mean 0.6585±0.256 g cm^{-3} in intermediate plots then decreased by mean 0.4931±0.112 g cm^{-3} in landward plots). Soil bulk density between accretion sites (A1, A2, A3) looked less variation compared to that between erosion sites (E1, E2, E3, E4) (Figure 12c). Site E1, a new and slight erosion site, was likely lower soil bulk density compared to other sites and site E3, a long-term and strong erosion site, was likely higher soil bulk density compared to other sites.

Mean value of soil bulk density in accretion sites are likely similar to distribution condition of mangrove forests in Northern Australia with soil bulk density 0.38 – 0.45 g cm^{-3} (Boto and Wellington 1984). This property was found much varied from 0.176 – 0.742 g cm^{-3} in the mangrove area of Caribbean Coast of Colombia (Cardona and Botero 1998), cover the mean values of soil bulk density in both accretion and erosion sites of the study.

Result of bulk density in depositional soil is associated with Thao (2017) in terms of variation tendency which is gradual rise from the sea going inside. This author was also asserted positive relation between soil bulk density and land surface elevation which corresponding with analysis result of this study mentioned below. This relation could be used to explain opposite scenes on change in soil bulk density by transect line due to contrary variation of relative elevation between depositional and erosional sites.

Soil moisture content at accretion sites (mean 53.38±9.27 %) was significantly much higher than that at erosion sites (mean 48.92±23.05 %) ($p < 0.05$). This property also showed a significant variation between seaward, intermediate and landward plots. Soil moistured dramatically decreased from seaward plots (mean 61.53±4.54 %) to intermediate plots (mean 53.59±8.26 %) and to landward plots (mean 51.01±10.62 %). Similarly, soil moisture in erosion landward plots (mean 46.34±18.93 %) was lowest value but it got highest value in intermediate plots (mean 50.61±21.91 %). Mean value of soil moisture at erosion sites had a high standard deviation might be due to some outliers found at site E3 (Figure 12d).

Soil moisture content in mangrove distribution condition was not much studied, it varied from 10% (in more mineral sediments, inundation during late dry season) to 70% (highly organic sediments, regularly flooded by tides) (Ball 1998).

Total organic soil carbon of accretion sites (mean 4.53±1.69 %) was significantly higher than that of erosion sites (mean 4.52±1.51 %) ($p < 0.05$). However, this property showed insignificance between seaward, intermediate and landward plots in both accretion and erosion sites ($p > 0.05$). In general, total organic carbon gradually increased toward landward plots (i.e., from mean 3.31±1.39 % in accretion seaward plots to mean 4.34±0.83 % in accretion intermediate plots to mean 5.93±1.74 % in accretion landward plots and from mean 3.99±1.49 % in erosion seaward plots to mean 4.51±1.52 % in erosion intermediate plots to 5.98±1.29 % in erosion landward plots). Total organic carbon at site E1, a new and slight erosion site, looked higher than other sites and that at site E3, a long-term and strong erosion site, looked lower than other sites (Figure 12e).

Much higher organic matter content was analyzed from study of Thao (2017) which is from 9.66 – 12.9% and the highest value is at the middle zone by transect line. It is explained because of the difference in sampling time. One of study purpose of Thao (2017) was litter fall decomposition which require sample to be collected at the highest period of litter fall causing rich value of organic matter.

4.1.3. Correlation between elevation and soil properties at accretion and erosion sites

According to the results of the Spearman correlation analysis (Table 5), soil salinity, soil bulk density and soil moisture had significant correlation with elevation ($p <0.01$). In which, soil salinity and soil BD were positively correlated with elevation, and soil moisture was negatively correlated with elevation. This means the soil salinity and soil bulk density increased as the elevation increased and soil moisture decreased as the elevation increased (Figure 13).

Table 5. Spearman correlation coefficients of elevation and soil characteristics.

	Elevation (m)	pH	Salinity (‰)	BD (g.cm^{-3})
Elevation (m)				
pH	0.046			
Salinity (‰)	0.244**	-0.052		
BD (g cm^{-3})	0.366**	0.337**	0.075	
Moisture (%)	-0.323**	-0.350**	-0.107	-0.928**
TOC (%)	0.111	-0.055	-0.265**	-0.084

**: Correlation is significant at the 0.01 level (2-tailed). BD: Bulk density, TOC: Total organic carbon.

Even though soil pH and total organic carbon did not show a significant correlation with elevation, they significantly affected other soil properties. There was a positive significant correlation between soil pH with soil bulk density but negative significant correlations between soil pH and soil moisture and between soil total organic carbon and soil salinity ($p < 0.01$).

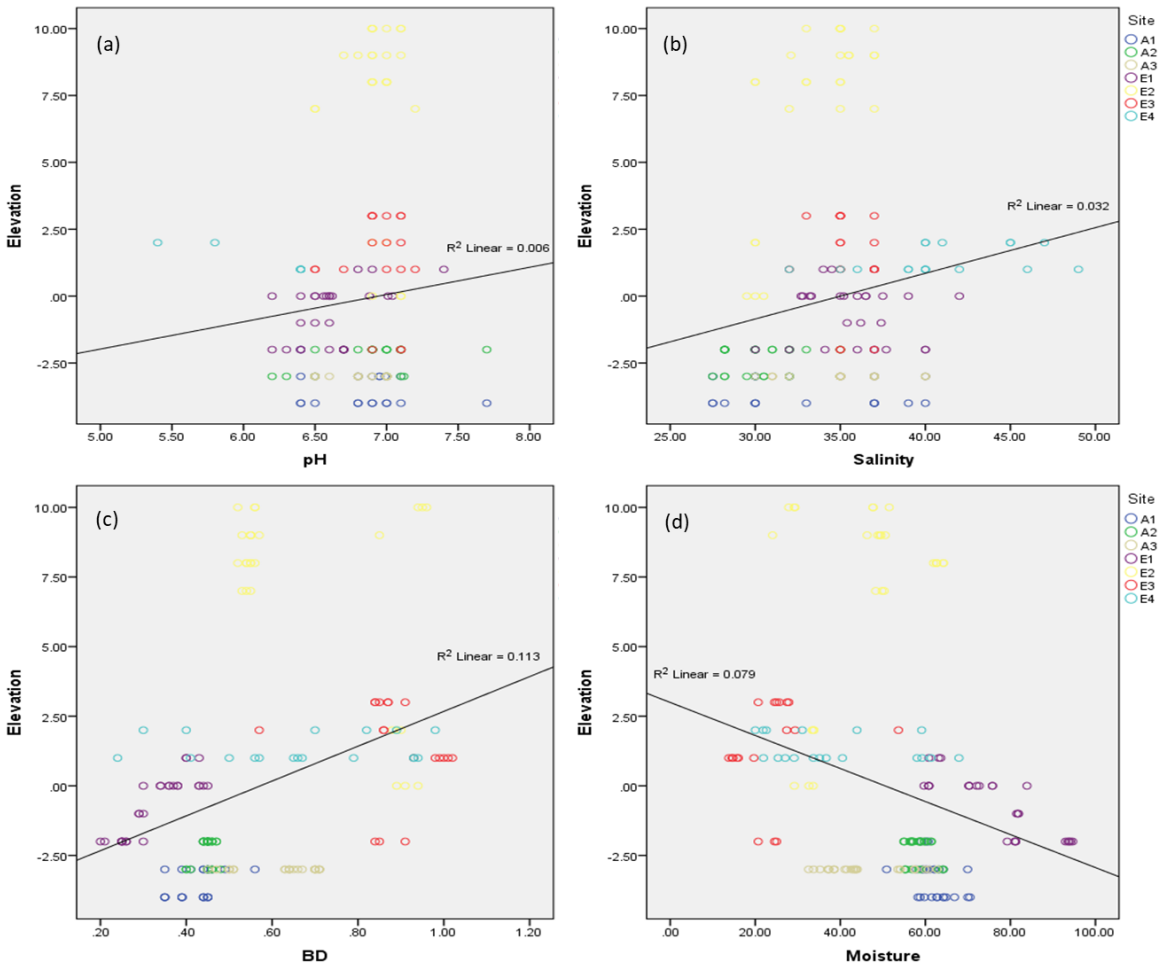

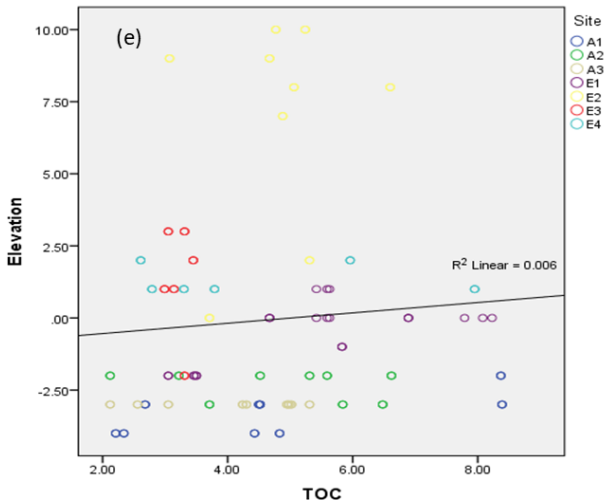

Figure 13. Correlation of elevation and soil properties from field measurements. Scatter plots of (a) soil pH, (b) soil salinity (‰), (c) soil bulk density (BD, g cm^{-3}), (d) soil moisture (%), € soil total organic carbon content (TOC, %) at accretion (A1, A2, and A3) and erosion (E1, E2, E3 and E4) sites.

Similar to previous studies, salinity and soil bulk density were two main properties strongly influenced by change in elevation. Salinity in mangrove forests in Northern Australia (Boto and Wellington 1984) varied 30 – 40 ‰ in < 1.4 m of elevation, 30 – 50 ‰ in 0.8 – 1.4 m of elevation, and 34 – 37 ‰ in 0.6 – 1.4 m of elevation. In this area, soil bulk density was 0.38 g cm-3 in 1.2 – 1.4 m of elevation and 0.45 g cm-3 in < 1.4 m of elevation. In the Caribbean Coast of Colombia, mangrove forests distrubution in the condition with salinity varied 19.8 – 53.5 ‰ in uneven topography, 40.2 – 103 ‰ in low topographic level (almost completely dead of mangroves), 34.4 – 93.1 ‰ in more inland position (narrow belt of poor developed mangrove trees), more inland showed lower soil bulk density (0.176 g cm^{-3}) (Cardona and Botero 1998).

4.2. Mangrove distribution and adaptation at accretion and erosion sites

4.2.1. Species distribution of overstory trees at accretion and erosion sites

4.2.1.1. Species richness, composition and density of overstory trees

Unlikely terrestrial forest types, species of mangroves are much more limited number due to unique conditions of habitats. At the study sites, within 120 m distance from the shoreline (the most sensitive area to accretion and erosion process), species richness of woody overstory trees (DBH ≥ 6 cm) was five (5) at accretion sites *(A. alba, A. marina, A. officinalis, R. apiculata, B. parviflora)* and lower than at erosion sites, species richness was six (6) (*A. alba, A. marina. A. officinalis, R. apiculata, B. parviflora, E. agallocha*).

In a previous study conducted in Ca Mau (Tri 1996), there were 8 communities with 9 dominant species in mangrove forest of Ca Mau peninsula including: 1) pure community of *Avicennia alba*; 2) pure community of *Avicennia marina*; 3) pure community of *Avicennia officinalis*, 4) mixed community of *Rhizophora apiculata* and *Bruguiera parviflora*; 5) mixed community of *Rhizophora apiculata* and *Rhizophora mucronata*; 6) mixed community of *Lumnitzera racemosa* and *Bruguiera parviflora*; 7) pure community of *Excoecaria agallocha*; and 8) pure community of *Phoenix paludosa.*

Seven (7) species was named for the whole mangrove area at Con Ngoai Ong Trang, Ca Mau (Tan 2008). Much higher result, a total of 22 species of mangrove species were surveyed at Adelaide River in northern Australia and varied from 7 to 15 species per transect. However, in this case, excepting for woody species, such other life forms as shrub, ground cover and vine trees number of species was also included (Ball 1998).

More species richness at erosion sites probably leaded to significantly higher average density of all species (1431±709 trees ha^{-1}) compared to those at accretion sites (1377±589 trees ha^{-1}) ($p < 0.05$). However, by species (Figure 14), accretion sites detected denser number of pioneer species (i.e., *A. alba*, *A. marina*, *A. officinalis*), whereas, erosion sites dected higher number of *R. apiculata* and *B. parviflora.* Only *E. agallocha* appeared in erosional site with extremely limited density (ca. 25 trees ha^{-1}).

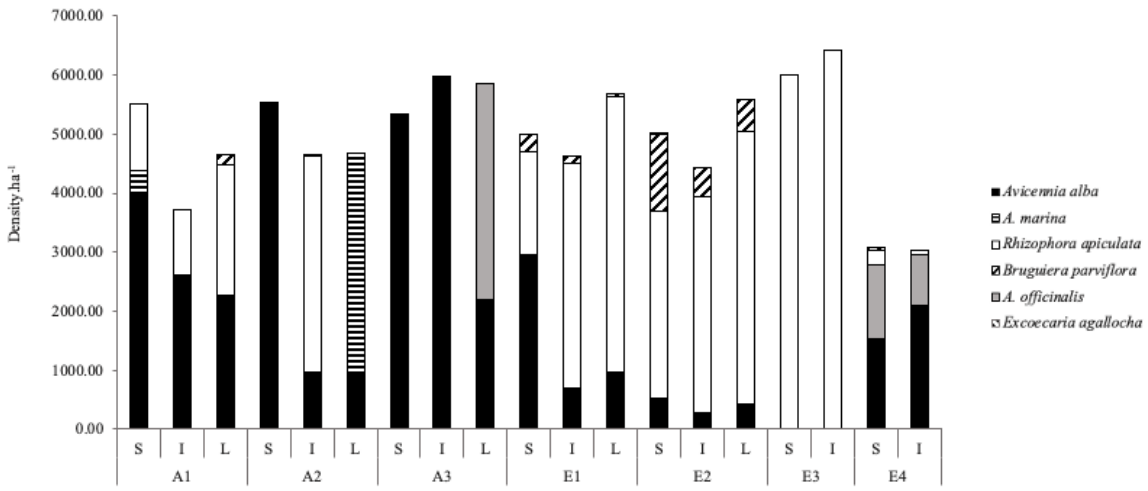

Figure 14. Density of species in seaward (S), intermediate (I), landward (L) at accretion (A1, A2, A3) and erosion sites (E1, E2, E3, E4).

Regarding species composition, *A. alba* and *R. apiculata* dominated the most at accretion and erosion sites, respectively. The ordination of species dominance with IV% > 10% (Figure 15) were *A. alba* > *R. apiculata* > *A. officinalis* at accretion sites and *R. apiculata* > *A. alba* > *B. parviflora* at erosion sites. *A. alba* dominated in seaward plots of all accretion sites. However, *R. apiculata* showed dominated in seaward plots of site E2 and E3 only. It might determined by different intensity and timescale of erosion process.

Avincennia alba and *Rhizophora apiculata* is native species in Ca Mau province. Primary succession of mangroves in Ca Mau (Figure 6, Hong and San 1993) clearly indicates the introduction of *A. alba* as a pioneer tree species in this mud fats during first stage. Mixed community of *A. alba, R. apiculata, C. tagal* and *A. officinalis* appeared at the next stage before *R. apiculata* predominates in stage 3, continuation of succession and mixed with B. *parviflora, C. tagal* and *C. decandra*. Over the long term, *A. alba* and *R. apiculata* still exhibit dominant showing the high adaptability of two species.

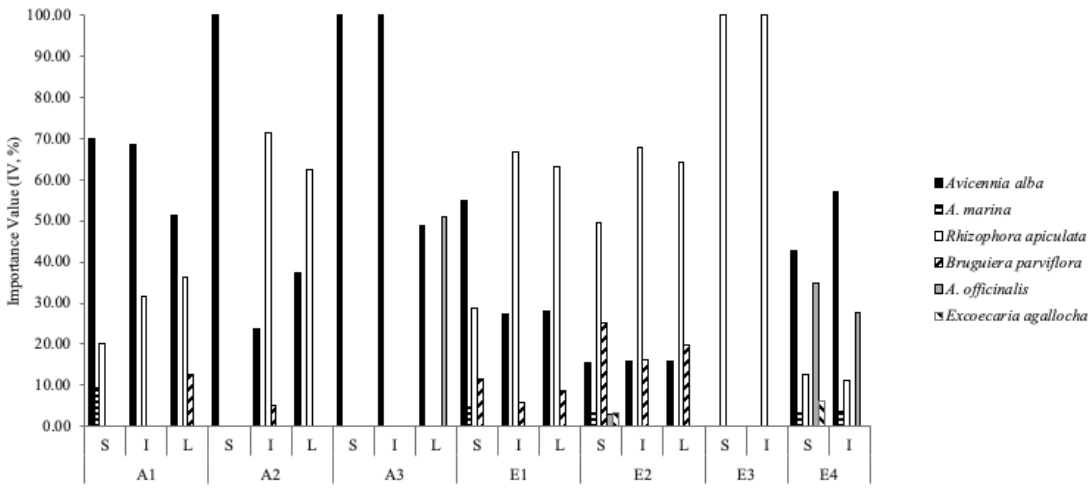

Figure 15. Importance value (IV, %) by species in seaward (S), intermediate (I), landward (L) at accretion (A1, A2, A3) and erosion sites (E1, E2, E3, E4).

A. marina is a pioneer species favorable growing in high salinity condition and mainly in coastal regions of East Sea and northern shore of Bay Hap River (Tri 1996). This species was early found at the seaward plots at either accretion site A1 and erosion site E1, E2 and even at the intermediate plots of site E4. This result was associated to the highest soil salinity examined at both seaward and intermediate plots of site E4. *E. agallocha* was solely found at erosion sites, even in seaward plots, associated with statement of (Tri 1996) that this species growths on high floor and near the sea.

4.2.1.2. Stem diameter and height distribution of overstory trees

At accretion sites, *A. alba* showed a L-shaped in seaward plots (except site A2) and bell-shaped in intermediate and landward plots (Figure 16). DBH distribution of *A. alba* at accretion sites gradually increaded from the shoreline. At site A1, most of trees were at 6-10 cm DBH in seaward plots, 10-15 cm DBH in intermediate plots, and 15-20 cm in landward plots. At site A2, most of trees were at 10-15 cm DBH in seaward plots and remaining concentration of DBH distribution mainly at 20-25 cm. At site A3, most of trees distributed at 6-10 cm DBH class in seaward plots, 15-20 cm in intermediate and reached 25-30 cm in landward plots. The smaller DBH classes were occupied by *R. apiculata* in landward plots at Sites A1 and A2, whereas *A. officinalis* was abundant in the smaller DBH classes in landward plots at

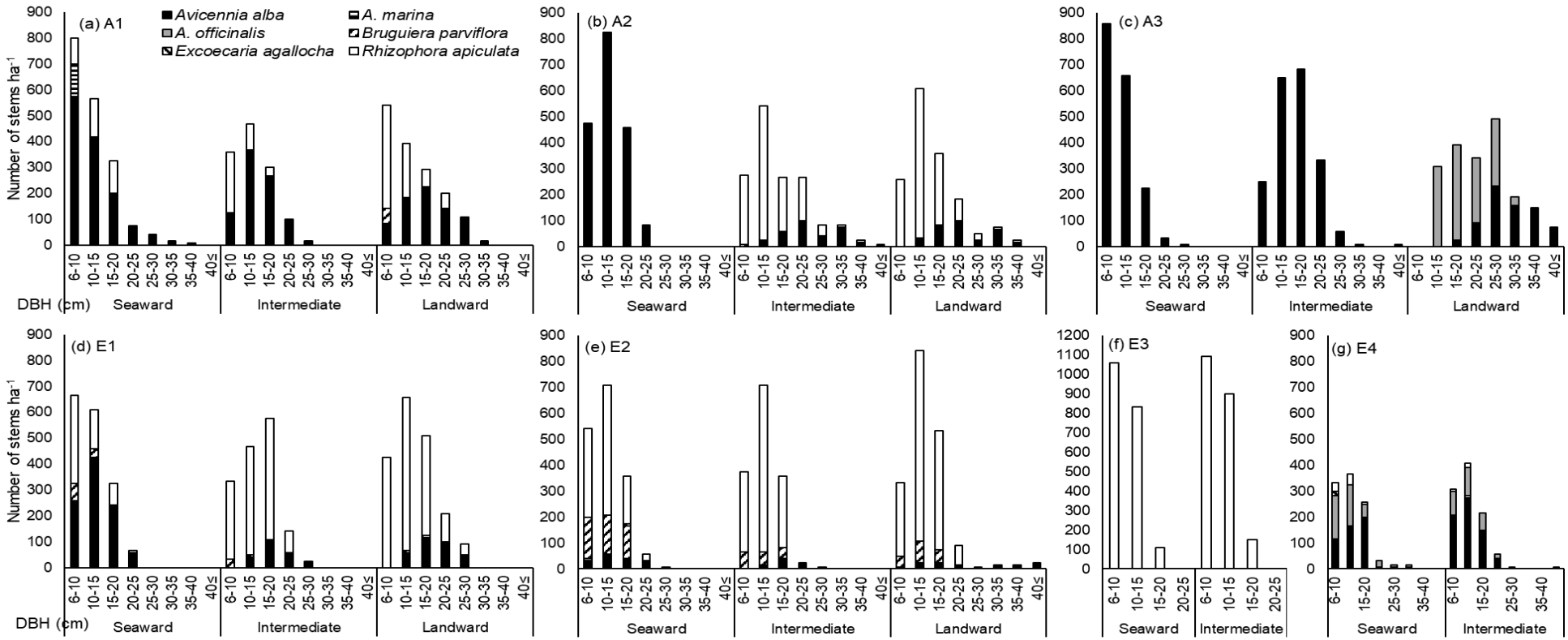

Figure 16. Diameter at breast height (DBH) distribution of overstory trees in seaward (S), intermediate (I), landward (L) at accretion (A1, A2, A3) and erosion sites (E1, E2, E3, E4).

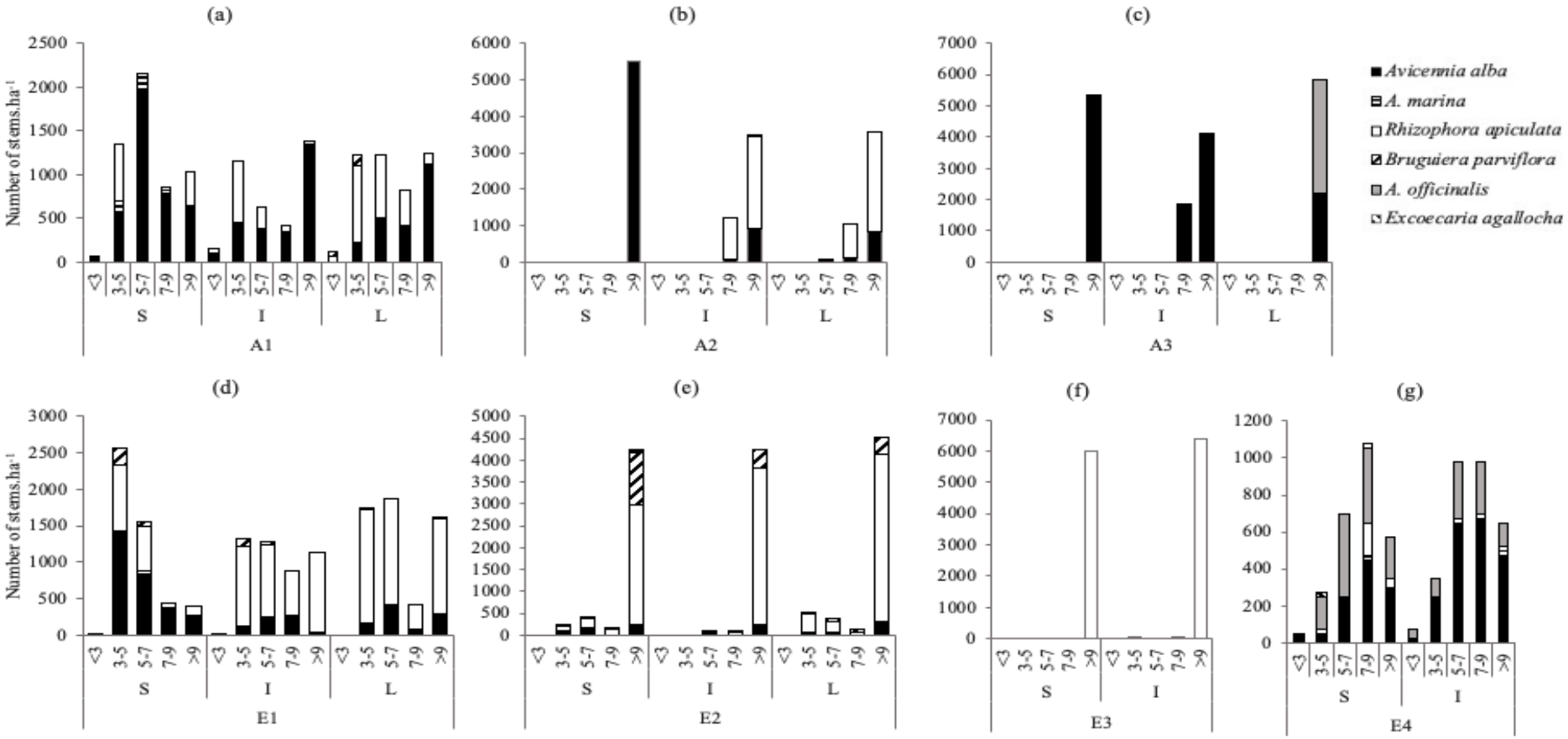

Figure 17. Height (H) distribution of overstory trees in seaward (S), intermediate (I), landward (L) at accretion A1 (a), A2 (b), A3 (c) and erosion sites E1 (d), E2 (e), E3 (f), E4 (g).

Site A3. Height of *A. alba* distributed the most at 5-7 m height in seaward plots and remaining at > 9 m height from intermediate to landward plots at site A1. The same height distribution of A. alba showed at site A2 and A2 with most of trees concentrated at > 9 m height class from seaward, intermediate to landward plots (Figure 17).

At erosion sites, the range of DBH classes of *R. apiculata* was U-shaped pattern along transect line from the shoreline at site E1, E2, E4 and L-shaped pattern at site E3 (Figure 16). *R. apiculata* was evenly distributed in almost DBH classes at all erosion sites. This species also had a uniform height distribution at most of the height levels at site E1, E4, but mainly distributed at height class > 9 m at site E2 and E3 (Figure 17). This showed the high adaptability of *R. apiculata* at erosion sites.

4.2.1.3. Spatial distribution of overstory trees

Spatial distribution of overstory trees not only reflected distribution position but also competition of light and nutrient among individuals of species. It was illustrated relied upon X, Y coordinate with X axis paralleled to the shoreline.

Majority of species display different spatial distribution patterns between accretion and erosion sites (Figure 18, Figure 19). For both *A. alba* and *A. officinalis*, there were regular and random patterns seen at accretion sites but aggregated patterns at erosion sites, especially when appearing with other species. The main cause is predicted to be the light competition. These are two pioneer and light demanding species which prefer distributing in the gaps once there is competition for light with other species in overstory layer.

B. parviflora was found several individuals under random pattern at accretion sites and both random and aggregated patterns at erosion sites and opposite for *A. marina* (i.e., aggregated pattern at accretion sites and random several individuals at erosion sites). The spatial distribution pattern of *B. parviflora* can be explained by the difference in substrate conditions. This species appears at the same stage of primary succession with Rhizophora genus, after the substrate has been relatively stable. At erosion sites were characterized with a significantly higher but uneven mean elevation and soil bulk density compared to accretion sites, explaining for the both random and aggregated patterns of *B. parviflora* at these sites. *A. marina* is a high salinity tolerant species (Wakushima et al. 1994) but also a pioneer and light demanding species. Therefore, even though soil salinity at erosion sites was significantly higher than accretion sites, *A. marina* was found higher number in accretion sites with aggregated pattern distribution, possibly under light competition with other species.

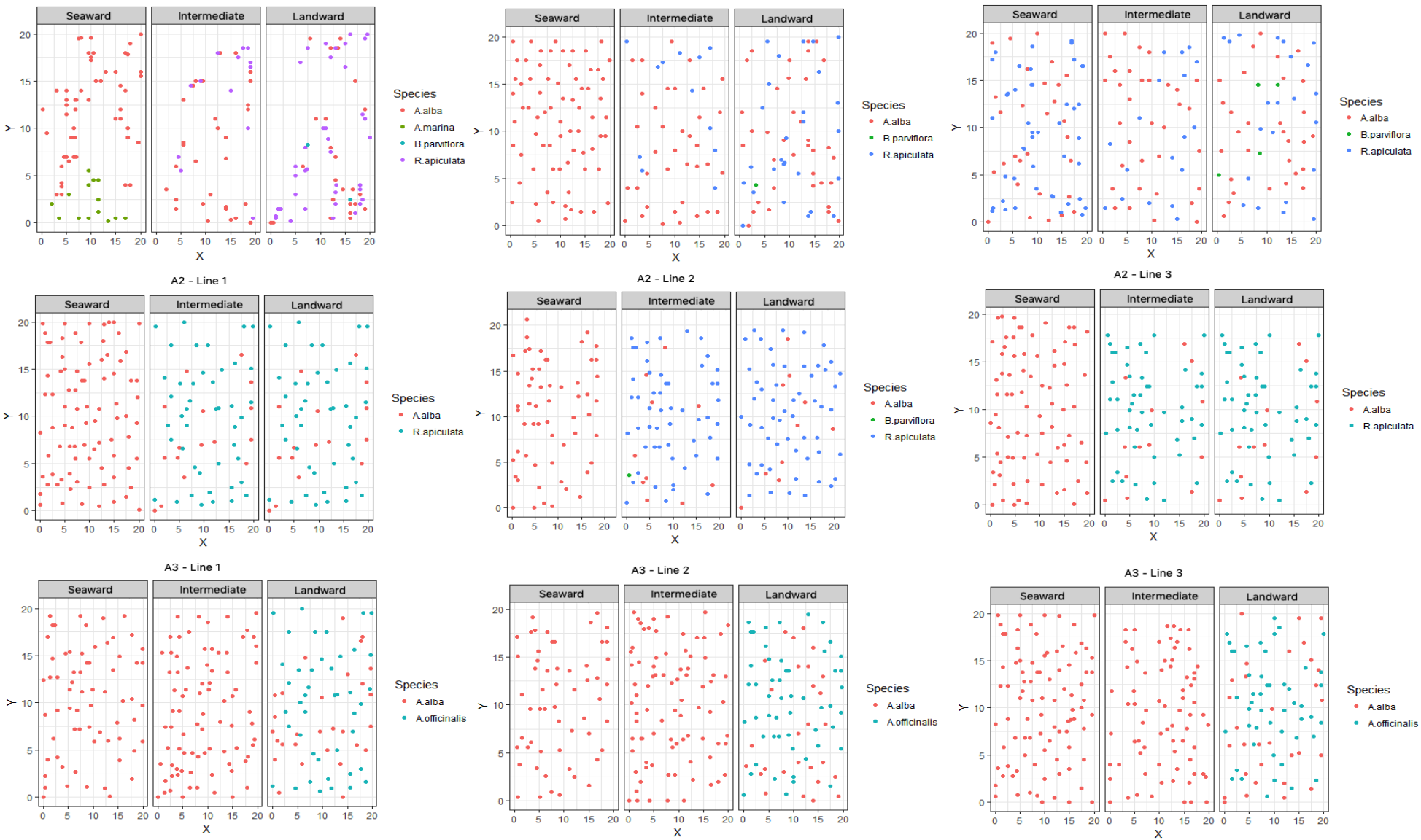

Figure 18. Spatial distribution of overstory trees in seaward, intermediate, landward plots at accretion sites (A1, A2 and A3)

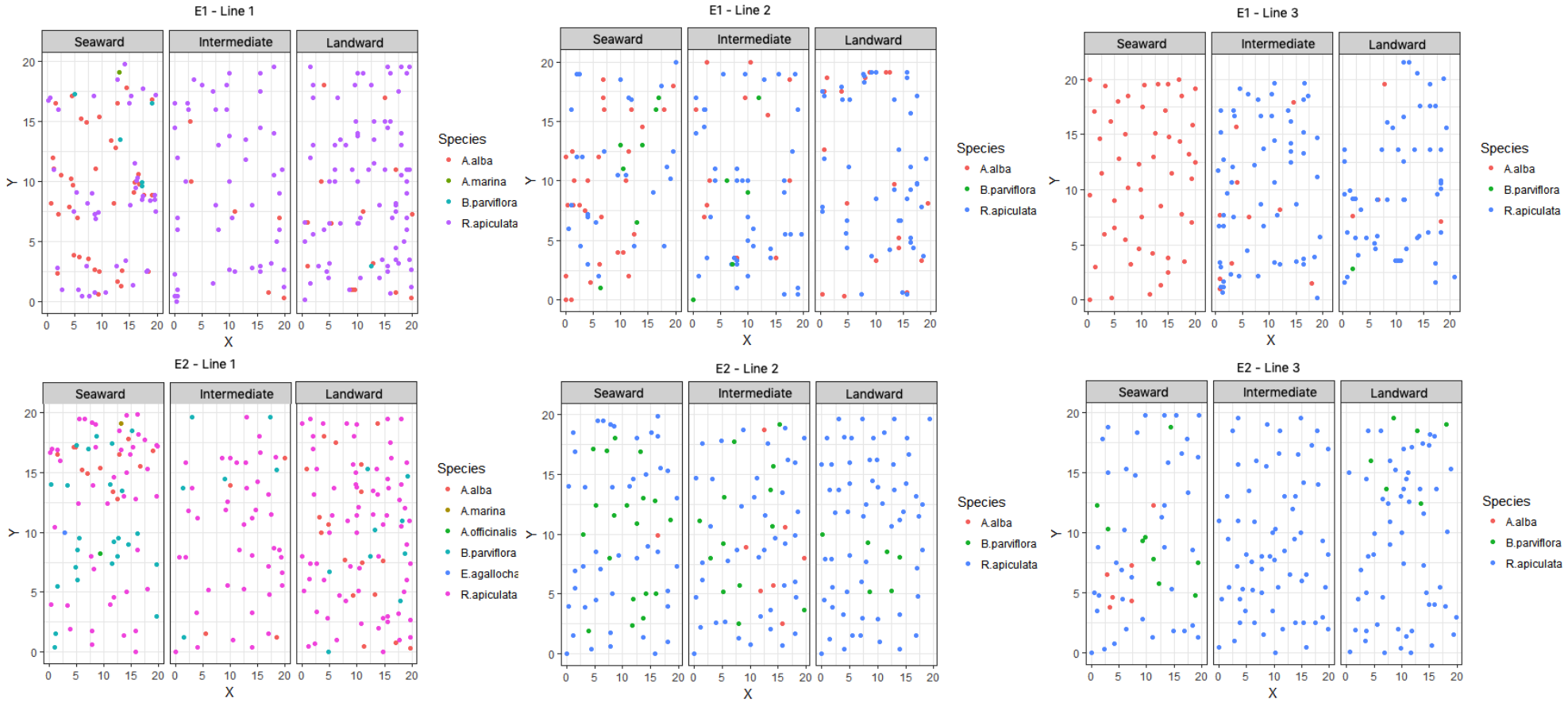
E1 - Line 1
Seaward
Intermediate
Landward
Species
A.alba
A.marina
B.parviflora
R.apiculata
E1 - Line 2
Species
A.alba
B.parviflora
R.apiculata
E1 - Line 3
Species
A.alba
B.parviflora
R.apiculata
E2 - Line 1
Species
A.alba
A.marina
A.officinalis
B.parviflora
E.agallocha
R.apiculata
E2 - Line 2
Species
A.alba
B.parviflora
R.apiculata
E2 - Line 3
Species
A.alba
B.parviflora
R.apiculata
X
Y

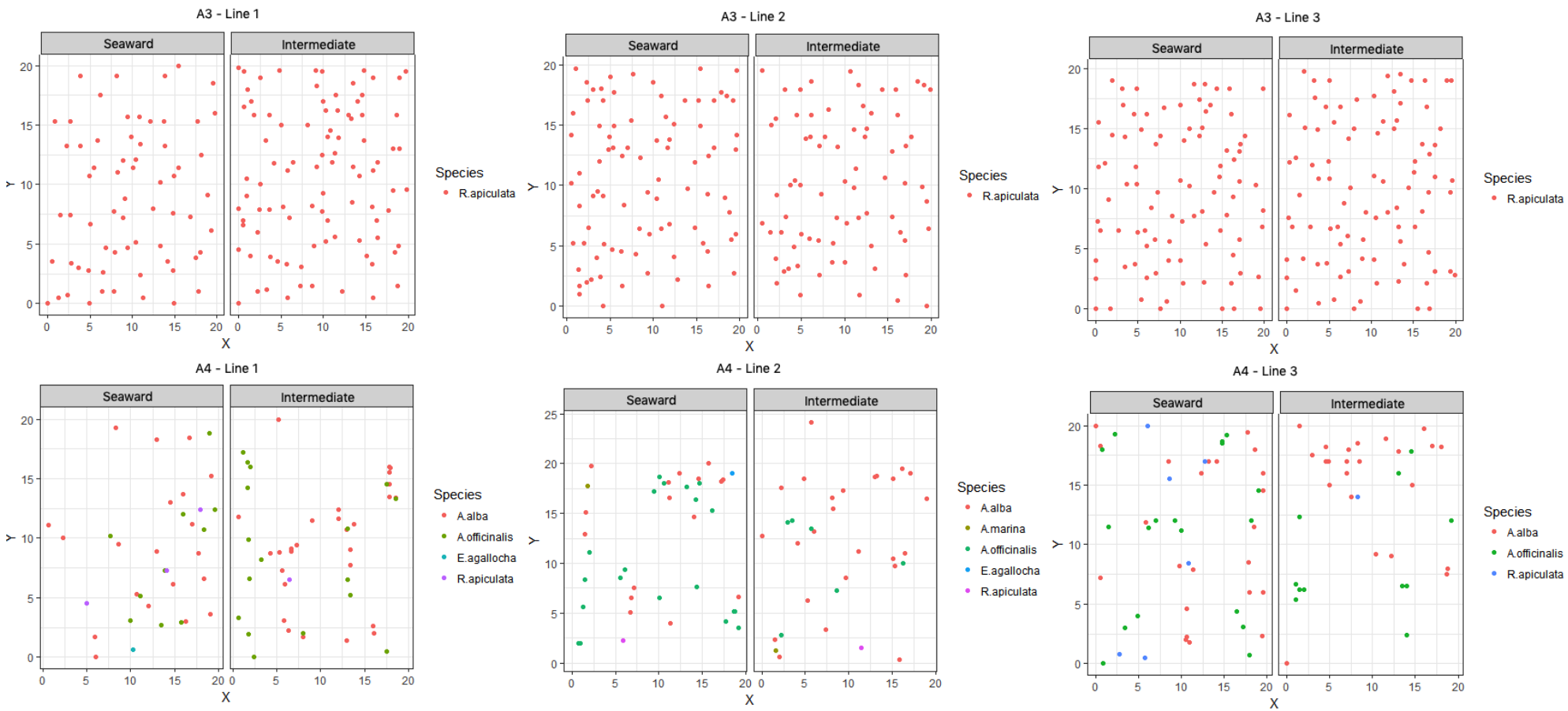

Figure 19. Spatial distribution of overstory trees in seaward, intermediate, landward plots at erosion sites (E1, E2, E3 and E4)

E. agallocha was also discovered limited individual under random pattern of distribution. This is a species favorable to growth in hard substrate conditions. Random pattern distribution possibly showed the adaptability of this species in terms of light, nutrion and substrate conditions in erosion sites.

Unlikely, *R. apiculata* presented similar patterns of distribution between accretion and erosion sites with multi-patterns of random, regular and aggregated but random pattern was the most popular. This distribution pattern illustrated the high adaptability of this species in both accretion and erosion sites because this species has a wide range of adaptation in terms of light tolerance, elevation, soil pH and salinity (e.g., Boto and Wellington 1984; McKee 1993).

At accretion sites (Figure 18), *A. marina* was first seen as pure community at the beginning muddy bank (nearest the sea) then behind by pure community of *A. alba* before *A. alba* was mixed with *R. apiculata.* *B. parviflora* started appearing to create mixed community of *R. apiculata, A. alba* and *B. parviflora* at the intermediate plots. *A. officinalis* replaced *B. parviflora* to create mixed community of *R. apiculata, A. alba* and *A. offficinalis* at the inland plots.

Along the transect line at erosion sites (Figure 19), pure community of *R. apiculata* was first seen before being mixed with other species. In general, species of *R. apiculata, A. alba* and *B. parviflora* were discovered remaining from the last position of seaward plots to inland plots.

The shift in dominance between *Avicennia* at accretion sites and *R. apiculata* at erosion sites could be explained by their species-specific characteristics and adaptation to coastal environments. *A. alba* was favoured over *R. apiculata* in areas of sediment accretion, relatively high disturbances or harsh environments, as well as higher intertidal locations (Duke, N. 2001). *R. apiculata* was more sensitive to sediment burial than *A. alba* (Terrados, J. et al. 1997). Furthermore, *A. marina* and *A. officinalis* are tolerant to a wide range of soil salinity, enabling dominance in seaward sites (Joshi, H. and Ghose, M. 2003). *Avicennia* occupies seaward frontlines, with their combination of reproduction and vegetative regrowth, whereas *R. apiculata* dominates more stable environments such as landward sites (Hinrichs, S. et al. 2009; Panapitukkul, N. et al. 1998).

4.2.2. Distribution of understory trees at accretion and erosion sites

4.2.2.1. Species richness and composition of understory trees

A. alba and *R. apiculata* are native species the study area. Ca Mau is close to the archipelagos of Indonesia and Malaysia, where mangrove species originate. Due to the warm streams and southwest wind bringing seeds or propagules to this area, along with the tropical monsoon climate (Hong, P.N. and San, H.T. 1993). The regeneration process of the secondary succession of mangroves in the study area was described as follows: *A. alba* regenerated on land previously occupied by *Rhizophora* forest. Seeds of *A. alba* were carried by tidal water from neighboring areas and growed rapidly. *Ceriops decandra* could be found underneath the tree canopy. If the forest is undisturbed, mangroves growing at the edge of the mudflats would be replaced after 10-15 years. A community of *Ceriops decandra-Lumnitzera racemosa* was regenerated on land flooded by high tide. The denuded flats of firm mud-clay along canals and those further inland are unsuitable for the regeneration of *Rhizophora*. If the land continues to be elevated, after some time *Ceriops* can be eventually replaced by *Excoecaria*. There is some regeneration of *Phoenix padulosa* on rarely-flooded land. After the forest of *Rhizophora* and *Bruguiera* was destroyed, the land was degenerated. The seeds of *Phoenix padulosa* established themselves in the denuded flats. In low-lying areas, where the flats are flooded, scattered *A. alba*, *A. marina* and *Ceriops tagal* were found. The former community of *Rhizophora-Avicennia alba* on land flooded by high tide was cut down for firewood. The regenerated succession is complex: euryhaline liane species such as *Sarcobolus globosus, Gymnanthera nitida* and some other species like *Lumnitzera racemosa, Dolichandrone spathacea* and *A. marina* invaded these areas, but *A. officinalis* remains dominant. If left undisturbed, the species diversity will eventually decrease due to the closing of the *Avicennia* canopy and the liane species will be reduced in number. *Sonneratia caseolaris* forests used to grow in muddy swamps along brackish water rivers. (Hong and San 1993)

In the study, species richness of understory trees significantly differed between accretion and erosion sites ($p < 0.01$). Similar to overstory trees, understory trees were richer species at erosion sites compared to accretion sites. It was 9 at erosion sites and 6 at accretion sites. Total number of different species was tested not significant change by distance from the shoreline at accretion sites ($p > 0.1$) but erosion sites ($p < 0.01$).

4.2.2.2. Density and height distribution of understory trees

Although more abundance of species richness than overstory trees, dominant species of understory trees are associated with overstory tree which are *A. alba* at accretion sites and *R. apiculata* at erosion sites (Figure 20). Apart from the most dominant species of *A. alba* and *R.*

apiculata, such other species of regeneration simultaneously found at overstory trees as *R. apiculata*, *A. officinalis* and *B. parviflora* at accretion sites and *B. parviflora*, *A. alba*, *A. marina* and *A. officinalis* at erosion sites. Nevertheless, either seedling or sapling of *A. marina* at accretion sites and *E. agallocha* at erosion sites, were not discovered regenerated on the forest floor. This phenomenon might be explained because of restriction in appropriate habitat. In details, *A. marina* was stated especially adapt with high salinity positions and mainly grows in coastal regions of East Sea and northern shore of Bay Hap river while *E. agallocha* grows well on high floor and near the sea (Tri 1996). Besides, new species of regeneration which absent at overstory layer were detected including *B. cylinica* and *S. alba* at accretion sites and *B. cylinica*, *C. tagal*, *X. mekongensis* and *L. racemosa* at erosion sites.

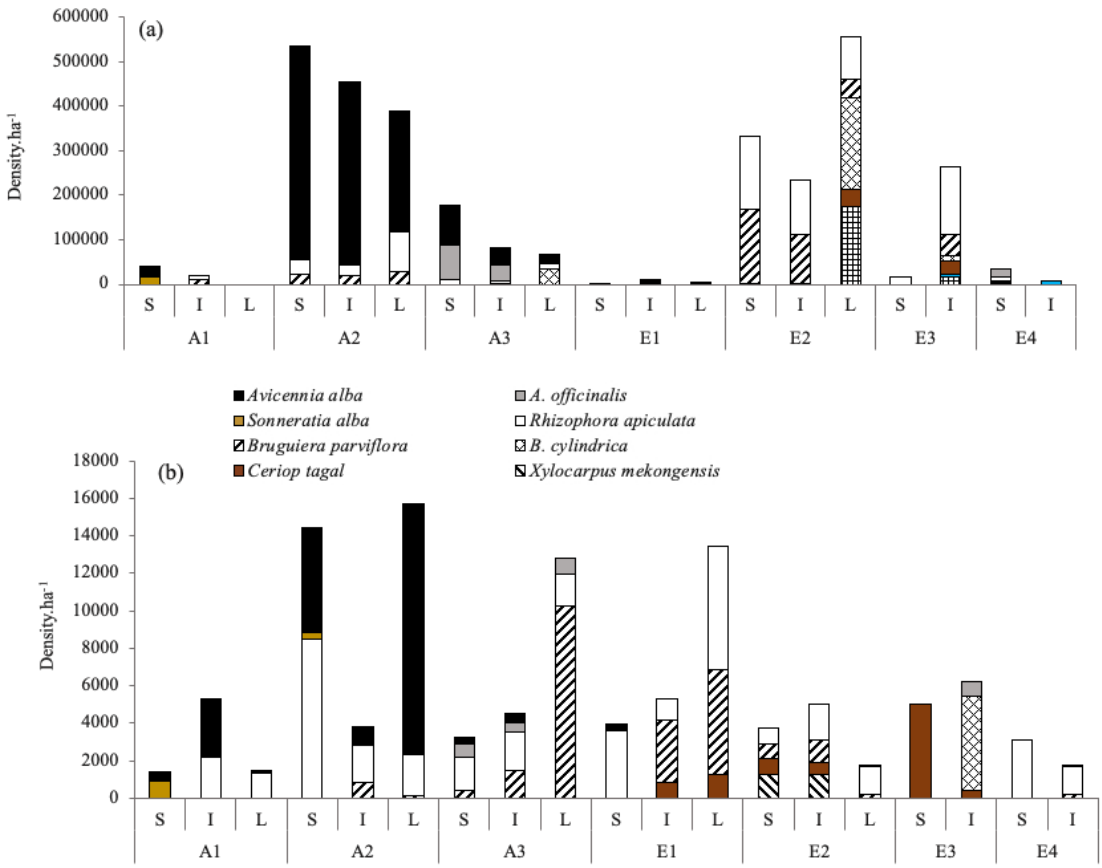

Figure 20. Density of seedlings (a) and saplings (b) in seaward (S), intermediate and landward (L) at accretion sites (A1, A2, A3) and erosion sites (E1, E2, E3, E4)

Appearance of *S. alba* at accretion sites reflected stabilization of *A. alba* stands. According to Tan (2008), *S. alba* was found in front of *A. alba* but actually formulated after suitable habitat was established by *A. alba*. However, in this study, there were only understory trees of *S. alba*

under canopies but overstory trees representing its early stage of colonization. In this case, viviparous seeds of *S. alba* brought from adjacent or even far areas by tide were trapped by root systems of *A. alba* and growth if meeting demands in environmental conditions.

At erosion sites, appearance of *B. cylinica, C. tagal, X. mekongensis* and *L. racemosa* displayed evidence of higher soil compaction compared to depositional soil compaction because those species were affirmed well adapted with firm floor (Tri 1996).

Along the distance from the shoreline (Figure 20), at accretion sites, except *A. alba* and *R. apiculata, S. alba, B. parviflora* and *A. officinalis* were early seen regenerating at the beginning position of muddy bank (seaward plots) under canopy of mixed community of *A. alba, R. apiculata* with several individuals of *A. marina*. As previously explained, *S. alba* was only growth in front of *A. alba* that the reason its understory trees disappear from the middle point of the transect line.

In addition, overstory trees of *B. parviflora* were found missing at the seaward plots but joining in overstory layer from the intermediate plots that was the origin of understory trees understory at the first point (i.e., seeds of *B. parviflora* were taken surrounding area by go up and down of tidal amplitude). Likely, understory trees of *A. officinalis* were investigated on the floor in seaward plots and missing after that point. Overstory trees of this species, however, were still absent until landward plots. Viviparous propagule of *A. officinalis* from mother trees in landward plots were considered to be taken down and growth in intermediate plots and seaward plots. In landward plots, appearance of *B. cylinica* in understory layer was forecasted originated from adjacent upstream zone as an added evidence of seawards succession processes at accretion region.

At erosion sites, although overstory trees of *A. alba* species were the second most abundant just behind *R. apiculata*, its understory trees were not much distribution as *B. parviflora* species and some new species. Pioneer species of *A. alba, A. marina* as well as *A. officinalis* were simultaneously discovered regenerating in seaward plots and gradual limitation then by transect lines even disappear all in landward plots. It was considered logically based on succession theory. However, understory trees of *C. tagal* and *X. mekongensis* were early detected in seaward plots then addition of *B. cylinica* and *L. racemosa*. Such species of *C. tagal, X. mekongensis, L. racemosa* and *B. cylinica* were reckoned originating from inland communities.

C. tagal, E. agallocha, L. racemosa, X. mekongensis reportedly adapt to a high firm floor or high tidal inundation position (Joshi and Ghose 2003; Tri 1996). The distribution of *E. agallocha* in the canopy layer and *C. tagal, L. racemosa, B. cylindrica,* and *X. mekongensis* in the seedling and sapling layers at erosion sites suggests that seaward plots on erosion sites might provide more inland-like floors than accretion sites.

Below the canopy layer were 6 layers of regenerative trees with 2 m intervals of height distribution as shown in Figure 21. However, among those regenerative trees, the potential to join canopy layer in the future is important to assess the adaptability of the species. In this study, potential regeneration species were estimated as good quality of growth and average height was equal or over average height of all regeneration species of each plot (Figure 22). Some species were investigated abundant at seedling period but under impacts of competition drivers or change in appropriate habitat they will be rejected before reaching potential understory trees. Therefore, this was a determining factor of species composition of forest story in the future and an important evidence of mangrove succession process prediction.

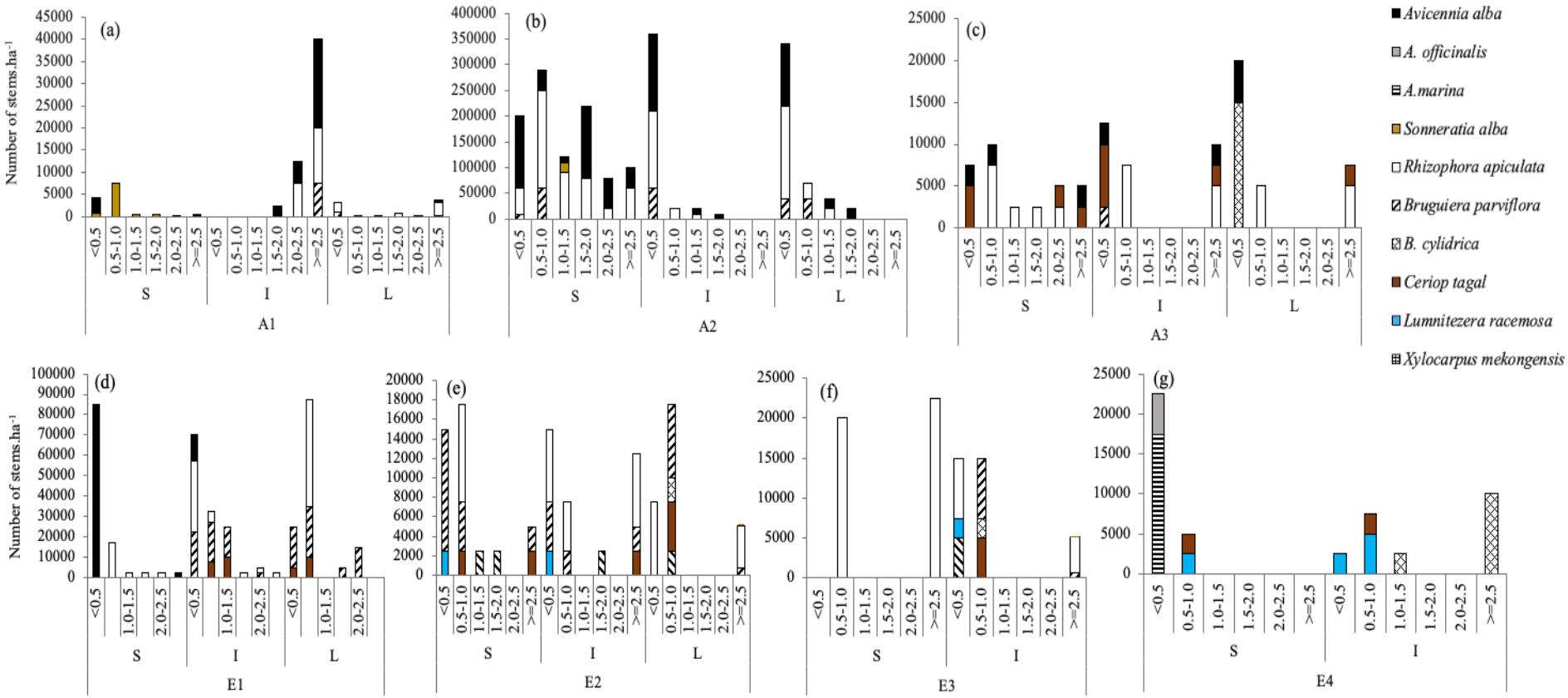

Figure 21. Height (H) distribution of regeneration in seaward (S), intermediate (I), landward (L) at accretion A1 (a), A2 (b), A3 (c) and erosion sites E1 (d), E2 (e), E3 (f), E4 (g)

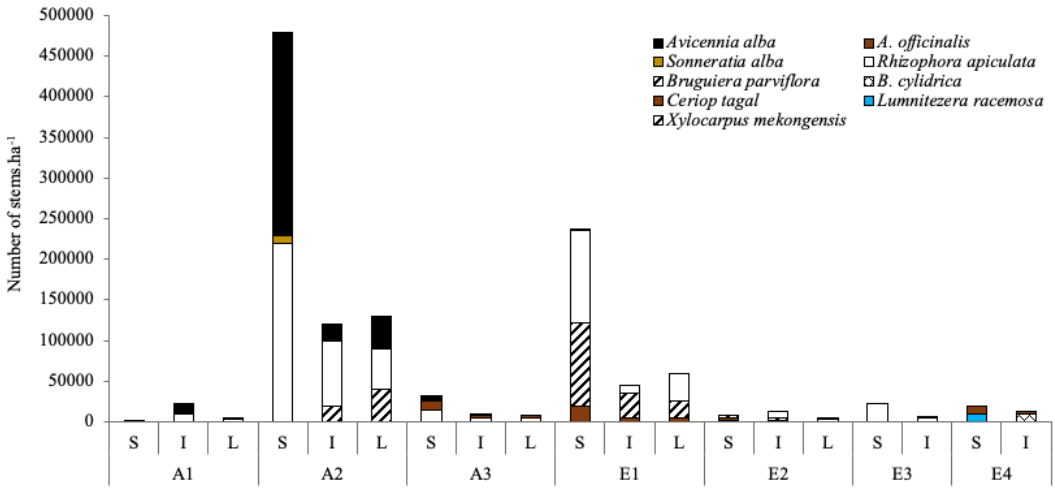

Figure 22. Number of trees by species with height upper mean height of understory trees in seaward (S), intermediate and landward (L) at accretion sites (A1, A2, A3) and erosion sites (E1, E2, E3, E4).

Among regeneration species, such species as *B. cylinica* and *S. alba* of accretion sites and *A. marina, A. officinalis, X. mekongensis* and *L. racemosa* of erosion sites were excluded in potential regeneration species composition. At accretion sites, despite *A. alba* was seen as the most abundant regeneration species; its potential tree number were less than those of *R. apiculata*. Similar to *B. cylinica* of erosion sites, it was the least abundant regeneration species but number of potential trees was the second most just behind *R. apiculata*.

Potential regeneration species were also varied along the transect line. At accretion sites, *A. officinalis* was detected the highest number of potential understory trees in seaward plots instead of *A. alba*. Likely, understory trees of *R. apiculata* were found potential more than *A. alba* at both intermediate plots and landward plots. At erosion sites, in contrast, number of potential trees of *R. apiculata* overwhelm others at all positions associated with its occupation at canopy layer.

A. alba seedlings survived in up to 7 cm sediment burial (Affandi et al. 2010), whereas the seedling mortality of *R. apiculata* increased linearly with increasing sediment accretion (Terrados et al. 1997). *A. alba* was a pioneer species and grows fast during the seedling stage, which enhances their ability to resist sediment disturbance (Balke et al. 2013; Hinrichs et al. 2009).

4.3. Roles of aerial roots in mangrove distribution and adaptation to coastal processes

4.3.1. Aerial root distribution at accretion and erosion sites

The frequency of appearance of aerial root types in sampling sub-plots varied in seaward, intermediate and landward plots at accretion and erosion sites (Figure 23).

Pneumatophores absolutely predominate in the seaward plots of all accretion sites, in the intermediate of site A1 and A3, and in the landward of site A3. This type of roots also appeared in seaward, intermediate and landward of site E1 and E2 but in intermediate plot only of site E3 and in seaward plot only of site E4.

Stilt roots share the occupation with pneumatophores in landward plot of site A2 and in intermediate and landward plots of site A2 at accretion sites. This root type showed the absolute occupation in seaward plot of site E3 and intermediate of site R4 and mostly dominated more than pneumatophore at site E2 and shared occupation with pneumatophores at site E2.

Knee roots were detected only in landward plot of site A1 and intermediate plot of site A2 at accretion sites. Meanwhile, this type of root appeared early from seaward plot to intermediate and landward plot at site E1 and E2 but was completely absented at site E3 and E4.

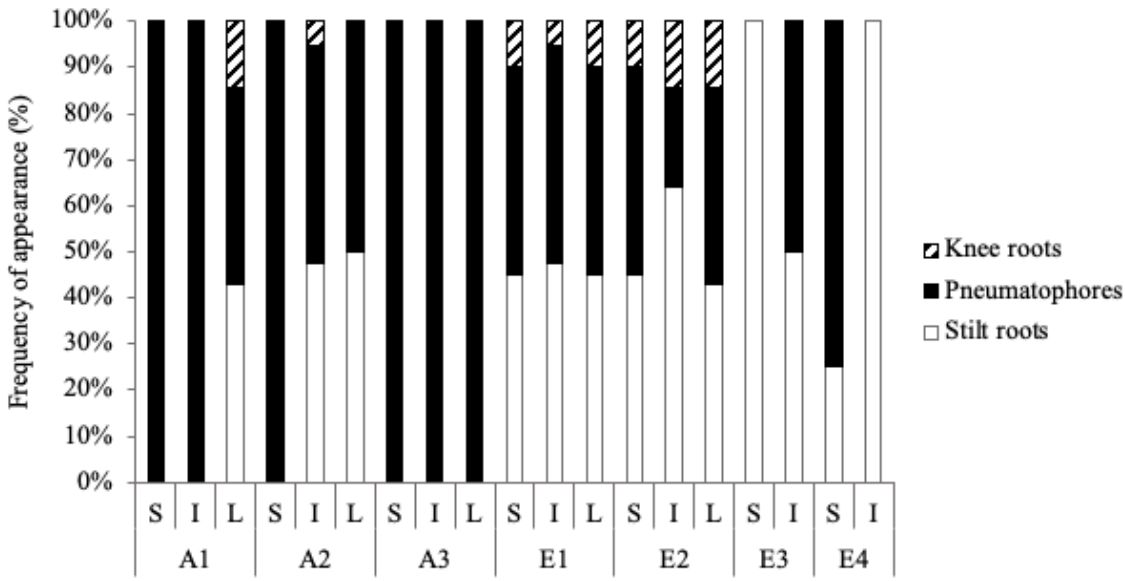

Figure 23. Frequency of appearance of aerial root types in seaward (I), intermediate (I), landward (L) at accretion sites (A1, A2, A3) and erosion sites (E1, E2, E3, E4)

4.3.2. Root morphology at accretion and erosion sites

4.3.2.1. Morphologies of stilt roots

The number of primary stilt roots and the aboveground stilt root height significantly differed among sites and the distance from the shoreline ($p < 0.01$). Stilt roots in seaward plots showed a greater number of primary roots per individual tree at erosion Sites E1 and E3 than at accretion sites ($p < 0.01$); however, the number of primary roots in landward plots was similar regardless of site (Figure 24a). No stilt roots were found at Site A3, which was due to the absence of *R. apiculata* at Site A3. The number of primary stilt roots per tree was greater in landward plots than in seaward and intermediate plots at Site A1, whereas Site E1 showed the opposite pattern. The number of primary stilt roots decreased significantly from intermediate to landward plots at Sites E1 and E2.

The aboveground stilt root height in seaward and intermediate plots significantly differed among sites ($p < 0.01$). However, the difference in landward sites was not significant. The aboveground stilt root height decreased from the seaward plots to the intermediate plots at the erosion sites. The aboveground stilt root height slightly increased from intermediate to landward plots at the accretion sites (Figure 24b). The stilt roots at E1 showed a significant decrease in the aboveground root height from the seashore toward inland plots ($p < 0.01$).

Stilt root biomass showed a negative relationship with the density and biomass of pneumatophores, corresponding to changes in dominance between *R. apiculata* and *A. alba*, and a positive relationship with elevation and TOC ($p < 0.01$; Table 6; Figure 25).

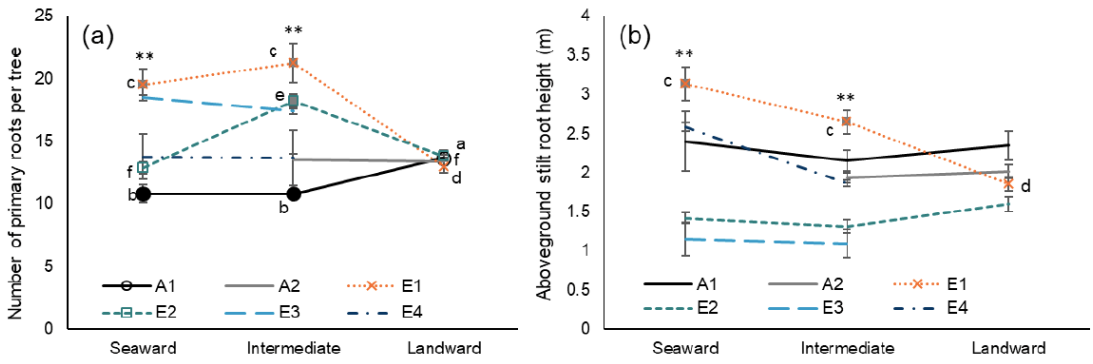

Figure 24. (a) Number of primary stilt roots of individual trees (Mean ± SE) and (b) the aboveground stilt root height of individual trees (Mean ± SE) in seaward, intermediate and

landward plots at accretion (A1, A2, and A3) and erosion (E1, E2, E3 and E4) sites. Means followed by different letters are significantly different among seaward, intermediate, and landward plots at the same site at $p < 0.05$, according to the Schéffe test. Labels are used as a and b for A1, c and d for E1, and e and f for E2. ** indicates means of seaward, intermediate and landward plots are significantly different among sites at $p < 0.05$.

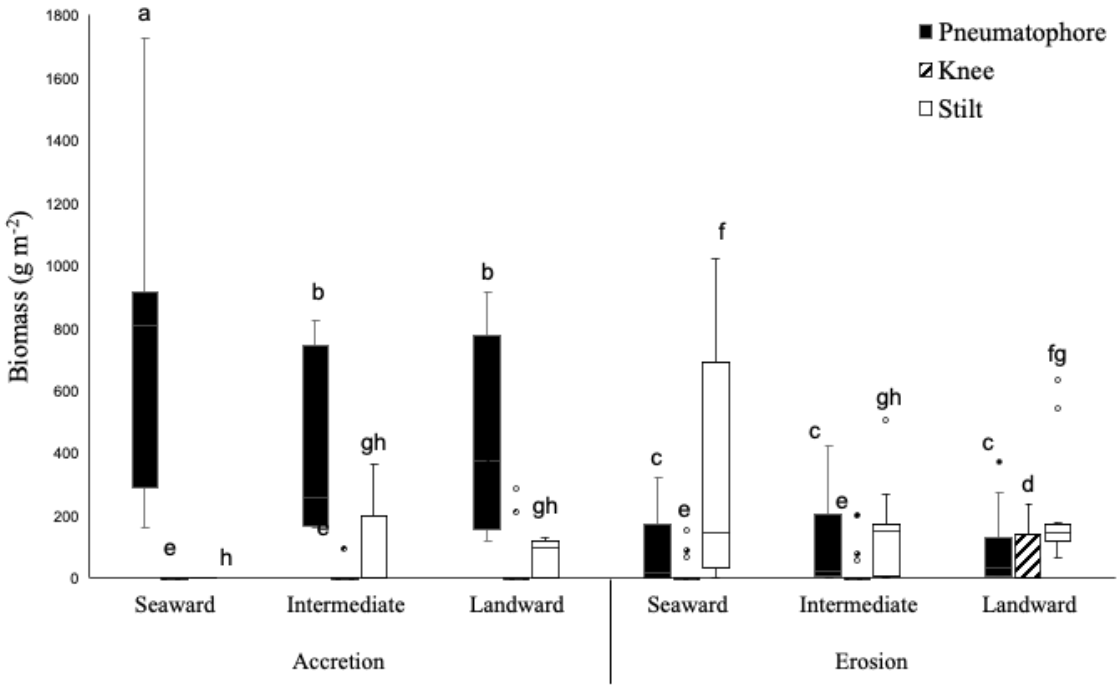

Figure 25. Box plot of root biomass of different root types in seaward, intermediate and landward plots at accretion and erosion sites. The line in the box indicates the mean. Different letters on the same root type indicate that means are significantly different among seaward, intermediate and landward plots at $p < 0.05$, according to the Schéffe test (n = 18–36). Labels are used as a, b and c for pneumatophore root, d and e for knee root, and f, g, and h for stilt root type.

4.3.2.2. Morphologies of pneumatophore and knee roots

The pneumatophore roots included pencil-like pneumatophores of *Avicennia* spp. and cone-like pneumatophores of *S. alba* at the study sites. Both the density and biomass of pneumatophore roots in seaward plots were significantly higher at accretion sites than at erosion sites ($p < 0.01$, Figure 26a, 26b). The mean density of pneumatophore roots at accretion sites was 331.2 roots m^{-2}, much greater than that of 97.8 roots m^{-2} at erosion sites. The density and biomass of pneumatophore roots at A1 and A3 were significantly greater than those at the other sites, even

in landward plots ($p < 0.05$). The density and biomass of pneumatophore roots significantly decreased from seaward to intermediate plots at accretion sites except for A1 ($p < 0.05$; Figure 26). At Site A1, both the density and biomass of pneumatophore roots were significantly higher in the intermediate plot than in the other plots ($p < 0.05$). In contrast, the density and biomass of pneumatophore roots at erosion sites were similar regardless of the distance from the shoreline.

Pneumatophores were distributed with significantly greater biomass in seaward plots than in intermediate or landward plots at accretion sites ($p < 0.05$). Pneumatophore biomass was similar regardless of the distance from the shoreline at the erosion sites.

Knee roots were not found in seaward plots at accretion sites, whereas knee roots were distributed in all plots at E1 and E2 at erosion sites. The biomass of knee roots ranged from 100–300 g m^{-2}, and landward plots had a greater biomass of knee roots than seaward and intermediate plots at erosion sites (Figure 26c). The biomass of knee roots in landward plots was significantly greater than that in seaward and intermediate plots at both accretion and erosion sites ($p < 0.05$).

The density and biomass of pneumatophores negatively correlated to above sea elevation, soil pH, soil BD and TOC. The biomass of pneumatophores additionally showed a negative relation to soil salinity ($p < 0.01$; Table 6).

Table 6. Spearman correlation coefficients for root density, root biomass of root types and elevation and soil characteristics.

	D Pneuma	B Pneuma	D knee	B knee	B stilt	Relative elevation	pH	Salinity	BD
B pneuma	0.885**								
D knee	-0.107	-0.079							
B knee	-0.107	-0.077	0.999**						
B stilt	-0.730**	-0.608**	0.178*	0.175*					
Relative elevation	-0.681**	-0.618**	0.040	0.040	0.648**				
pH	-0.246**	-0.198*	0.063	0.066	0.070	0.178*			
Salinity	-0.055	-0.202**	0.019	0.017	-0.139	-0.117	-0.052		
BD	-0.335**	-0.390**	-0.062	-0.060	0.069	0.289**	0.335**	0.072	
TOC	-0.200**	-0.022	0.135	0.140	0.198**	0.037	-0.055	-0.265**	-0.086

**: $p < 0.01$, *: $p < 0.05$, pneuma: pneumatophore root, knee: knee root, stilt: stilt root, D: root density (number of roots m^{-2}), B: root biomass (g m^{-2}), Relative elevation (m), salinity (‰), BD: soil bulk density (g cm^{-3}), and TOC: soil organic carbon (%).

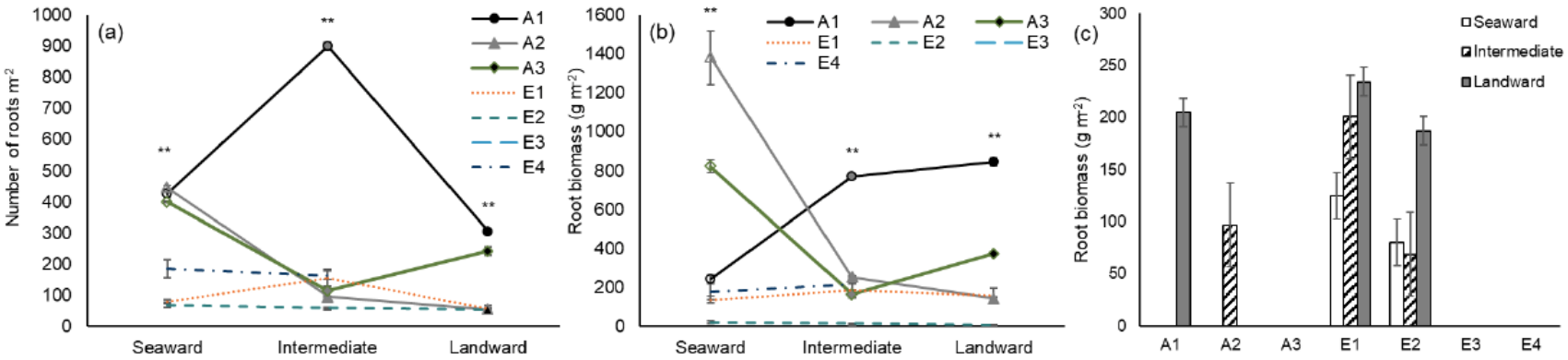

Figure 26. (a) Number (m^{-2}) and (b) biomass (mean ± SE, g m^{-2}) of pneumatophore roots and (c) biomass of knee roots (mean ± SE, g m-2) in seaward, intermediate and landward plots at accretion (A1, A2, and A3) and erosion (E1, E2, E3 and E4) sites. Means with symbols of different colors are significantly different among seaward, intermediate and landward plots at the same site at $p < 0.05$, according to the Schéffe test. ** indicates means of seaward, intermediate and landward plots are significantly different among sites at $p < 0.05$.

4.3.3. Adaptive morphologies of aerial root supporting mangrove distribution and adaptation at accretion and erosion sites

4.3.3.1. Stilt root adaptation and dominance of Rhizophora at erosion sites

Mangrove species have their own specific root morphology, which has different adaptability to the coastal processes of accretion and erosion. Mangroves at erosion sites need mechanical support to anchor them firmly on erosive substrates (Gill and Tomlinson 1969). Seaward plots had higher primary stilt roots than landward plots at erosion sites except for E2. The number of primary stilt roots per tree in landward plots was similar among sites. Mangroves develop more stilt roots to withstand erosional processes when the impact is higher (Balke, T. et al. 2013). Since mangroves in landward plots needed less support and experienced less tidal impact than those in seaward plots, landward plot mangroves required less stilt roots. The erosion sites were dominated by *R. apiculata*, likely because the root system of *Rhizophora* mangroves is adapted to withstand erosion (Kibler et al. 2022).

Mangroves showed a decrease in aboveground stilt root height from seaward to intermediate plots at erosion sites, whereas higher number of trees larger than 15 cm DBH were distributed in landward plots than in seaward plots. The aboveground stilt root height was significantly higher in the seaward plots than in the intermediate and landward plots at E1 and E4 ($p < 0.05$). Erosion at these sites resulted in a lowering of the ground surface and exposed roots, resulting in increased aboveground root height in stilt roots, which was more noticeable in seaward plots at erosion sites (Ola et al. 2019). The erosion intensity differed among sites, resulting in various stilt root heights at the sites.

Branched lateral roots were found on *R. apiculata* and some *Avicennia* trees at erosion sites. At our sites, branched lateral roots were developed even above the branch separation point on *R. apciulata*. The branched lateral roots improved the anchorage on unstable eroding mud to uphold the tree to confront strong waves and high tidal stress, supporting the tree's survival at erosion sites (Kitaya et al. 2002). Even *Avicennia* spp. developed some branched stilt roots at erosion sites, verifying the adaptive role of stilt roots to erosion (Saifullah et al. 2004; Purnobasuki 2017).

4.3.3.2. Adaptation of pneumatophores and the dominance of Avicennia at accretion sites

The dominance of *A. alba* in seaward plots at accretion sites indicated that *A. alba* invaded and fit newly accreted sites better than other mangrove species in the study area. *Avicennia* has pneumatophores that enable the species to withstand accretion processes, which continue to create anaerobic conditions with a high-water table, high salinity and less developed substrates (Balke, T. et al. 2013). *Avicennia marina* also had pneumatophores and was distributed in seaward plots at A1.

The higher density and biomass of pneumatophores in seaward plots at accretion sites showed the ability of pneumatophores to adapt to accretion over other aerial root types (Hao et al. 2021). The density of pneumatophores in seaward plots was 20–965 m^{-2}, which was higher than that of 56–520 m^{-2} in *A. marina* in Karachi, Pakistan (Saifullah and Elahi 1992). Pneumatophores adapt to anaerobic and water-logged conditions (Srikanth et al. 2016). Pneumatophore density increases to support gas exchange, and vice versa, the density of pneumatophores decreases in more aerobic soil condition (Young and Harvey 1996), which corresponded to a decrease in pneumatophore density and biomass from seaward to intermediate plots at A2 and A3 in our study. Pneumatophores bind and stabilize unstable sediment by having more rootlets at the immediate belowground soil surface, which also contribute to the competitiveness of Avicennia at accretion sites (Spenceley 1977).

At Site A1, both the density and biomass of the pneumatophore roots were significantly higher in the intermediate plot than in the seaward plot ($p < 0.05$). A1 has been forming since the 1980s and was the newest accredited site with the lowest elevation among sites with active accretion processes. The impact of accretion extended to intermediate plots, putting seaward and intermediate plots under similar accredited conditions as A1, which explained the increase in pneumatophore density and biomass from seaward to intermediate plots at A1 as mangroves responded to active accretion in intermediate plots. The density of *A. alba* in the intermediate plot at A1 was less than that in the seaward plot at A1 and the seaward and intermediate plots at A3. In contrast, pneumatophore density in the intermediate plot at A1 was the highest among the plots. At accretion sites, pneumatophore density did not correspond to tree density and was affected by other factors, such as soil or accretion processes or microtopography (Dahdouh-Guebas et al. 2007). However, stilt root density corresponded to *R. apiculata* density at erosion sites. Stilt roots and branched pneumatophore roots were detected on *Avicennia* trees at erosion sites (Figure 10k, 10l, and 10m), which were additionally developed to support the tree from being washed away by erosion (Saifullah et al. 2004).

4.3.3.3. Mangrove species distribution interacting with accretion and erosional processes

Each of the six mangrove species had their own distribution patterns interacting with site characteristics and distance from the shoreline, reflecting the time since coastal processes had occurred. Elevation, soil bulk density and soil TOC increased from seaward to landward plots, implying that seaward plots could be considered newly accreted, and the muddy flat became more stable with the distance from the shoreline at accretion sites. Thus, changes in soil, topography and species distribution along the transect from the seaward to landward direction reflected the tendency of mangrove species succession and stand development at accretion sites (Alongi 2008; Linh et al. 2020).

The density and dominance of *A. alba* decreased, whereas the density of *R. apiculata* or *A. officinalis* increased from seaward to intermediate to landward plots at accretion sites, demonstrating the succession and stand development pattern in mangrove stands in this area (Gustavo et al. 2013; Linh et al. 2020). In landward plots, *A. alba* remained in higher DBH classes, and lower DBH classes were occupied by *R. apiculata* or *A. officinalis*. The DBH distribution of *A. alba* was a bell shape in most intermediate and landward plots, whereas that in seaward plots of A1 and A3 was a reverse J shape, indicating that *A. alba* was still invading the newly accreted sites at A1 and A3. The elevation of A2 was slightly higher than that of A1 and A3. The number of primary stilt roots per tree was greater in landward plots than in seaward and intermediate plots, while the density of pneumatophores in landward plots were lower than those in seaward and intermediate plots at Site A1, indicating that stilt roots that anchored the tree became more competitive than pneumatophore roots that had less tidal inundation and less oxygen stress as elevation increased and soil was stabilized (Stachew et al. 2021).

Rhizophora appiculata dominated the erosion sites; however, the density of *A. alba* was also high in the seaward plots of E1 and E4. Erosional processes probably worked as minor disturbances, creating gaps that provided space for *A. alba* to invade. The occurrence of *A. alba* in seaward plots at erosion sites showed the ability of *A. alba* to invade disturbed sites. The elevation slightly decreased from seaward to landward plots at E3 and E4, which recently experienced severe erosional processes. In addition to surface erosion, underwater soil erosion had developed and continued to expand landwards into mangrove stands, disrupting the continuity of mangrove belts and worsening soil erosion at extreme erosion sites (GIZ 2014). As a

consequence, soil particles were eroded seawards, causing sand flats at the beginning of the shoreline or from sand dunes, which explained the decrease in elevation landwards at erosion sites (Thao, V.N. 2017). Mangroves at E2 showed an increase in primary stilt roots from seaward to intermediate plots, which might indicate the continuous impact of erosion even in intermediate plots at E2.

E4 was located in an area of extreme erosional processes, which started only several years ago. *Avicennia* dominated E4, developing a very thin band between the sea and a soil dam, which made E4 a sort of island, surrounded by a muddy bank both seaward and toward the soil dam. The muddy bank and new erosional processes provided competitiveness to *Avicennia* spp. over *R. apiculata*, resulting in the dominance of *Avicennia* spp. at E4. A newly established mangrove band at E4 protected the soil dam behind the band. The *Avicennia* band of E4 showed that mangrove distribution was affected by substrate and the period of erosional processes as disturbances (Semeniuk 1980).

Bruguiera parviflora was distributed in lower DBH classes in intermediate or landward plots at accretion and erosion sites. The density of *B. parviflora* was the highest at E2, where the elevation was higher, and the distance from the shoreline was farther than the other sites, implying that this species favored more stable conditions than *R. apiculata* and *A. alba*. The distribution of *B. parviflora* with knee roots under lower DBH classes in intermediate or landward plots showed the potential of *B. parviflora* dominance after *R. apiculata* if the site and substrate were more stabilized (Krauss et al. 2003).

The changes in species composition and DBH distribution from seaward to landward plots at accretion and erosion sites showed the stand development pattern of mangroves interacting with disturbances of accretion and erosion as well as the role of root morphology in coastal processes. Mangroves are adapted to coastal processes and intertidal areas and interact with erosion and accretion, contributing to diverse ecosystem functions in this area. Mangroves with different root morphologies have site-specific roles in regard to coastal processes, which should be considered in mangrove restoration studies.

Our study demonstrated the zonation of aerial root types and its support for mangrove species along various distances from shoreline and the impact of costal processes (Chen et al. 2023). Pneumatophores showed a positive relationship with soil moisture content, a negative relationship with surface elevation, and higher density and biomass in seaward plots at accretion sites, which explained the dominance of *Avicennia* at accretion sites, suggesting that pneumatophore was better than stilt root at adapting to newly accredited sites where soil was often inundated and oxygen-poor mud had accumulated. *Avicennia alba* with pneumatophore roots are

a potential solution for the restoration of areas with frequent inundation, newly accredited site, or unstable substrate. *Avicennia alba* grew over 40 cm DBH and aboveground pneumatophore biomass estimated over 1500 g m^{-2}, showing high potential to sequester carbon. *Rhizophora apiculata* with stilt root might have competitiveness at erosion sites as shown in stilt root distribution by sites and could be applied to the restoration of erosive sites. *Bruguiera parviflora* with knee root could be applied to the restoration of more stable sites.

Coastal exploitation has destroyed mangrove forests and efforts to restore and conserve mangrove ecosystems are actively underway (Mentaschi et al. 2018; Ellison et al. 2020; Winterwerp et al. 2020). However, detailed field information for mangrove restoration such as species-specific distribution and adaptation to coastal processes, mangrove forest structure or mangrove stand dynamics is still limited. Our study explored mangrove roots' role in the adaptation to coastal processes by investigating the density and biomass of aboveground aerial roots with mangrove species distribution at accretion and erosion sites. We did not investigate belowground roots. Future work on belowground roots, microstructure or genetic characteristics of aerial root types will provide better understanding the role of mangrove aerial roots. More information on growth, regeneration and carbon pool of mangroves interacting with coastal processes is required to assist mangrove restoration and enhance management of mangroves and coastal ecosystems.

4.4. Suggestions on mangrove-based solutions for coastal protection and development

4.4.1. Selection of silvicultural measures and species for mangrove restoration

The silvicultural measures applied in forest rehabilitation in Vietnam need to comply with Circular 29/2018/TT-BNNPTNT issued by MARD on stipulating silvicultural measures, dated November 11, 2018. The given measures include:

(1) Zoning to promote natural regeneration: Applicable to areas that do not meet the criteria of becoming a forest, with a density of regenerated purpose trees over 0.5 m height is greater than 500 trees ha^{-1} and relatively evenly distributed over the entire area. Contents of measures: Protecting and combating cutting of existing regenerated trees; preventing and fighting forest fires; clearing vines, shrubs and cutting down crooked trees, pests, and non-purpose trees to facilitate natural regeneration.

(2) Zoning to promote natural regeneration with additional planting: Applicable to areas that do not meet the criteria of becoming a forest, with a density of regenerated purpose trees over 0.5 m height is greater than 500 trees ha^{-1} and relatively unevenly distributed over the entire area. Contents of measures: Contents of measures: Depending on the density of existing regenerated trees to determine the additional planting density, ensuring no more than 800 trees ha^{-1}.

(3) Nurturing natural forests: Applicable to protection forests and special-use forests (except for strictly protected subdivisions) with timber trees in overstory is greater than 400 trees ha^{-1} or regenerating trees over 1 m height is greater than 500 trees ha^{-1} and relatively evenly distributed over the area. Contents of measures: Cutting vines, crooked, diseased and broken top trees, do not disturb shrubs, fresh vegetation and keep healthy growing trees, ensure a minimum canopy cover of 0.6.

(**4) Enrichment of natural forests:** Applicable to protection forests and special-use forests (except for strictly protected areas) with timber trees in overstory is less than 400 trees ha^{-1} or regenerating trees over 1 m height is less than 500 trees ha^{-1} and relatively unevenly distributed

over the area. Contents of measures: Planting density is maximum 500 trees ha^{-1}, in banks or in clusters.

(5) Plant new protection forests: Bare land on alluvial area or have regenerated purpose trees with over 0.5m height is less than 300 trees ha^{-1}. Contents of measures: Depending on the specific conditions and the selected species to determine the appropriate planting density, ensuring the density of the main species is more than 400 trees ha^{-1}. Techniques for planting mangrove species apply the guidance at Decision 5365/QD-BNN-TCLN issued by MARD, dated December 23, 2016.

(6) Reforestation: The forest area damaged by natural disasters and other causes is not capable of natural restoration into forest. Contents of measures: Apply techniques for planting mangrove species at Decision 5365/QD-BNN-TCLN issued by MARD, dated December 23, 2016.

Based on the research results on mangrove stand structure of two dominant sepcies (i.e., *Avicennia alba* - Aa and *Rhizophora apiculata* – Ra) by distance and intensity and timescale of accretion and erosion (Figure 27), applicable silvicultural measures to each location in the study area are as follows:

New and slight accretion (site A1):

- For the seaward locations, the applicable technique is zoning to promote natural regeneration with additional planting due to the density of regenerated purpose trees over 0.5 m height is greater than 500 trees ha^{-1} but unevenly distributed over the entire area. Additional planting density should not exceed 800 trees ha^{-1}. According to the distribution and adaptation characteristics of the species, the suitable species for additional planting in this position is *A. alba*.

- For intermediate and landward locations, the appropriate measure is nurturing natural forests dute to density of regenerating trees over 1 m height is greater than 500 trees ha^{-1} and relatively evenly distributed over the area. Contents of measures: Cutting vines, crooked, diseased and broken top trees, do not disturb shrubs, fresh vegetation and keep healthy growing trees, ensure a minimum canopy cover of 0.6.

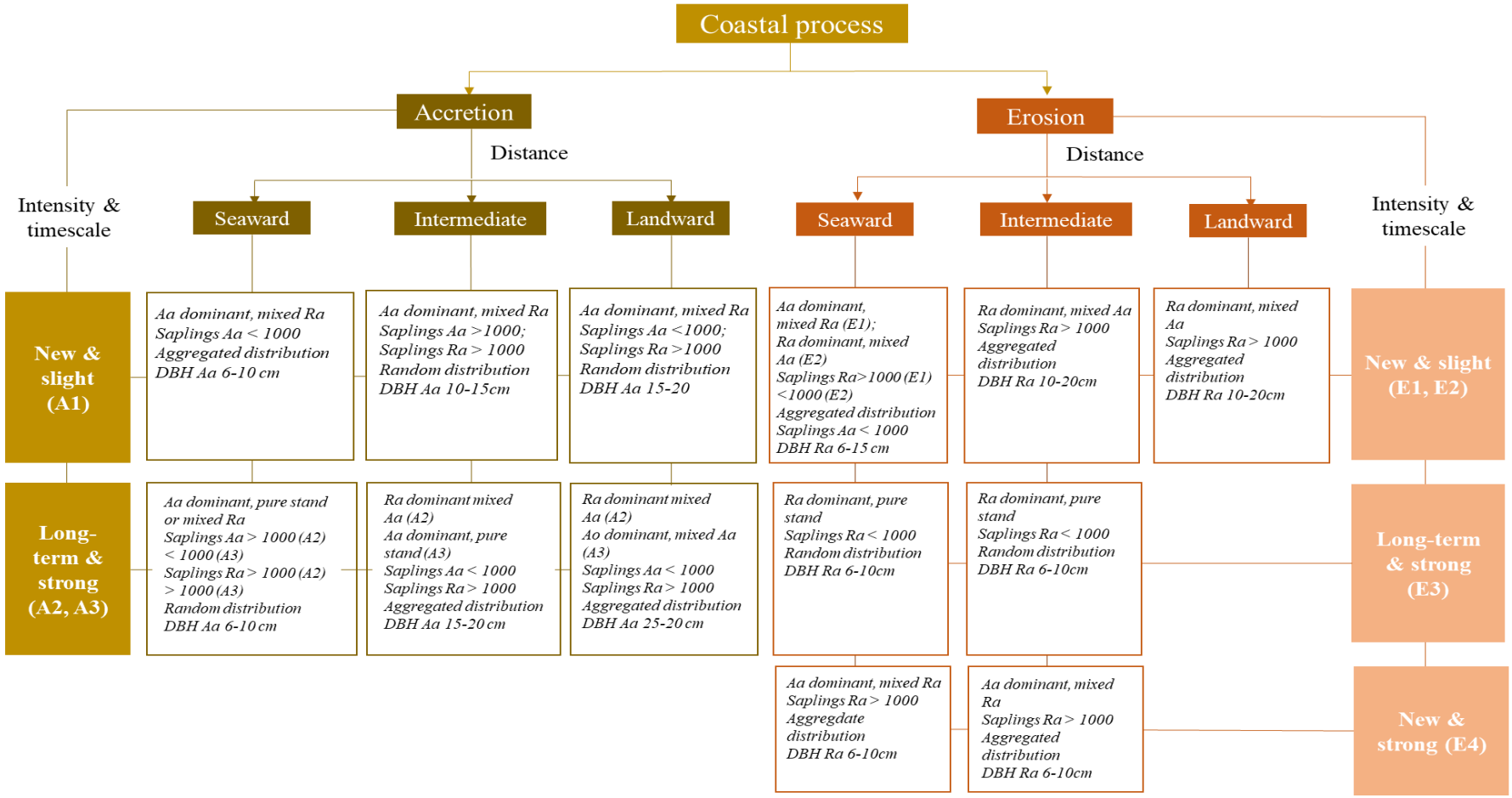

Figure 27. Mangrove stand structure of two dominance species (*Avicennia alba* – Aa and *Rhizophora apiculata* – Ra) by distance (seaward, intermediate, landward) and intensity and timescale of accretion (new and slight accretion – site A1, long-term and strong accretion – site A2, A3) and erosion (new and slight erosion – site E1, E2; long-term and strong erosion – site E3; new and strong erosion – site E4). DBH: Diameter at breast height. Saplings means number of trees ha^{-1}.

Long-term and strong accretion (site A2, A3):

- The appropriate measure for the seaward locations is zoning to promote natural regeneration due to high number of regeneration trees and relative even distribution. Contents of measures: Protecting and combating cutting of existing regenerated trees; preventing and fighting forest fires; clearing vines, shrubs and cutting down crooked trees, pests, and non-purpose trees to facilitate natural regeneration.

- For intermediate and landward locations, the appropriate measure is is zoning to promote natural regeneration with additional planting due to the density of regenerated purpose trees over 0.5 m height is greater than 500 trees ha^{-1} but unevenly distributed over the entire area. Additional planting density should not exceed 800 trees ha^{-1}. According to the distribution and adaptation characteristics of the species, the suitable species for additional planting in this position is both *A. alba* and/or *R. apiculata*. *R. apiculata* can be planted under the canopy but *A. alba* must be planed in open canopy or gaps due to its high light requirements.

New and slight erosion (site E1, E2):

- Applicable measure for the seaward, intermediate and landward locations is zoning to promote natural regeneration with additional planting due to the density of regenerated purpose trees over 0.5 m height is greater than 500 trees ha^{-1} but unevenly distributed over the entire area. Additional planting density should not exceed 800 trees ha^{-1}. According to the distribution and adaptation characteristics of the species, the suitable species for additional planting in this position is *R. apiculata*.

Long-term and strong erosion (site E3):

- Applicable measure for the seaward and intermediate locations is zoning to promote natural regeneration with additional planting due to the distribution of regenerated trees is evenly but density of regenerated *R. apiculata* is less than 500 trees ha^{-1}. Additional planting density should not exceed 800 trees ha^{-1}. According to the distribution and adaptation characteristics of the species, the suitable species for additional planting in this position is *R. apiculata*.

New and strong erosion (site E4):

- Applicable measure for the seaward and intermediate locations is zoning to promote natural regeneration with additional planting due to density of regenerated trees is less than 500 trees ha^{-1} but distribution of regenerated trees is relatively even. Additional planting density should not exceed 800 trees ha^{-1}. According to the distribution and adaptation characteristics of the species, the suitable species for additional planting in this position is *R. apiculata*. Although *A. alba* was dominant over *R. apiculata* in the overstory layer, *R. apiculata* was dominant in the understory layer showing the high adaptability of this species.

Planting of *A. alba* and *R. apiculata* requires to comply with the technical guidance on planting A. alba has been issued by MARD (Decision 5365/QD-BNN-TCLN dated December 23, 2016). The guidance provides specific techniques on 1) Collecting and preserving viviparous fruits; 2) Create seedlings in the nursery; 3) Two methods of planting techniques (including planting, tending and protecting): i) directly using viviparous and ii) using seedlings.

4.4.2. Other suggestions of mangrove-based solutions for coastal protection

According to the literature review in Chapter 2, accretion and erosion are combined processes of geomorphology and biology. Of which, geomorphological process is a complicated, challenging and expensive process because it depends mainly on natural conditions such as currents, wind direction, waves, sea level rise etc. Besides, biological process promotes the process by promoting the process, mangrove succession (natural or close to natural succession) can be considered as cost-effective and ecological-benefit solutions.

Based on the literature review of studies on distribution conditions of mangrove species, lessons learned from mangrove restoration programs in countries around the world, particularly in Asian countries adjacent to Vietnam such as Indonesia, Thailand, Philippines, India and Bangladesh, the principles to achieve ecological mangrove restoration should be considered as: Understand the autecology (species-specific ecology) of the mangrove species at the site, in particular the patterns of reproduction, propagule distribution, and successful seedling establishment (Lewis III 2009). The wrong in selection of tree species and planting sites caused the failure of many projects in many countries (Winterwerp et al. 2013).

Planting *A. alba* in bare alluvial area or seaward plots: To promote a high rate of survival, making nets or fences in front of the mudflats to limit impacts of wave and tide regime. Strong waves combined with high and low tide might easily pushes the viviparous fruits of *A. alba* out of the sea. In this case, proposed solutions aimed at gradually fixing the sediments to facilitate the first colonization of other species (i.e., Rhizophora genus, Bruguiera genus, etc.). By this way, sedimentary is also regulated under development of mangrove succession to be more accumulated landwards and encroached seawards.

In strong erosion area: The immediate solution is to reduce the direct impact of strong waves and high tides on mangroves, like the construction of concrete sea dam at site E3. According to study results, at sites E3, the role of sea dam in sediment accumulation in seaward position looked effectively since the mean elevation in seaward plot was higher than that in intermediate plots. However, the sea dam system must be an open system, which needs to be studied carefully so as not to obstruct completely the convection of current flow and sediment in and out of the dam and evenly distributed sediments.

Nowsaday, variety of nature-based solutions of coastline protection were implemented as an alternative to hard infrastructure sea dams such as mangrove planting and permeable barriers (e.g., bamboo fences, brushwood dams etc.). This application was successfully applied in Guyana, Indonesia, Suriname, Thailand and Vietnam (Figure 4). The basic philosophy behind the construction of permeable dams was the rehabilitation of mangrove habitat by restoring the net sediment balance (Winterwerp et al. 2020). In another aspect, sediment flats is a suitable condition for the formation and development of mangrove forests and promotes the natural succession process.

Chapter 5. CONCLUSIONS

The study showed the differences in species richness, species composition and distribution from the shoreline, reflecting the timescale and intensity of accretion or erosion process at both accretion and erosion sites. *Avicennia alba* BL. and *Rhizophora apiculata* BL. dominated seaward plots at accretion and erosion sites, respectively. The elevation, soil salinity, bulk density, moisture content and total organic soil carbon showed significant difference between accretion sites and erosion sites ($p < 0.05$). The elevation decreased gradually from the sea to the land and proportional correlated with soil salinity and soil bulk density and negatively correlated to soil moisture ($p < 0.05$).

Different aerial root types of mangroves have their own adaptations to the coastal processes of accretion and erosion, supporting the site-specific distribution of mangrove species. Stilt roots provide mechanical stability on erosive substrates, improving anchorage on unstable mud. *Rhizophora apiculata*, with stilt roots, dominated erosion sites where stabilizing support was important. The high density and biomass of pneumatophores supported *A. alba* dominance of accretion sites and invasion of newly accreted sites by improving gas exchange for trees to endure tidal inundation and anaerobic conditions. Knee roots occurred in landward plots at both accretion and erosion sites, showing their adaptation to more stable conditions than stilt roots at erosion sites and pneumatophores at accretion sites. Mangrove species with different root types at accretion sites showed a sequential distribution along the distance from the shoreline, changing dominance from *A. alba* to *R. apiculata*, which reflected the mangrove stand development from newly accreted to more stable conditions. Different functional characteristics of aerial root types play a crucial role in mangrove distribution in coastal areas. The site-specific and zonal distribution of mangrove species should be considered in coastal mangrove restoration, together with the degree of erosion or accumulation, soil stability, and coastal processes. Future work on growth, regeneration, and carbon pool of mangrove ecosystems in different coastal processes is required to advance understanding and restoration techniques of mangroves in coastal ecosystems.

Selection of right species and planting site is one of critical factors determining the success of forest restoration. Applicable measures in accretion sites proposed for new and slight accretion (site A1) is zoning to promote natural regeneration with additional planting of *A. alba* in seaward locations and nurturing natural forests in intermediate and landward locations; and for long-term

and strong accretion (site A2, A3) is zoning to promote natural regeneration in seaward locations and zoning to promote natural regeneration with additional planting of *A. alba* (in open gaps) and/or *R. apiculata*. Applicable measures in erosion sites proposed for new and slight erosion (site E1, E2) is zoning to promote natural regeneration with additional planting of *R. apiculata* in seaward, intermediate and landward locations; in long-term and strong erosion (site E3) is zoning to promote natural regeneration with additional planting of *R. apiculata* in seaward and intermediate locations; and in new and strong erosion (site E4) is zoning to promote natural regeneration with additional planting of *R. apiculata* in seaward and intermediate locations.

In addition, in order to increase the survival of planted seedlings or the ability to regenerate naturally, it is necessary to apply temporary measures such as using net systems or fences or permeable barriers (e.g., bamboo fences, brushwood dams etc.) to protect the impact of waves and tides and support the accumulation of sediment and creating favorable conditions for the development of mangroves.

Literature cited

Abonyi, J. and Feil, B. 2007. Cluster Analysis for Data Mining and System Identification; Birkhäuser Verlag AG: Berlin, Germany.

Affandi, N.A.M., Kamali, B., Mz, R., Tamin, N.M. and Hashim, R. 2010. Early growth and survival of *Avicennia alba* seedlings under excessive sedimentation. Sci. Res. Essays, 5, pp. 2801–2805.

Alejandro, B. 2001. Relationship between species richness and morphodynamics in sandy beaches: what are the underlying factors? Marine Ecology Progress Series, Vol. 224, pp. 35-44. Doi:10.3354/meps224035.

Alongi, D.M. 2002. Present state and future of the world's mangrove forests. Environ. Conserv., 29, pp. 331–349.

Alongi, D.M. 2008. Mangrove forests: Resilience, protection from tsunamis, and responses to global climate change. Estuar. Coast. Shelf Sci., 76 (1), pp. 1–13.

Andreetta, A., Fusi, M., Cameldi, I., Cimò, F., Carnicelli, S. and Cannicci, S. 2014. Mangrove carbon sink. Do burrowing crabs contribute to sediment carbon storage? Evidence from a Kenyan mangrove system. J. Sea Res., 85, pp. 524–533.

Asp, N.E., Gomes, V.J.C., Schettini, C.A.F., Souza-Filho, P.W.M., Siegle, E., Ogston, A.S., Nittrouer, C.A., Silva, J.N.S., Nascimento Jr., Souza, S.R., Pereira, L.C.C. and Queiroz, M.C. 2018. Sediment dynamics of a tropical tide-dominated estuary: Turbidity maximum, mangroves and the role of the Amazon River sediment load. Estuar. Coast. Shelf S., 214, pp. 10–24.

Babak, K. and Roslan, H. 2011. Mangrove restoration without planting. Ecological Engineering, Volume 37, Issue 2 (2011), pp. 387-391, ISSN 0925-8574, https://doi.org/10.1016/j.ecoleng.2010.11.025.

Baldwin, H.A., Egnotovich, M., Ford, M. and Platt, W.J. 2001. Regeneration in fringe mangrove forests damaged by Hurricane Andrew. Plant Ecol., 157, pp. 151–164.

Balke, T., Webb, E.L., Elzen, E., Galli, E., Herman, P.M.J., and Bouma, T.J. 2013. Seedling establishment in a dynamic sedimentary environment: a conceptual framework using mangroves. J. Appl. Ecol., 50, pp. 740–747.

Ball, M.C. 1980. Patterns of secondary succession in a mangrove forest of Southern Florida. Oecologia, Vol. 44, pp. 226-235. Doi:0029-8549/80/0044/0226/S2.00.

Ball, M.C. 1998. Mangrove species richness in relation to salinity and waterlogging: a case study along the Adelaide River floodplain, northern Australia. Global Ecology and Biogeography Letters 7, pp. 73-82.

Bird, E.C.F. 1986. Mangroves and intertidal morphology in Westernport Bay, Victoria, Australia. Mar. Geol., 69, pp. 251–271.

Boto, K. G. and Wellington, J. T. 1984. Soil characteristics and nutrient status in a Northern Australian mangrove forest. Estuaries 7, pp. 61-69.

Braat, L., Leuven, J.R.F.W., Lokhorst, I.R. and Kleinhans, M.G. 2019. Effects of estuarine mudflat formation on tidal prism and large-scale morphology in experiments. Earth Surf. Process. Landforms, 44, pp. 417–432.

Breanyn, M., Joanne, B., Pinegina, T.K., and Ekaterina, A.K. 2009. Tsunami geomorphology: Erosion and deposition from the 15 November 2006 Kuril Island tsunami. Geology, 37, pp. 995–998.

Bui, L.H.N. and Bui, L.T. 2020. Modelling bank erosion dependence on natural and anthropogenic factors-case study of Ganh Hao estuary, Bac Lieu - Ca Mau, Vietnam. Environ. Technol. Innov., 19, 100975.

Cahoon, D.R. and Turner, R.E. 1989. Accretion and canal impacts in a rapidly subsiding wetland II. Feldspar marker horizon technique. Esturies, 12, pp. 2060 - 2068. Doi:0160-8347/89/040260-09801.50/0.

Cardona, P. and Botero, L. 1998. Soil Characteristics and Vegetation Structure in a Heavily Deteriorated Mangrove Forest in the Caribbean Coast of Colombia. Biotropica 30, pp. 24-34.

Carlton, J. 1974. Land-building and stabilization by mangroves. Environ. Conserv., 1, 285–294.

Central Steering Committee for Disaster Prevention, 2022. Online map of landslide management: URL: http://satlo.vndss.com/#11/8.7782/104.9335/c0. Accessed on 23 October 2022.

Chaudhuri, P., Chaudhuri, S. and Gosh, R. 2019. Sedimentary Processes: Examples from Asia, Turkey and Nigeria. Chapter 6: The role of mangroves in coasal and estuarine sedimentary accretion in Southeast Asia, pp. 89 - 111. Doi: http://dx.doi.org/10.5772/intechopen.85591.

Chen, G., Hong, W., Gu, X., Krauss, K.W., Zhao, K., Fu, H., Chen, L., Wang, M. and Wang, W. 2023. Coupling near-surface geomorphology with mangrove community diversity at the estuarine scale: A case study at Dongzhaigang Bay, China. Sedimentology, 70, pp. 31–47.

Choowong, M., Murakoshi, N., Hisada, K., Charusiri, P., Daorerk, V., Charoentitirat, T., Chutakositkanon, V., Jankaew, K. and Kanjanapayont, P. 2007. Erosion and deposition by

the 2004 Indian Ocean tsunami in Phuket and Phang-nga Provinces, Thailand. J. Coast. Res., 23, pp. 1270–1276.

Clarke, P.J. and Allaway, W.G. 1993. The regeneration niche of the grey mangrove (*Avicennia marina*): Effects of salinity, light and sediment factors on establishment, growth and survival in the field. Oecologia, 93, pp. 548–556.

Cunha-Lignon, M., Mahiques, M.M., Schaeffer-Novelli, Y., Rodrigues, M., Klein, D.A., Goya, S.C., Menghini, R.P., Tolentino, C.C., Cintrón-Molero, G. and Dahdouh-Guebas, F. 2009. Analysis of mangrove forest succession, using sediment cores: A case study in the Cannéia-Iguape coastal system, São Paulo-Brazil. Brazilian Journal of Oceanography, Vol. 57, pp. 161-174.

Curtis, J.T. and McIntosh, R.P. 1951. An upland forest continuum in the prairie-forest border region of Wisconsin. Ecology, 32, pp. 476–496.

Dahdouh-Guebas, F., Kairo, J. G., Bondt, R. D. and Koedam, N. 2007. Pneumatophore height and density in relation to micro-topography in the grey mangrove *Avicennia marina*. Belgian J. Bot., 140, pp. 213–221.

Dalling, J.W. 2008. Pioneer species. In *Encyclopedia of Ecology*; Jørgensen, S.E., Fath, B.D, Eds.; Academic Press: Oxford, UK, pp. 2779–2782.

DARD of Ca Mau (Department of Agriculture and Rural Development of Ca Mau province), 2019. Report on Environmental and Social Impact Assessment. Project: Mekong Delta Integrated Climate Resilience and Sustainable Livelihoods (MD-ICRSL). Sub-project: Infrastructure to prevent coastal erosion, supply fresh water and for production of shrimp – forest model to improve livelihoods and adapting to climate change in the coastal area of Ca Mau province. Ca Mau, July, 2019, pp. 70–80.

Duke, N. 2001. Gap creation and regenerative processes driving diversity and structure of mangrove ecosystems. Wetl. Ecol. Manag., 9, pp. 267–279.

Dyer, K.R. 1988. Fine sediment particle transport in estuaries. In *Physical Processes in Estuaries*; van Leussen, W., Dronkers, J., Eds.; Springer: Berlin/Heidelberg, Germany, pp. 295–310.

Du, Q., Qin, A., Ming, S. and Zhang, C. 2021. Differences in the vertical accretion of sediment among mangrove species with different aerial root types. Estuarine, Coastal and Shelf Science, 256, 107375. Doi:10.1016/j.ecss.2021.107375.

Duarte, C.M., Losada, I.J., Hendriks, I.E., Mazarrasa, I., and Marbà, N. 2013. The role of coastal plant communities for climate change mitigation and adaptation. Nat. Clim. Change, 3, pp. 961–968.

El Banna, M.M.. and Frihy, O.E. 2009. Human-induced changes in the geomorphology of the northeastern coast of the Nile delta, Egypt. Geomorphology, 107, pp. 72-78. Doi:10.1016/j.geomorph.2007.06.025.

Ellison, A.M., Felson, A.J. and Friess, D.A. 2020. Mangrove rehabilitation and restoration as experimental adaptive management. Front. Mar. Sci., 7, 327. doi: 10.3389/fmars.2020.00327.

Emma, A., Richard, L., Catherine, T. and Peter, B. 2016. Mangrove response to environmental change in Australia's Gulf of Carpentaria. Ecol. Evol., 6, pp. 3523–3539.

Estrada, G., Mário, L., Filipe, O. and Viviane, F. 2013. Analysis of the structural variability of mangrove forests through the physiographic types approach. Aquat. Bot, 111, pp. 135–143.

Faas, R.W. 1995. Mudbanks of the southwest coast of India III: Role of non-Newtonian flow properties in the generation and maintenance of mudbanks. J. Coast. Res., 11, pp. 911–917.

FAO, 2020. Soil Organic Carbon Walkley-Black Method: Titration and Colorimetric Method. (Standard operating procedure for soil organic carbon. https://www.fao.org/3/ca7471en/ca7471en.pdf (29 January 2023).

Fromard, F., Puig, H., Mougin, E., Marty, G., Betoulle, J.L. and Cadamuro, L. 1998. Structure, above-ground biomass and dynamics of mangrove ecosystems: New data from French Guiana. Oecologia, 115, pp. 39–53.

Fromard, F., Vega, C. and Proisy, C. 2004. Half a century of dynamic coastal change affecting mangrove shorelines of French Guiana. A case study based on remote sensing data analyses and field surveys. Marine Geology 208, pp. 265-280. Doi: 10.1016/j.margeo.2004.04.018.

Garcia, K., Malabrigo, P., Gevaña, D. 2014. Philippines' Mangrove Ecosystem: Status, Threats and Conservation. Mangrove Ecosystem of Asia, 81-94 In: Faridah-Hanum, I., Latiff, A., Hakeem, K., Ozturk, M. (eds) Mangrove Ecosystems of Asia. Springer, New York, NY. https://doi.org/10.1007/978-1-4614-8582-7_5.

Gensac, E., Martinez, J-M, Vantrepotte, V. and Anthony, E.J. 2016 Seasonal and inter-annual dynamics of suspended sediment at the mouth of the Amazon river: The role of continental and oceanic forcing, and implications for coastal geomorphology and mud bank formation. Cont. Shelf Res., 118, pp. 49–62.

Gill, A.M. and Tomlinson, P.B. 1969. Studies on the growth of red mangrove (*Rhizophora mangle* L.). I. habit and general morphology. Biotropica, 1, pp. 1–9.

Gill, A.M. and Tomlinson, P.B. 1977. Studies on the growth of red mangrove (*Rhizophora mangle* L.). 4. the adult root system. Biotropica, 9, pp. 145–155.

Giri, C., Ochieng, E., Tieszen, L.L., Zhu, Z., Singh, A., Loveland, T., Masek, J. and Duke, N. 2011. Status and distribution of mangrove forests of the world using earth observation satellite data. Glob. Ecol., 20, pp. 154–159.

GIZ (Deutsche Gesellschaft für Internationale Zusammenarbeit GmbH), 2013. Shoreline Protection in Cuu Long Delta of Vietnam. Engineering Consultants Report.

GIZ (Deutsche Gesellschaft für Internationale Zusammenarbeit GmbH), 2014. Shoreline Protection of Ca Mau, Vietnam. Engineering Consultants Report.

Gustavo, C.D., Mário, L.G., Filipe, C. and Viviane, F.C. 2013. Analysis of the structural variability of mangrove forests through the physiographic types approach. Aquat. Bot., 111, pp. 135–143.

Hai, N.T., Dell, B., Phuong, V.T. and Harper, R.J. 2020. Towards a more robust approach for the restoration of mangroves in Vietnam. Annals of Forest Sciences 77, 18. Doi:10.1007/s13595-020-0921-0.

Hao, S., Su, W. and Li, Q.Q. 2021. Adaptive roots of mangrove *Avicennia marina*: structure and gene expressions analyses of pneumatophores. Sci. Total Env., 757, 143994.

Hatton, J.C. and Couto, A.L. 1992. The effect of coastline changes on mangrove community structure, Portuguese Island, Mozambique. Hydrobiologia, 247, pp. 49–57.

Hauser, L.T., Vu, G.N., Nguyen, B.A., Dade, E., Nguyen, H.M., Nguyen, T.T.Q., Le, T.Q., Vu, L.H., Tong, A.T.H. and Pham, H.V. 2017. Uncovering the spatio-temporal dynamics of land cover change and fragmentation of mangroves in the Ca Mau peninsula, Vietnam using multi-temporal SPOT satellite imagery (2004–2013). Appl. Geogr., 86, pp. 197–207.

Hesp, P.A. 1991. Ecological processes and plant adaptations on coastal dunes. J. Arid Environ., 21, pp. 165–191.

Hien, N.M. 2017. Research the Changes in Coastal Shoreline of Ca Mau, Vietnam from Landsat Database. Hanoi University of Natural Resources and Environment, Hanoi, Vietnam.

Hinrichs, S., Nordhaus, I. and Geist, S.J. 2009. Status, diversity and distribution patterns of mangrove vegetation in the Segara Anakan lagoon, Java, Indonesia. Reg. Environ. Chang., 9, pp. 275–289.

Hochard, J.P., Hamilton, S. and Barbier, E.B. 2019. Mangroves shelter coastal economic activity from cyclones. Proc. Natl. Acad. Sci., 116, pp. 12232–12237.

Hogarth, P.J. 2015. The Biology of Mangroves and Seagrasses. Oxford University Press, Oxford, UK.

Hong, P.N. 1984. Distribution of mangroves in Vietnam. In the 1st National Symposium on Mangrove Ecosystem, Hanoi, Dec. 1984. Hanoi: pp. 41-55.

Hong, P.N. 1991. Mangrove ecosystem in Vietnam. Some management considerations. In conservation and sustainable utilization of mangrove ecosystem genetic resources. Project formulation workshop, Jan. 15-19/91, Madras, India. Proceedings No.2: pp. 53-64.

Hong, P.N. and San, H.T. 1993. Mangroves of Vietnam. IUCN, Bangkok, Thailand.

Jenny, A.R., José, E.M. and Héctor, T. 2021. Mangrove restoration in Colombia: Trends and lessons learned. Forest Ecology and Management, Vol. 496 (2021), 119414, ISSN 0378-1127. https://doi.org/10.1016/j.foreco.2021.119414.

Jie, S.; Bingchao, Y., Luzhen, C. and Alexandros, G. 2022. Priority areas for mixed-species mangrove restoration: the suitable species in the right sites. Environmental Research Letters, Vol. 17, No. 6. 065001. DOI 10.1088/1748-9326/ac6b48

Joshi, H. and Ghose, M. 2003. Forest structure and species distribution along soil salinity and pH gradient in mangrove swamps of the Sundarbans. J. Trop. Ecol., 2, pp. 197–206.

Kandasamy, K. and Bingham, B. 2001. Biology of mangroves and mangrove ecosystems. Adv. Mar. Biol., 40, pp. 81–251.

Kazemi, A., Castillo, L. and Curet, O.M. 2021. Mangrove roots model suggest an optimal porosity to prevent erosion. Sci. Rep., 11, 9969. https://doi.org/10.1038/s41598-021-88119-5.

Khan, T. M. A., Razzaq, D. A., Chaudhry, Q.-U.-Z., Quadir, D. A., Kabir, A. And Sarker, M. A. 2002. Sea Level Variations and Geomorphological Changes in the Coastal Belt of Pakistan. Marine Geodesy, 25(1-2), pp. 159–174. doi:10.1080/014904102753516804.

Khiem, H.T. 2012. Research on the environmental factors and the nitrogen components in mangroves at Con Ong Trang, Ca Mau province. Master Thesis, Can Tho University, Can Tho, Vietnam.

Kibler, K.M., Pilato, C., Walters, L.J., Donnelly, M. and Taye, J. 2022. Hydrodynamic limitations to mangrove seedling retention in subtropical estuaries. Sustainability 2022, 14, 8605. https://doi.org/ 10.3390/su14148605.

Kida, M. and Fujitake, N. 2020. Organic carbon stabilization mechanisms in mangrove soils: a review. Forests 2020, 11, 981. doi:10.3390/f11090981.

Kitaya, Y., Jintana, V., Piriyayotha, S., Jaijing, D., Yabuki, K., Izutani, S., Nishimiya, A. and Iwasaki, M. 2002. Early growth of seven mangrove species planted at different elevations in a Thai estuary. Trees, 16, pp. 150–154.

Koh, H., Teh, S., Kh'ng, X. and Raja, B.R. 2018. Protection against and resilience to coastal disturbances mangrove forests. J. Trop. For. Sci., 30, pp. 446–460.

Krauss, K. W., Allen, J. A. and Cahoon, D. R. 2003. Differential rates of vertical accretion and elevation change among aerial root types in Micronesian mangrove forests. Estuarine, Coastal and Shelf Science, 56, pp. 251–259. Doi:10.1016/S0272-7714(02)00184-1.

Krishna Prasad, M.B. and Ramanathan, A.L. 2008. Sedimentary nutrient dynamics in a tropical estuarine mangrove ecosystem. Estuar. Coast. Shelf Sci., 80, pp. 60–66.

Lap, N.V. and Oanh, T.T.K. 2012. Sedimentary characteristics of tidal flats and coastline changes in Ca Mau coastal area, Mekong River Delta. Vietnam J. Earth Sci., 34, pp. 1–9.

Lee, K., Tan, W.H. and Havanond, S. 1996. Regeneration and colonisation of mangrove on clay-filled reclaimed land in Singapore. Hydrobiologia, 319, pp. 23–35.

Lefebvre, J. P., Dolique, F. and Gratiot, N. 2004. Geomorphic evolution of a coastal mudflat under oceanic influences: an example from the dynamic shoreline of French Guiana. Marine Geology, 208(2-4), pp. 191–205. doi:10.1016/j.margeo.2004.04.008.

Lewis III, R.R. 2009. Methods and Criteria for Successful Mangrove Forest Restoration. In Gerardo, M.E.P., Eric, W., Donalr, R.C. and Mark, M.B., editors, Coastal Wetlands: An Integrated Ecosystem Approach. Elsevier, 2009, p. 787. ISBN: 978-0-444-53103-2.

Lovelock, C., Sorrell, B., Hancock, N., Hua, Q. and Swales, A. 2010. Mangrove forest and soil development on a rapidly accreting shore in New Zealand. Ecosystems, 13, pp. 437–451.

Lugo, A.E. and Snedaker, S. C. 1974. The Ecology of Mangroves. Annu. Rev. of Ecol. Eovl. Syst., 5, pp. 39–64.

Lugo, A.E. 1980. Mangrove Ecosystém: Successional or Steady State? Biotropica, Vol. 12, No. 2, pp. 65-72. Doi:10.2307/2388158.

Li, J., Chen, X., Townend, I., Shi, B., Du, J., Gao, J., Chuai, X., Gong, Z. and Wang, Y.P. 2021. A comparison study on the sediment flocculation process beween a bare tidal flat and a clam aquaculture mudflat: The important role of sediment concentration and biological processes. Marine Geology, Vol. 434, 106443. Doi:10.1016/j.margeo.2021.106443.

Li, Y.-F., Du, F.-Y., Gu, Y.-G., Ning, J.-J. and Wang, L.-G. 2017. Changes of the macrobenthic faunal community with stand age of a non-native mangrove species in Futian Mangrove National Nature Reserve, Guangdong, China. Zool. Stud., 56, e19.

Lu, X.X. and Siew, R.Y. 2006. Water discharge and sediment flux changes over the past decades in the Lower Mekong River: Possible impacts of Chinese Dams. Hydrol. Earth Syst. Sci. 2006, 10, pp. 181–195.

Ma, W., Wang, W., Tang, C., Chen, G. and Wang, M. 2022. Zonation of mangrove flora and fauna in a subtropical estuarine wetland based on surface elevation. Ecol. Evol., 10, pp. 7404–7418.

Malini, B.H. and Rao, K.N. 2004. Coastal erosion and habitat loss along the Godavari delta front—A fallout of dam construction. Curr. Sci., 87, pp. 1232–1236.

MARD 2014. Coastal forest protection and development plan to respond to climate change for the period 2015 – 2020 (approved at decision 120/QD-TTg dated 22 January 2015 of Vietnamese Prime Minister). Ministry of Agriculture and Rural Development, Hanoi, Vietnam.

MARD 2016. Mangrove Forest Inventory Report. Ministry of Agriculture and Rural Development, Hanoi, Vietnam.

MARD 2020. Forest status data. Ministry of Agriculture and Rural Development, Hanoi, Vietnam.

MARD 2016. Decision No. 5365/QD-BNN-TCLN, dated 23 December 2016 on Techincal guidance for planting 6 mangrove species: *Avicennia alba* (Mấm trắng), *Avicennia marina* (Mấm biển), *Rhizophora apiculata* (Đước đôi), *Rhizophora mucronata* (Đưng), *Sonneratia alba* (Bần trắng), and *Lumnitzea racemosa* (Cóc trắng). Ministry of Agriculture and Rural Development, Hanoi, Vietnam

MARD 2018. Circular 29/2018/TT-BNNPTNT stipulating slivicultural measures, dated November 11, 2018. Ministry of Agriculture and Rural Development, Hanoi, Vietnam.

Mariem, B.S. 2021. Spatial point-pattern analysis as a powerful tool in identifying pattern-process relationships in plant ecology: an updated review. Ecological Processes, (2021) 10:56. https://doi.org/10.1186/s13717-021-00314-4.

Masselink, G., Russell, P., Rennie, A., Brooks, S. and Spencer, T. 2020. Impacts of climate change on coastal geomorphology and coastal erosion relevant to the coastal and marine environment around the UK. MCCIP Science Review 2020, pp. 158-189. Doi:10.14465/2020.arc08.cgm.

Matsui, N., Songsangjinda, P. and Keiyo, M. 2012. Mangrove rehabilitation on highly eroded coastal shorelines at Samut Sakhon, Thailand. Int. J. Ecol., 2012, pp. 1–11.

Mazda, Y., Magi, M., Nanao, H., Kogo, M., Miyagi, T., Kanazawa, N. and Kobashi, D. 2002. Coastal erosion due to long-term human impact on mangrove forests. Wetl. Ecol. Manag., 10, pp. 1–9.

McKee, K. L. 1993. Soil Physicochemical Patterns and Mangrove Species Distribution--Reciprocal Effects? Journal of Ecology 81, pp. 477-487.

McKee, K.L. 1996. Growth and physiological responses of neotropical mangrove seedlings to root zone hypoxia. Tree Physiol., 16, pp. 883–889.

McKee, K.L. 2011. Biophysical controls on accretion and elevation change in Caribbean mangrove ecosystems. Estuarine, Coastal and Shelf Science, Vol. 91, Issue 4, pp. 475-483.

Méndez-Alonzo, R., Moctezuma, C., Ordoñez, V.R., Angeles, G., Martínez, A.J. and López-Portillo, J. 2015. Root biomechanics in Rhizophora mangle: anatomy, morphology and ecology of mangrove's flying buttresses. Ann. Bot., 115, pp. 833–840.

Mentaschi, L., Vousdoukas, M.I., Pekel, J-F., Voukouvalas, E. and Feyen, L. 2018. Global long-term observations of coastal erosion and accretion. Sci. Rep., 8, 12876.

MHEN (Institute of Meteorology, Hydrology and Environment), 2011. Climate Change Impact and Adaptation Study in the Mekong Delta Ca Mau Atlas. ADB Consultants' Reports. IMHEN, Ha Noi, Vietnam.

MOST (Ministry of Science and Technology), 2011. Soil Quality – determination of total organic carbon – Walkley Black method. A National Standard of Viet Nam TCVN 8941:2011, compiled by the Institute of Agricultural Planning and Design, proposed by the Ministry of Agriculture and Rural Development, appraised by the General Department of Standards, Metrology and Quality, and announced by the Ministry of Science and Technology.

Mujabar, P.S. and Chandrasekar, N. 2011. Coastal erosion hazard and vulnerability assessment for southern coastal Tamil Nadu of India by using remote sensing and GIS. Natural Hazards, 69, pp. 1295-1314. Doi:10.1007/s11069-011-9962-x.

Ngoc, H.M. 2011. Research on structure of woody mangrove trees in Ong Trang river mouth, Ngoc Hien district, Ca Mau province. Master thesis, National University of Ho Chi Minh City, University of Natural Sciences. Ho Chi Minh City 2011.

Nardin, W., Locatelli, S., Pasquarella, V., Rulli, M.C., Woodcock, C.E. and Fagherazzi, S. 2016. Dynamics of a fringe mangrove forest detected by Landsat images in the Mekong River Delta, Vietnam. Earth Surf. Proc. Landf., 41, pp. 2024–2037.

Nascimento, W.R., Souza-Filho, P.W.M., Proisy, C., Lucas, R.M. and Rosenqvist, A. 2013. Mapping changes in the largest continuous Amazonian mangrove belt using object-based classification of multisensor satellite imagery. Estuar. Coast. Shelf Sci., 117, pp. 83–93.

Nayak, S.R., Hegde, V.S., Shalini, G., Rajawat, A.S., Girish, K.H., Jayakumar, S. and Suryanarayana, A. 2010. Geomorphic Processes in the Vicinity of the Venkatapur River Mouth, Central West Coast of India: Implications for Estuarine Sedimentation. Journal of Coastal Research (2010) 26 (5 (265)): pp. 925-934.

Nitto, D.D., Neukermans, G., Koedam, N., Defever, H., Pattyn, F., Kairo, J.G. and Dahdouh-Guebas, F. 2014. Mangroves facing climate change: Landward migration potential in response to projected scenarios of sea level rise. Biogeosciences, 11, pp. 857–871.

Nguyen, H.H., Nghia, N.H., Nguyen, H.T.T., Le, A.T., Tran, L.T.N., Duong, L.V.K., Bohm, S. and Furniss, M.J. 2020. Classification methods for mapping mangrove extents and drivers of change in Thanh Hoa Province, Vietnam during 2005–2018. For. Soc., 4, pp. 225–242.

Linh, T.M.N., Hanh, T.H., Han, V.T. and Pil, S.P. 2020. Comparison of mangrove stand development on accretion and erosion sites in Ca Mau, Vietnam. Forests, 11, 615. Doi:10.3390/f11060615.

Linh, T.M.N., Hanh, T.H., Euho, C. and Pil, S.P. 2023. Distribution of mangroves with different aerial root morphologies at accretion and erosion sites in Ca Mau province, Vietnam. Estuarine, Coastal and Shelf Science 287 (2023) 108324; doi: 10.1016/j.ecss.2023.108324.

Odum, E.P. 1969. The strategy of ecosystem development. Science, Vol. 164, Issue 3877, pp. 262-270.

Oertel, G.F. 1997. Geomorphic cycles in ebb deltas and related patterns of shore erosion and accretion. Journal of Sedimentary Petrology, Vol. 47, No. 3, pp. 1121-1131. Doi:10.1306/212F72F2-2B24-11D7-8648000102C1865D.

Ohira, W., Honda, K., Nagai, M. and Ratanasuwan, A. 2013. Mangrove stilt root morphology modeling for estimating hydraulic drag in tsunami inundation simulation. Trees, 27, pp. 141–148.

Ola, A., Gauthier, A.R.G., Xiong, Y. and Lovelock, C.E. 2019. The roots of blue carbon: responses of mangrove stilt roots to variation in soil bulk density. Biol. Lett., 15, 20180866. http://dx.doi.org/10.1098/rsbl.2018.0866.

Ong, J.E. and Gong, W.K. 2013. Structure, Function and Management of Mangrove Ecosystems. ISME Mangrove Educational Book Series No. 2. International Society for Mangrove Ecosystems (ISME), Okinawa, Japan, and International Tropical Timber Organization (ITTO), Yokohama, Japan.

Panapitukkul, N., Duarte, C.M., Thampanya, U., Kheowvongsri, P., Srichai, N., Geertz-Hansen, O., Terrados, J. and Boromthanarath, S. 1998. Mangrove colonization: Mangrove progression over the growing Pak Phanang (SE Thailand) mud flat. Estuar. Coast. Shelf Sci., 47, pp. 51–61.

Pham, L.T.H., Vo, T.Q., Dang, T.D. and Nguyen, U.T.N. 2019. Monitoring mangrove association changes in the Can Gio biosphere reserve and implications for management. Remote Sens. Appl.: Soc. Environ., 13, pp. 298–305.

Pi, N., Tam, N.F.Y., Wu, Y. and Wrong, M.H. 2009. Root anatomy and spatial pattern of radial oxygen loss of eight true mangrove species. Aquat. Bot., 90, pp. 222–230.

Phuong, V.T.; Linh, N.T.M.; Trang, D.L.H.; and Truong, N.V. 2020. Integrated management of mangrove forest to respond to climate change: current situation and policy recommendations. Vietnam Journal of Forest Science (2020), pp. 75-89. ISSN: 1859-0373.

Plaziat, J. and Augustinus, P. 2004. Evolution of progradation/erosion along the French Guiana mangrove coast: A comparison of mapped shorelines since the 18th century with Holocene data. Mar. Geol., 208, pp. 127–143.

Proffitt, C. and Devlin, D. 2005. Long-Term Growth and Succession in Restored and Natural Mangrove Forests in Southwestern Florida. Wetlands Ecol Manage 13, pp. 531–551 (2005). https://doi.org/10.1007/s11273-004-2411-9

Purnobasuki, H., Putut, R.P. and Kazutaka, K. 2017. Morphology of four root types and anatomy of root-root junction in relation gas pathway of Avicennia Marina (Forsk) Vierh roots. Vegetos, 30, 2.

Reed, D.J. 1990. The impact of sea-level rise on coastal salt marshes. Prog. Phys. Geog., 14, pp. 465–481.

Rodtassana, C. and Poungparn, S. 2012. Quantitative analysis of the root system of Avicennia alba based on the pipe model theory. Sci. Asia, 38, pp. 414–418.

Rogers, K., Saintilan, N. and Heijnis, H. 2005. Mangrove encroachment of salt marsh in Western Port Bay, Victoria: The role of sedimentation, subsidence, and sea level rise. Estuaries, 28, pp. 551–559.

Rogers, K., Wilton, K.M. and Saintilan, N. 2006. Vegetation change and surface elevation dynamics in estuarine wetlands of southeast Australia. Estuar. Coast. Shelf Sci., 66, 3-4, pp. 559-569. https://doi.org/10.1016/j.ecss.2005.11.004.

Saengsupavanich, C., Chonwattana, S. and Naimsampao, T. 2009. Coastal erosion through integrated management: A case of Southern Thailand. Ocean Coast. Manag., 52, pp. 307–316.

Saifullah, S., Gul, S. and Rasool, F. 2004. Anomalous aerial roots in grey mangroves of an Arid climate lagoon, Pakistan J. Bot., 36 (2), pp. 463–466.

Saifullah, S. M. and Elahi, E. 1992. Pneumatophore density and size in mangroves of Karachi, Pakistan. Pakistan J. Bot., 24, pp. 5–10.

Semeniuk, V. 1980, Mangrove zonation along an eroding coastline in King Sound, North-Western Australia. J. Ecol., 68(3), pp. 789–812. https://doi.org/10.2307/2259456.

Sherman, R.E., Fahey, T.J. and Battles, J.J. 2000. Small-scale disturbance and regeneration dynamics in a neotropical mangrove forest. J. Ecol., 88, pp. 165–178.

Shi, B., Pratolongo, P.D., Du, Y., Li, J., Yang, S.L., Wu, J., Xu, K. and Wang, Y.P. 2019. Influence of Macrobenthos (Meretrix meretrix Linnaeus) on Erosion-Accretion Processes in Intertidal Flats: A case study from a cultivation zone. Journal of Geophysical Research: Biogeosciences, Vol. 125, Issue 1. Doi:10.1029/2019JG005345.

Siddiqui, M.N. and Maajid, S. 2004. Montiorting of geomorphological changes for planning reclamation work in coastal area of Karichi, Pakistan. Advances in Space Research, 33 (2004), pp. 1200-1205. Doi:10.1016/S0273-1177/(03)00373-9.

SIWRP (Southern Institute for Water Resources Planning), 2013. Final Report to Japan International Cooperation Agency: The Project for Climate Change Adaptation for Agriculture and Rural Sustainable Development of Coastal Area of Cuu Long Delta, Vietnam; Southern Institute of Water Resources Planning: Ho Chi Minh, Vietnam, 2013; pp. 252.

Southern Institute of Water Resources Research. 2018. Verifying the Erosion Status in Provinces of Bac Lieu and Ca Mau; Southern Institute of Water Resources Planning: Ho Chi Minh, Vietnam.

Spenceley, A.P. 1977. The role of pneumatophores in sedimentary processes. Mar. Geol., 24, pp. M31–M37.

Srikanth, S. Lum, S.K.Y. and Chen, Z. 2016. Mangrove root: adaptations and ecological importance. Trees, 30, pp. 451–465. Doi:10.1007/s00468-015-1233-0.

Stachew, E., Houette, T. and Gruber, P. 2021. Root systems research for bioinspired resilient design: a concept framework for foundation and coastal engineering. Front. Robot. AI 8:548444. doi: 10.3389/frobt.2021.548444

Sukristijono, S. 1994. Soils in the mangrove forests of the Apar Nature Reserve, Tanah Grogot, East Kalimantan, Indonesia. Southeast Asian Studies, 32, 3, pp. 385-398.

Tan, T.D. 2008. Research on Influence of Ecological Environmental Drivers on Adaptability of Mangrove Species at Con Ngoai Ong Trang, Ca Mau; Forest Science Institute of South Vietnam: Ho Chi Minh, Vietnam.

Terrados, J., Thampanya, U., Srichai, N., Kheowvongsri, P., Geertz-Hansen, O., Boromthanarath, S., Panapitukkul, N. and Duarte, C.M. 1997. The effect of increased sediment accretion on the survival and growth of Rhizophora apiculata seedlings. Estuar. Coast. Shelf Sci., 45, pp. 697–701.

Thampanya, U., Vermaat, J.E., sinsakul, S. and Panapitukkul, N. 2006. Coastal erosion and mangrove progradation of Southern Thailand. For. Ecol. Manag., 68, pp. 75–85.

Thao, V.N. 2017. Research on the Structure and Nutrient at Ong Trang Mangrove Islet, Ca Mau Province in Environmental Soil and Water. Ph.D. Thesis, Can Tho University, Can Tho, Vietnam.

Thi, T.V., Xuan, A.T.T., Nguyen, H.P., Dahdouh-Guebas, F. and Koedam, N. 2014. Application of remote sensing and GIS for detection of long-term mangrove shoreline changes in Mui Ca Mau, Vietnam. Biogeosciences, 11, pp. 3781–3795.

Thomas, N., Lucas, R., Bunting, P., Hardy, A., Rosenqvist, A. and Simard, M. 2017. Distribution and drivers of global mangrove forest change, pp. 1996–2010. PLoS ONE, 12, e0179302.

Thorsten, B. and Daniel, A.F. 2015. Geomorphic knowledge for mangrove restoration: a pan-tropical categorization. Earth surface processes and landforms, Vol. 41, Issue 2, pp. 231-239. https://doi.org/10.1002/esp.3841.

Tri, N.H. 1996. Mangrove Species of Vietnam; Education Publishing House of Hanoi: Hanoi, Vietnam.

Trincardi, F., Correggiari, A. and Roveri, M. 1994. Late Quaternary transgressive erosion and deposition in a modern epicontinental shel: The Adriatic semienclosed basin. Geo-Mar. Lett., 14, pp. 41–51.

Tu L.X., Thanh V.Q., Reyns J., Van, S.P., Anh, D.T., Dang, T.D. and Roelvink, D. 2019. Sediment transport and morphodynamical modeling on the estuaries and coastal zone of the Vietnamese Mekong Delta. Cont. Shelf Res., 186, pp. 64–76.

Twilley, R.R. 2008. Mangrove wetlands. In Encyclopedia of Ecology; Jørgensen, S.E., Fath, B.D., Eds.; Academic Press: Oxford, UK, pp. 2198–2208.

Ursula, L.K. and Geoffrey, P.J. 1998. Mangrove restoration: A potential tool for coastal management in Tropical developing countries. Building for Coastal Management, Vol. 27, No.8, pp. 656-661, https://www.jstor.org/stable/4314812.

Veettil, B.K., Ward, R.D., Quang, N.X., Trang, N.T.T and Giang, T.H. 2019. Mangroves of Vietnam: Historical development, current state of research and future threats. Estuarine, Coastal and Shelf Science, Vol. 218, 212-236. Doi:10.1016/j.ecss.2018.12.021.

Vogt, D.G.J. 2012. Modeling gap dynamics, succession, and disturbance regimes of mangrove forests. Doctoral dissertation. Technische Universität Dresden.

Vousdoukas, M. I. 2012. Erosion/accretion patterns and multiple beach cusp systems on a meso-tidal, steeply-sloping beach. Geomorphology, 141-142, pp. 34–46. doi:10.1016/j.geomorph.2011.12.003.

Vu, P.T., Minh, V.Q., Tri, L.Q. and Thang, Q.T. 2011. Soils of the Mekong delta classified by WRB-FAO (2006) classification system. Can Tho Univ. J. Sci., 18b, pp.10–17.

Wakushima, S., Kuraishi, S. and Sakurai, N. 1994. Soil salinity and pH in Japanese mangrove forests and growth of cultivated mangrove plants in different soil conditions. J. Plant Res., 107, pp. 39–46.

Widdows, J., Brown, S., Brinsley, M.D., Salked, P. N. and Eliott, M. 2000. Temporal changes in intertidal sediment erodability: influence of biological and climatic factors. Continental Shelf Research, Vol. 20, issue 10-11, pp. 1275-1289. Doi:10.1016/S0278-4343(00)00023-6.

Widdows, J., Blauw, A., Heip, C.H.R., Herman, P.M.J., Lucas, C.H., Middelburg, J.J., Schmidt, S., Brinsley, M.D., Twisk, F. and Verbeek, H. 2004. Role of physical and biological processes in sediment dynamics of a tidal flat in Westerschelde Estuary, SW Netherlands. Marine Ecology Progress Series, Vol. 274, pp. 41-56. Doi:10.3354/meps274041.

William, K.M., Elizabeth R.B., Keith, L.B., Mark, M.B. and Leonard, R.G. 1997. Climate Change, Hurricanes and Tropical storms, and rising sea level in coastal wetlands. Ecol. Appl., 7 (3), pp. 770–801.

Winterwerp, J.C., Erftemeijer, P.L.A., Suryadiputra, N., Eijk, P.V. and Zhang, L. 2013. Defining Eco-morphodynamic requirements for rehabilitating eroding mangrove-bud coasts. Wetlands, Vol. 33, pp. 515-526. Doi:10.1007/s13157-013-0409-x.

Winterwerp, J., Albers, T., Edward, J.A., Friess, D., Mancheño, A.G., Moseley, K., Muhari, A., Naipal, S., Noordermeer, J., Oost, A., Saengsupavanich, C., Tas, S.A.J., Tonneijck, F.H., Wilms, T., Bijsterveldt, C.V., Eijk, P.V., Lavieren, E.V. and Wesenbeeck, B.K.V. 2020. Managing erosion of mangrove-mud coasts with permeable dams – lessons learned. Ecol. Eng., 158, 106078. Doi:10.1016/j.ecoleng.2020.106078.

Woodroffe, C. 1992. Coastal and Estuarine Studies. Chapter 2: Mangrove sediments and geomorphology. Tropical Mangrove Ecosystem, Vol. 41, pp. 7-41. Doi:10.1029/CE041p0007.

Woodroffe, C.D., Rogers, K., McKee, K.L., Lovelock, C.E., Mendelssohn, I.A. and Saintilan, N. 2016, Mangrove sedimentation and response to relative sea-level rise. Annu. Rev. Mar. Sci., 8, pp. 243–266. Doi: 10.1146/annurev-marine-122414-034025.

Young, B.M. and Harvey, E.L. 1996. A spatial analysis of the relationship between mangrove (Avicennia marina var.australasica) physiognomy and sediment accretion in the Hauraki Plains, New Zealand. Estuar. Coast. Shelf Sci., 42, pp. 231–246.

APPENDICES

Appendix 1. List of mangrove species in study sites

Latin name	Local name	Abbreviation	
Avicennia alba BL.	Mấm trắng	*A. alba*	Aa
Avicennia marina (Forssk.) Vierh.	Mấm biển, Mấm ổi	*A. marina*	Am
Avicennia officinalis L.	Mấm đen	*A. officinalis*	Ao
Sonneratia alba J. Smith	Bần trắng, Bần đắng	*S. alba*	Sa
Rhizophora apiculata BL.	Đước đôi	*R. apiculata*	Ra
Bruguiera parviflora (Roxb.) W. ex Griff.	Vẹt tách	*B. parviflora*	Bp
Bruguiera cylinica (L.) Blume.	Vẹt trụ, Vẹt hôi, Vẹt thăng	*B. cylinica*	Bc
Ceriop tagal (Perr.) C. B. Rob.	Dà vôi	*C. tagal*	Ct
Xylocarpus mekongensis Piere	Su Mekong	*X. mekongensis*	Xm
Lumnitezera racemosa Wild.	Cóc trắng	*L. racemosa*	Lr
Excoecaria agallocha L.	Giá	*E. agallocha*	Ea

Appendix 2. Site characteristics in seaward, intermediate, landward plots at accretion sites (A1, A2, A3) and erosion sites (E1, E2, E3)

Site	Line	Plot	Latitude	Longitude	Subplot	A.s.l elevation (m)	pH	Salinity (‰)	Bulk Density (BD, g cm^{-3})	Moisture (%)	Total Organic Carbon (TOC, %)
A1	1	Seaward			1	-4	6.9	33.0	0.3935	61.51	2.21
A1	1	Seaward	8°43'48.31"N	104°48'33.79"E	2	-4	7.0	37.0	0.3925	64.27	
A1	1	Seaward			3	-4	7.0	39.0	0.3536	70.00	
A1	1	Intermediate			1	-4	6.4	27.5	0.4446	62.80	4.43
A1	1	Intermediate	8°43'46.81"N	104°48'35.07"E	2	-4	6.4	30.0	0.4436	62.68	
A1	1	Intermediate			3	-4	6.5	30.0	0.4534	64.86	
A1	1	Landward			1	-4	6.9	27.5	0.4397	59.76	4.83
A1	1	Landward	8°43'45.55"N	104°48'36.06"E	2	-4	7.7	28.2	0.4533	58.26	
A1	1	Landward			3	-4	-	30.0	0.4485	58.78	
A1	2	Seaward			1	-4	6.8	37.0	0.3489	66.85	2.34
A1	2	Seaward	8°43'45.29"N	104°48'32.65"E	2	-4	7.1	40.0	0.3925	64.27	
A1	2	Seaward			3	-4	6.8	37.0	0.3497	70.49	
A1	2	Intermediate	8°43'44.07"N	104°48'34.17"E	1	-3	6.5	27.5	0.4495	62.12	4.52

Site	Line	Plot	Latitude	Longitude	Subplot	A.s.l elevation (m)	pH	Salinity (‰)	Bulk Density (BD, g cm^{-3})	Moisture (%)	Total Organic Carbon (TOC, %)
A1	2	Intermediate			2	-3	6.5	30.0	0.4593	61.04	
A1	2	Intermediate			3	-3	7.0	30.0	0.4888	57.85	
A1	2	Landward			1	-3	6.9	30.0	0.4426	59.43	8.39
A1	2	Landward	8°43'43.00"N	104°48'35.41"E	2	-3	6.4	30.0	0.4473	60.29	
A1	2	Landward			3	-3	6.8	32.0	0.4490	60.11	
A1	3	Seaward			1	-3	6.8	37.0	0.4121	59.38	2.68
A1	3	Seaward	8°43'42.53"N	104°48'30.95"E	2	-3	7.1	40.0	0.3930	64.21	
A1	3	Seaward			3	-3	6.8	37.0	0.3540	69.95	
A1	3	Intermediate			1	-3	7.0	32.0	0.5574	50.89	4.50
A1	3	Intermediate	8°43'41.35"N	104°48'32.51"E	2	-3	7.0	35.0	0.4396	63.24	
A1	3	Intermediate			3	-3	7.0	35.0	0.4501	62.05	
A1	3	Landward			1	-2	6.4	30.0	0.4462	59.04	8.37
A1	3	Landward	8°43'40.39"N	104°48'33.75"E	2	-2	-	-	0.4477	60.25	
A1	3	Landward			3	-2	-	-	0.4439	60.68	
A2	1	Seaward	8°43'20.95"N	104°49'15.30"E	1	-3	6.5	30.5	0.4004	64.23	5.84

Site	Line	Plot	Latitude	Longitude	Subplot	A.s.l elevation (m)	pH	Salinity (‰)	Bulk Density (BD, g cm^{-3})	Moisture (%)	Total Organic Carbon (TOC, %)
A2	1	Seaward			2	-3	6.2	29.5	0.4103	63.09	
A2	1	Seaward			3	-3	6.3	30.0	0.4023	64.02	
A2	1	Intermediate			1	-3	7.0	27.5	0.4515	58.46	3.71
A2	1	Intermediate	8°43'21.26"N	104°49'17.35"E	2	-3	7.0	28.2	0.4466	59.00	
A2	1	Intermediate			3	-3	7.0	28.2	0.4799	55.41	
A2	1	Landward			1	-3	7.1	30.5	0.4475	56.82	6.48
A2	1	Landward	8°43'17.78"N	104°49'19.17"E	2	-3	7.1	32.0	0.4623	55.24	
A2	1	Landward			3	-3	7.0	32.0	0.4634	55.12	
A2	2	Seaward			1	-2	7.0	32.0	0.4397	59.76	2.12
A2	2	Seaward	8°43'14.42"N	104°49'16.09"E	2	-2	6.5	30.0	0.4387	61.26	
A2	2	Seaward			3	-2	7.0	30.0	0.4370	61.45	
A2	2	Intermediate			1	-2	6.8	28.2	0.4632	57.19	4.52
A2	2	Intermediate	8°43'14.58"N	104°49'18.08"E	2	-2	6.7	28.2	0.4488	56.68	
A2	2	Intermediate			3	-2	6.9	28.2	0.4521	56.33	
A2	2	Landward	8°43'14.62"N	104°49'19.67"E	1	-2	7.1	31.0	0.4637	55.08	6.62

Site	Line	Plot	Latitude	Longitude	Subplot	A.s.l elevation (m)	pH	Salinity (‰)	Bulk Density (BD, g cm^{-3})	Moisture (%)	Total Organic Carbon (TOC, %)
A2	2	Landward			2	-2	7.1	35.0	0.4488	56.68	
A2	2	Landward			3	-2	-	31.0	0.4521	58.40	
A2	3	Seaward			1	-2	7.1	32.0	0.4396	59.77	3.22
A2	3	Seaward	8°43'14.42"N	104°49'16.09"E	2	-2	7.0	32.0	0.4620	58.69	
A2	3	Seaward			3	-2	7.1	33.0	0.4466	60.38	
A2	3	Intermediate			1	-2	6.9	28.2	0.4479	56.78	5.31
A2	3	Intermediate	8°43'14.58"N	104°49'18.08"E	2	-2	6.9	28.2	0.4654	54.91	
A2	3	Intermediate			3	-2	6.9	28.2	0.4500	58.62	
A2	3	Landward			1	-2	7.7	35.0	0.4479	58.85	5.59
A2	3	Landward	8°43'14.62"N	104°49'19.67"E	2	-2	7.1	30.0	0.4654	56.95	
A2	3	Landward			3	-2	7.0	30.0	0.4477	58.87	
A3	1	Seaward			1	-3	6.8	35.0	0.4986	57.48	4.95
A3	1	Seaward	8°38'43.16"N	104°42'55.30"E	2	-3	6.6	37.0	0.4691	59.96	
A3	1	Seaward			3	-3	6.8	35.0	0.4681	60.75	
A3	1	Intermediate	8°38'43.37"N	104°42'57.48"E	1	-3	6.5	30.0	0.6372	43.54	4.24

Site	Line	Plot	Latitude	Longitude	Subplot	A.s.l elevation (m)	pH	Salinity (‰)	Bulk Density (BD, g cm^{-3})	Moisture (%)	Total Organic Carbon (TOC, %)
A3	1	Intermediate			2	-3	6.8	35.0	0.6323	43.97	
A3	1	Intermediate			3	-3	6.5	35.0	0.6657	41.08	
A3	1	Landward			1	-3	7.0	31.0	0.6965	38.52	5.02
A3	1	Landward	8°38'43.34"N	104°42'58.90"E	2	-3	7.0	32.0	0.7112	37.33	
A3	1	Landward			3	-3	7.0	32.0	0.7124	37.24	
A3	2	Seaward			1	-3	7.0	35.0	0.4500	62.76	2.12
A3	2	Seaward	8°38'40.03"N	104°42'54.07"E	2	-3	6.5	37.0	0.4976	57.59	
A3	2	Seaward			3	-3	7.0	35.0	0.5059	54.07	
A3	2	Intermediate			1	-3	6.8	35.0	0.6489	42.52	2.56
A3	2	Intermediate	8°38'40.18"N	104°42'56.32"E	2	-3	6.8	35.0	0.6346	43.77	
A3	2	Intermediate			3	-3	6.5	37.0	0.6378	43.49	
A3	2	Landward			1	-3	7.0	31.0	0.7127	32.54	4.98
A3	2	Landward	8°38'40.27"N	104°42'57.77"E	2	-3	7.0	35.0	0.6977	33.71	
A3	2	Landward			3	-3	-	31.0	0.7010	35.22	
A3	3	Seaward	8°38'36.89"N	104°42'53.07"E	1	-3	7.0	37.0	0.4985	57.50	4.30

Site	Line	Plot	Latitude	Longitude	Subplot	A.s.l elevation (m)	pH	Salinity (‰)	Bulk Density (BD, g cm^{-3})	Moisture (%)	Total Organic Carbon (TOC, %)
A3	3	Seaward			2	-3	7.0	35.0	0.5108	53.56	
A3	3	Seaward			3	-3	7.0	35.0	0.5054	54.11	
A3	3	Intermediate			1	-3	6.9	37.0	0.6429	43.04	5.31
A3	3	Intermediate	8°38'37.00"N	104°42'55.27"E	2	-3	7.0	37.0	0.6604	41.53	
A3	3	Intermediate			3	-3	6.5	35.0	0.6426	43.07	
A3	3	Landward			1	-3	6.9	40.0	0.6969	38.49	3.05
A3	3	Landward	8°38'36.97"N	104°42'56.63"E	2	-3	7.0	40.0	0.7143	37.08	
A3	3	Landward			3	-3	7.0	40.0	0.6966	38.52	
E1	1	Seaward			1	-2	6.4	32.0	0.2607	93.54	3.05
E1	1	Seaward	8°43'20.19"N	104°49'8.60"E	2	-2	6.4	30.0	0.2539	93.79	
E1	1	Seaward			3	-2	6.7	36.0	0.2594	92.95	
E1	1	Intermediate			1	0	6.6	33.2	0.4340	59.69	6.89
E1	1	Intermediate	8°43'21.16"N	104°49'6.94"E	2	0	6.6	32.7	0.3368	72.06	
E1	1	Intermediate			3	0	6.6	33.3	0.3380	72.65	
E1	1	Landward	8°43'21.92"N	104°49'5.43"E	1	0	6.6	35.2	0.3743	70.27	7.79

Site	Line	Plot	Latitude	Longitude	Subplot	A.s.l elevation (m)	pH	Salinity (‰)	Bulk Density (BD, g cm^{-3})	Moisture (%)	Total Organic Carbon (TOC, %)
E1	1	Landward			2	0	6.6	32.8	0.3771	70.27	8.08
E1	1	Landward			3	0	6.4	36.5	0.3777	70.27	8.23
E1	2	Seaward			1	-2	6.3	40.0	0.2508	81.25	3.50
E1	2	Seaward	8°43'17.16"N	104°49'7.52"E	2	-2	6.2	37.0	0.2533	81.01	
E1	2	Seaward			3	-2	6.7	37.0	0.2450	81.19	
E1	2	Intermediate			1	0	6.2	37.5	0.3004	83.89	4.67
E1	2	Intermediate	8°43'18.08"N	104°49'5.79"E	2	0	6.5	42.0	0.3623	75.78	
E1	2	Intermediate			3	0	6.5	39.0	0.3612	75.78	
E1	2	Landward			1	1	6.9	34.5	0.4250	60.80	5.63
E1	2	Landward	8°43'18.77"N	104°49'4.28"E	2	1	7.4	37.0	0.4032	63.14	5.59
E1	2	Landward			3	1	6.8	34.0	0.3957	63.61	5.42
E1	3	Seaward			1	-2	6.7	34.1	0.2015	94.63	3.46
E1	3	Seaward	8°43'14.21"N	104°49'6.18"E	2	-2	6.6	37.7	0.2143	94.14	
E1	3	Seaward			3	-2	6.7	40.0	0.2966	79.25	
E1	3	Intermediate	8°43'15.12"N	104°49'4.44"E	1	-1	6.4	35.4	0.2890	81.92	5.83

Site	Line	Plot	Latitude	Longitude	Subplot	A.s.l elevation (m)	pH	Salinity (‰)	Bulk Density (BD, g cm^{-3})	Moisture (%)	Total Organic Carbon (TOC, %)
E1	3	Intermediate			2	-1	6.6	37.4	0.2925	81.79	
E1	3	Intermediate			3	-1	6.5	36.2	0.2960	81.47	
E1	3	Landward			1	0	7.0	36.0	0.4350	60.80	5.63
E1	3	Landward	8°43'15.89"N	104°49'2.98"E	2	0	7.0	36.5	0.4331	60.80	5.59
E1	3	Landward			3	0	6.9	35.0	0.4453	60.80	5.42
E2	1	Seaward			1	0	6.9	29.5	0.8934	33.62	3.71
E2	1	Seaward	8°41'46.40"N	104°50'38.05"E	2	0	7.1	30.5	0.9077	32.62	
E2	1	Seaward			3	0	7.1	30.0	0.9352	29.18	
E2	1	Intermediate			1	9	6.9	35.5	0.5471	49.25	3.07
E2	1	Intermediate	8°41'48.18"N	104°50'38.91"E	2	9	6.9	35.5	0.5451	49.57	
E2	1	Intermediate			3	9	6.8	32.1	0.5499	48.85	
E2	1	Landward			1	10	6.9	35.0	0.5574	47.68	4.77
E2	1	Landward	8°41'49.59"N	104°50'39.71"E	2	10	7.1	37.0	0.5573	47.69	
E2	1	Landward			3	10	7.1	35.0	0.5182	51.50	
E2	2	Seaward	8°41'45.12"N	104°50'41.10"E	1	2	7.0	30.0	0.8930	33.65	5.31

Site	Line	Plot	Latitude	Longitude	Subplot	A.s.l elevation (m)	pH	Salinity (‰)	Bulk Density (BD, g cm^{-3})	Moisture (%)	Total Organic Carbon (TOC, %)
E2	2	Seaward			2	2	6.9	30.0	0.8832	33.81	
E2	2	Seaward			3	2	-	-	0.8970	33.37	
E2	2	Intermediate			1	8	7.0	30.0	0.5410	64.18	5.06
E2	2	Intermediate	8°41'46.97"N	104°50'41.95"E	2	8	6.9	30.0	0.5499	62.59	
E2	2	Intermediate			3	8	7.0	33.0	0.5488	62.71	
E2	2	Landward			1	7	6.5	32.0	0.5417	49.83	4.88
E2	2	Landward	8°41'48.35"N	104°50'42.67"E	2	7	7.2	37.0	0.5303	50.30	
E2	2	Landward			3	7	6.5	35.0	0.5506	48.33	
E2	3	Seaward			1	10	6.9	35.0	0.955	27.87	5.24
E2	3	Seaward	8°41'44.08"N	104°50'44.25"E	2	10	7.0	33.0	0.948	29.33	
E2	3	Seaward			3	10	6.9	35.0	0.936	29.16	
E2	3	Intermediate			1	8	6.9	35.0	0.5378	62.57	6.60
E2	3	Intermediate	8°41'45.79"N	104°50'45.13"E	2	8	7.0	33.0	0.5564	61.92	
E2	3	Intermediate			3	8	6.9	35.0	0.5220	64.26	
E2	3	Landward	8°41'47.25"N	104°50'46.03"E	1	9	6.7	37.0	0.5277	50.55	4.67

Site	Line	Plot	Latitude	Longitude	Subplot	A.s.l elevation (m)	pH	Salinity (‰)	Bulk Density (BD, g cm^{-3})	Moisture (%)	Total Organic Carbon (TOC, %)
E2	3	Landward			2	9	7.1	35.0	0.5722	46.30	
E2	3	Landward			3	9	7.0	37.0	0.8538	24.07	
E3	1	Seaward			1	2	7.0	37.0	0.8578	29.36	3.45
E3	1	Seaward	8°36'35.14"N	104°43'1.45"E	2	2	7.1	35.0	0.8627	27.39	
E3	1	Seaward			3	2	6.9	35.0	0.5668	53.67	
E3	1	Intermediate			1	-2	6.9	35.0	0.8398	25.01	3.31
E3	1	Intermediate	8°36'35.14"N	104°43'3.51"E	2	-2	7.1	37.0	0.8471	24.52	
E3	1	Intermediate			3	-2	7.1	35.0	0.9058	20.69	
E3	2	Seaward			1	3	6.9	35.0	0.8398	25.01	3.31
E3	2	Seaward	8°36'28.94"N	104°43'2.85"E	2	3	7.1	37.0	0.8471	24.52	
E3	2	Seaward			3	3	7.1	35.0	0.9058	20.69	
E3	2	Intermediate			1	1	6.5	32.0	0.9303	19.67	2.99
E3	2	Intermediate	8°36'29.01"N	104°43'4.85"E	2	1	7.2	37.0	0.9823	16.03	
E3	2	Intermediate			3	1	6.5	35.0	1.0216	13.77	
E3	3	Seaward	8°36'28.94"N	104°43'2.85"E	1	3	6.9	35.0	0.8672	27.46	3.05

Site	Line	Plot	Latitude	Longitude	Subplot	A.s.l elevation (m)	pH	Salinity (‰)	Bulk Density (BD, g cm^{-3})	Moisture (%)	Total Organic Carbon (TOC, %)
E3	3	Seaward			2	3	7.0	33.0	0.8377	27.88	
E3	3	Seaward			3	3	6.9	35.0	0.8699	25.67	
E3	3	Intermediate			1	1	6.7	37.0	1.0039	14.78	3.14
E3	3	Intermediate	8°36'29.01"N	104°43'4.85"E	2	1	7.1	35.0	0.9888	15.65	
E3	3	Intermediate			3	1	7.0	37.0	1.0086	14.51	
E4	1	Seaward			1	4	6.4	46.0	0.6505	35.11	7.95
E4	1	Seaward	8°49'7.97"N	104°46'50.69"E	2	4	-	49.0	0.5730	36.68	
E4	1	Seaward			3	4	-	-	0.6608	33.67	
E4	1	Intermediate			1	3	6.4	40.0	0.9359	29.14	2.79
E4	1	Intermediate	8°49'7.96"N	104°46'52.79"E	2	3	-	42.0	0.6723	40.52	
E4	1	Intermediate			3	3	-	40.0	0.9273	21.93	
E4	2	Seaward			1	4	6.4	32.0	0.2389	67.90	3.30
E4	2	Seaward	8°49'11.18"N	104°46'51.06"E	2	4	-	35.0	0.4125	61.34	
E4	2	Seaward			3	4	-	36.0	0.7891	27.04	
E4	2	Intermediate	8°49'11.18"N	104°46'53.20"E	1	3	6.4	39.0	0.5557	58.03	3.79

Site	Line	Plot	Latitude	Longitude	Subplot	A.s.l elevation (m)	pH	Salinity (‰)	Bulk Density (BD, g cm^{-3})	Moisture (%)	Total Organic Carbon (TOC, %)
E4	2	Intermediate			2	3	-	40.0	0.9325	25.36	
E4	2	Intermediate			3	3	-	39.0	0.5002	59.22	
E4	3	Seaward			1	6	5.4	45.0	0.3035	43.92	2.61
E4	3	Seaward	8°49'14.49"N	104°46'51.29"E	2	6	-	47.0	0.8233	21.86	
E4	3	Seaward			3	6	-	45.0	0.4006	59.13	
E4	3	Intermediate			1	5	5.8	40.0	0.9763	20.00	5.96
E4	3	Intermediate	8°49'14.35"N	104°46'53.29"E	2	5	-	41.0	0.8940	22.60	
E4	3	Intermediate			3	5	-	40.0	0.6967	31.05	

“-“ means missing data

Appendix 3. Importance Value (IV%) and density by species in seaward, intermediate, landward plots at accretion sites (A1, A3, A3) and erosion sites (E1, E2, E3, E4)

Site	Plot	Species	RD	RC	RF	IV (%)	Density ha^{-1}
A1	Seaward	*A. alba*	0.73	0.77	0.6	70.07	4000
		A. marina	0.07	0.02	0.2	9.57	375
		R. apiculata	0.20	0.21	0.2	20.36	1125
A1	Intermediate	*A. alba*	0.70	0.85	0.5	68.54	2625
		R. apiculata	0.30	0.15	0.5	31.46	1100
A1	Landward	*A. alba*	0.49	0.72	0.33	51.26	2275
		B. parviflora	0.04	0.01	0.33	12.62	175
		R. apiculata	0.47	0.28	0.33	36.13	2200
A2	Seaward	*A. Alba*	1	1	1	100	5525
A2	Intermediate	*A. alba*	0.21	0.07	0.43	23.58	975
		B. parviflora	0.01	0.00	0.14	5.01	25
		R. apiculata	0.78	0.93	0.43	71.41	3650
A2	Landward	*A. alba*	0.21	0.41	0.50	37.42	975
		R. apiculata	0.79	0.59	0.50	62.58	3700
A3	Seaward	*A. alba*	1	1	1	100	5350
A3	Intermediate	*A. alba*	1	1	1	100	5975

Site	Plot	Species	RD	RC	RF	IV (%)	Density ha^{-1}
A3	Landward	*A. alba*	0.38	0.59	0.50	48.96	2200
		A. officinalis	0.62	0.41	0.50	51.04	3650
E1	Seaward	*A. alba*	0.59	0.69	0.38	55.05	2925
		A. marina	0.01	0.01	0.13	4.78	25
		B. parviflora	0.06	0.03	0.25	11.48	300
		R. apiculata	0.35	0.26	0.25	28.69	1750
E1	Intermediate	*A. alba*	0.15	0.24	0.43	27.18	700
		B. parviflora	0.03	0.01	0.14	5.96	125
		R. apiculata	0.82	0.76	0.43	66.87	3800
E1	Landward	*A. alba*	0.17	0.29	0.38	28.03	975
		B. parviflora	0.01	0.01	0.25	8.84	50
		R. apiculata	0.82	0.70	0.38	63.13	4650
E2	Seaward	*A. alba*	0.09	0.13	0.25	15.67	475
		A. marina	0.00	0.01	0.08	3.37	25
		A. officinalis	0.00	0.00	0.08	3.04	25
		B. parviflora	0.26	0.25	0.25	25.17	1300
		E. agallocha	0.00	0.01	0.08	3.18	25
		R. apiculata	0.63	0.61	0.25	49.57	3175

Site	Plot	Species	RD	RC	RF	IV (%)	Density ha^{-1}
		A. alba	0.06	0.13	0.29	15.94	275
E2	Intermediate	*B. parviflora*	0.11	0.09	0.29	16.19	475
		R. apiculata	0.83	0.78	0.43	67.86	3675
		A. alba	0.08	0.26	0.14	16.00	425
E2	Landward	*B. parviflora*	0.09	0.07	0.43	19.88	525
		R. apiculata	0.83	0.67	0.43	64.12	4625
E3	Seaward	*R. apiculata*	1	1	1	100	6000
E3	Intermediate	*R. apiculata*	1	1	1	100	6425
		A. alba	0.49	0.54	0.25	42.68	1500
		A. marina	0.01	0.01	0.08	3.32	25
E4	Seaward	*A. officinalis*	0.41	0.39	0.25	34.92	1250
		E. agallocha	0.02	0.00	0.17	6.26	50
		R. apiculata	0.08	0.05	0.25	12.82	250
		A. alba	0.69	0.73	0.30	57.21	2075
E4	Intermediate	*A. marina*	0.01	0.01	0.10	3.83	25
		A. officinalis	0.28	0.25	0.30	27.63	850
		R. apiculata	0.02	0.01	0.30	11.33	75

Appendix 4. Attributions of aerial root types in seaward, intermediate and landward plots at accretion sites (A1, A2, A3) and erosion sites (E1, E2, E3, E4).

Site	Line	Plot	Subplot	Root type	Density m^{-2}	Number of Primary root	Highest root height (m)	Biomass ($g\ m^{-2}$)
A1	1	Seaward	1	Pneumatophore	471			321.78
A1	1	Seaward	2	Pneumatophore	462			246.66
A1	1	Seaward	3	Pneumatophore	359			223.74
A1	1	Intermediate	1	Pneumatophore	866			741.39
A1	1	Intermediate	2	Pneumatophore	965			826.15
A1	1	Intermediate	3	Pneumatophore	942			806.46
A1	1	Landward	1	Pneumatophore	275			777.34
A1	1	Landward	1	Stilt		13.54	1.97	118.76
A1	1	Landward	2	Knee	2			214.70
A1	1	Landward	2	Pneumatophore	298			842.12
A1	1	Landward	2	Stilt		13.54	1.97	103.92
A1	1	Landward	3	Pneumatophore	321			906.90
A1	1	Landward	3	Stilt		13.54	1.97	89.07
A1	2	Seaward	1	Pneumatophore	409			288.08
A1	2	Seaward	2	Pneumatophore	425			201.19

Site	Line	Plot	Subplot	Root type	Density m^{-2}	Number of Primary root	Highest root height (m)	Biomass ($g\ m^{-2}$)
A1	2	Seaward	3	Pneumatophore	407			159.12
A1	2	Intermediate	1	Pneumatophore	872			746.53
A1	2	Intermediate	2	Pneumatophore	892			763.65
A1	2	Intermediate	3	Pneumatophore	887			759.37
A1	2	Landward	1	Pneumatophore	313			777.30
A1	2	Landward	1	Stilt		11.2	2.19	118.80
A1	2	Landward	2	Knee	3			288.20
A1	2	Landward	2	Pneumatophore	323			913.40
A1	2	Landward	2	Stilt		11.2	2.19	87.60
A1	2	Landward	3	Pneumatophore	286			808.40
A1	2	Landward	3	Stilt		11.2	2.19	111.60
A1	3	Seaward	1	Pneumatophore	440			344.34
A1	3	Seaward	2	Pneumatophore	405			215.48
A1	3	Seaward	3	Pneumatophore	456			202.88
A1	3	Intermediate	1	Pneumatophore	923			790.18
A1	3	Intermediate	2	Pneumatophore	835			714.85
A1	3	Intermediate	3	Pneumatophore	912			780.77

Site	Line	Plot	Subplot	Root type	Density m^{-2}	Number of Primary root	Highest root height (m)	Biomass ($g\ m^{-2}$)
A1	3	Landward	1	Pneumatophore	300			777.30
A1	3	Landward	1	Stilt		13.8	2.67	102.70
A1	3	Landward	2	Knee	2			112.20
A1	3	Landward	2	Pneumatophore	314			888.00
A1	3	Landward	2	Stilt		13.8	2.67	93.40
A1	3	Landward	3	Pneumatophore	322			910.70
A1	3	Landward	3	Stilt		13.8	2.67	88.20
A2	1	Seaward	1	Pneumatophore	412			1554.68
A2	1	Seaward	2	Pneumatophore	446			842.12
A2	1	Seaward	3	Pneumatophore	481			906.90
A2	1	Intermediate	1	Pneumatophore	106			278.55
A2	1	Intermediate	1	Stilt		13.36	1.93	155.15
A2	1	Intermediate	2	Pneumatophore	81			213.01
A2	1	Intermediate	2	Stilt		13.36	1.93	362.02
A2	1	Intermediate	3	Pneumatophore	98			257.25
A2	1	Intermediate	3	Stilt		13.36	1.93	222.39
A2	1	Landward	1	Pneumatophore	55			145.09

Site	Line	Plot	Subplot	Root type	Density m^{-2}	Number of Primary root	Highest root height (m)	Biomass ($g\ m^{-2}$)
A2	1	Landward	1	Stilt		13.36	1.93	116.28
A2	1	Landward	2	Pneumatophore	62			163.15
A2	1	Landward	2	Stilt		13.36	1.93	106.40
A2	1	Landward	3	Pneumatophore	50			131.57
A2	1	Landward	3	Stilt		13.36	1.93	123.68
A2	2	Seaward	1	Pneumatophore	431			1627.05
A2	2	Seaward	2	Pneumatophore	458			1729.53
A2	2	Seaward	3	Pneumatophore	425			1602.46
A2	2	Intermediate	1	Knee	2			96.80
A2	2	Intermediate	1	Pneumatophore	101			265.12
A2	2	Intermediate	1	Stilt		13.5	1.92	197.56
A2	2	Intermediate	2	Pneumatophore	95			249.00
A2	2	Intermediate	2	Stilt		13.5	1.92	248.44
A2	2	Intermediate	3	Pneumatophore	101			264.80
A2	2	Intermediate	3	Stilt		13.5	1.92	198.56
A2	2	Landward	1	Pneumatophore	55			143.84
A2	2	Landward	1	Stilt		13.09	2.16	116.97

Site	Line	Plot	Subplot	Root type	Density m^{-2}	Number of Primary root	Highest root height (m)	Biomass ($g\ m^{-2}$)
A2	2	Landward	2	Pneumatophore	49			127.96
A2	2	Landward	2	Stilt		13.09	2.16	125.65
A2	2	Landward	3	Pneumatophore	45			119.63
A2	2	Landward	3	Stilt		13.09	2.16	130.21
A2	3	Seaward	1	Pneumatophore	449			777.34
A2	3	Seaward	2	Pneumatophore	438			1651.64
A2	3	Seaward	3	Pneumatophore	458			1727.85
A2	3	Intermediate	1	Pneumatophore	99			259.32
A2	3	Intermediate	1	Stilt		13.7	1.96	215.85
A2	3	Intermediate	2	Pneumatophore	83			218.22
A2	3	Intermediate	2	Stilt		13.7	1.96	345.59
A2	3	Intermediate	3	Pneumatophore	103			270.24
A2	3	Intermediate	3	Stilt		13.7	1.96	181.39
A2	3	Landward	1	Pneumatophore	68			178.85
A2	3	Landward	1	Stilt		13.64	1.95	97.81
A2	3	Landward	2	Pneumatophore	48			127.25
A2	3	Landward	2	Stilt		13.64	1.95	126.04

Site	Line	Plot	Subplot	Root type	Density m^{-2}	Number of Primary root	Highest root height (m)	Biomass ($g\ m^{-2}$)
A2	3	Landward	3	Pneumatophore	60			158.14
A2	3	Landward	3	Stilt		13.64	1.95	109.14
A3	1	Seaward	1	Pneumatophore	408			589.33
A3	1	Seaward	2	Pneumatophore	397			842.12
A3	1	Seaward	3	Pneumatophore	391			906.90
A3	1	Intermediate	1	Pneumatophore	113			163.72
A3	1	Intermediate	2	Pneumatophore	101			163.23
A3	1	Intermediate	3	Pneumatophore	136			166.57
A3	1	Landward	1	Pneumatophore	305			382.47
A3	1	Landward	2	Pneumatophore	239			372.58
A3	1	Landward	3	Pneumatophore	210			367.72
A3	2	Seaward	1	Pneumatophore	384			777.34
A3	2	Seaward	2	Pneumatophore	394			913.38
A3	2	Seaward	3	Pneumatophore	405			808.43
A3	2	Intermediate	1	Pneumatophore	125			164.89
A3	2	Intermediate	2	Pneumatophore	112			163.46
A3	2	Intermediate	3	Pneumatophore	122			163.78

Site	Line	Plot	Subplot	Root type	Density m^{-2}	Number of Primary root	Highest root height (m)	Biomass ($g\ m^{-2}$)
A3	2	Landward	1	Pneumatophore	253			375.00
A3	2	Landward	2	Pneumatophore	264			376.90
A3	2	Landward	3	Pneumatophore	191			364.80
A3	3	Seaward	1	Pneumatophore	409			773.42
A3	3	Seaward	2	Pneumatophore	403			887.98
A3	3	Seaward	3	Pneumatophore	400			910.66
A3	3	Intermediate	1	Pneumatophore	112			164.29
A3	3	Intermediate	2	Pneumatophore	108			166.04
A3	3	Intermediate	3	Pneumatophore	101			164.26
A3	3	Landward	1	Pneumatophore	280			379.40
A3	3	Landward	2	Pneumatophore	186			363.90
A3	3	Landward	3	Pneumatophore	243			373.20
E1	1	Seaward	1	Pneumatophore	116			220.72
E1	1	Seaward	1	Stilt		17.82	2.74	246.11
E1	1	Seaward	2	Pneumatophore	93			191.65
E1	1	Seaward	2	Stilt		17.82	2.74	329.01
E1	1	Seaward	3	Knee	3			93.50

Site	Line	Plot	Subplot	Root type	Density m^{-2}	Number of Primary root	Highest root height (m)	Biomass (g m^{-2})
E1	1	Seaward	3	Pneumatophore	94			100.80
E1	1	Seaward	3	Stilt		17.82	2.74	237.56
E1	1	Intermediate	1	Pneumatophore	77			115.00
E1	1	Intermediate	1	Stilt		17.31	2.86	33.90
E1	1	Intermediate	2	Pneumatophore	50			74.50
E1	1	Intermediate	2	Stilt		17.31	2.86	86.50
E1	1	Intermediate	3	Pneumatophore	90			130.70
E1	1	Intermediate	3	Stilt		17.31	2.86	44.00
E1	1	Landward	1	Knee	5			238.50
E1	1	Landward	1	Pneumatophore	99			273.87
E1	1	Landward	1	Stilt		10.8	1.43	545.50
E1	1	Landward	2	Pneumatophore	87			370.12
E1	1	Landward	2	Stilt		10.8	1.43	636.98
E1	1	Landward	3	Pneumatophore	90			220.65
E1	1	Landward	3	Stilt		10.8	1.43	520.54
E1	2	Seaward	1	Pneumatophore	54			69.31
E1	2	Seaward	1	Stilt		21.4	3.58	196.53

Site	Line	Plot	Subplot	Root type	Density m^{-2}	Number of Primary root	Highest root height (m)	Biomass ($g\ m^{-2}$)
E1	2	Seaward	2	Pneumatophore	62			120.01
E1	2	Seaward	2	Stilt		21.4	3.58	67.12
E1	2	Seaward	3	Knee	2			155.60
E1	2	Seaward	3	Pneumatophore	75			146.68
E1	2	Seaward	3	Stilt		21.4	3.58	35.14
E1	2	Intermediate	1	Pneumatophore	178			225.00
E1	2	Intermediate	1	Stilt		28.93	2.63	504.80
E1	2	Intermediate	2	Pneumatophore	333			421.80
E1	2	Intermediate	2	Stilt		28.93	2.63	232.10
E1	2	Intermediate	3	Knee	2			200.60
E1	2	Intermediate	3	Pneumatophore	133			106.70
E1	2	Intermediate	3	Stilt		28.93	2.63	149.20
E1	2	Landward	1	Pneumatophore	65			127.37
E1	2	Landward	1	Stilt		12.18	1.87	135.55
E1	2	Landward	2	Pneumatophore	32			145.92
E1	2	Landward	2	Stilt		12.18	1.87	106.54
E1	2	Landward	3	Pneumatophore	20			113.81

Site	Line	Plot	Subplot	Root type	Density m^{-2}	Number of Primary root	Highest root height (m)	Biomass ($g\ m^{-2}$)
E1	2	Landward	3	Stilt		12.18	1.87	135.55
E1	3	Seaward	1	Pneumatophore	76			105.74
E1	3	Seaward	1	Stilt		16.31	2.45	106.71
E1	3	Seaward	2	Pneumatophore	87			183.70
E1	3	Seaward	2	Stilt		16.31	2.45	150.98
E1	3	Seaward	3	Pneumatophore	53			111.50
E1	3	Seaward	3	Stilt		16.31	2.45	35.47
E1	3	Intermediate	1	Pneumatophore	166			177.92
E1	3	Intermediate	1	Stilt		16.31	2.45	268.57
E1	3	Intermediate	2	Pneumatophore	217			253.32
E1	3	Intermediate	2	Stilt		16.31	2.45	157.35
E1	3	Intermediate	3	Pneumatophore	157			158.70
E1	3	Intermediate	3	Stilt		16.31	2.45	174.22
E1	3	Landward	1	Knee	2			230.00
E1	3	Landward	1	Pneumatophore	35			47.82
E1	3	Landward	1	Stilt		16.07	2.3	66.85
E1	3	Landward	2	Pneumatophore	62			62.53

Site	Line	Plot	Subplot	Root type	Density m^{-2}	Number of Primary root	Highest root height (m)	Biomass ($g\ m^{-2}$)
E1	3	Landward	2	Stilt		16.07	2.3	81.87
E1	3	Landward	3	Pneumatophore	20			67.08
E1	3	Landward	3	Stilt		16.07	2.3	74.13
E2	1	Seaward	1	Pneumatophore	57			14.17
E2	1	Seaward	1	Stilt		13.33	1.47	151.03
E2	1	Seaward	2	Pneumatophore	121			78.11
E2	1	Seaward	2	Stilt		13.33	1.47	102.19
E2	1	Seaward	3	Pneumatophore	62			15.45
E2	1	Seaward	3	Stilt		13.33	1.47	144.95
E2	1	Intermediate	1	Pneumatophore	57			14.17
E2	1	Intermediate	1	Stilt		19	1.45	151.03
E2	1	Intermediate	2	Knee	1			57.50
E2	1	Intermediate	2	Pneumatophore	58			14.39
E2	1	Intermediate	2	Stilt		19	1.45	149.65
E2	1	Intermediate	3	Pneumatophore	66			16.44
E2	1	Intermediate	3	Stilt		19	1.45	136.90
E2	1	Landward	1	Pneumatophore	57			7.09

Site	Line	Plot	Subplot	Root type	Density m^{-2}	Number of Primary root	Highest root height (m)	Biomass ($g\ m^{-2}$)
E2	1	Landward	1	Stilt		12.73	1.4	151.03
E2	1	Landward	2	Knee	2			115.20
E2	1	Landward	2	Pneumatophore	40			21.31
E2	1	Landward	2	Stilt		12.73	1.4	171.18
E2	1	Landward	3	Pneumatophore	70			8.64
E2	1	Landward	3	Stilt		12.73	1.4	136.21
E2	2	Seaward	1	Pneumatophore	66			16.30
E2	2	Seaward	1	Stilt		14.3	1.48	140.70
E2	2	Seaward	2	Knee	1			69.80
E2	2	Seaward	2	Pneumatophore	69			17.20
E2	2	Seaward	2	Stilt		14.3	1.48	136.60
E2	2	Seaward	3	Pneumatophore	65			16.20
E2	2	Seaward	3	Stilt		14.3	1.48	141.20
E2	2	Intermediate	1	Stilt		16.25	0.98	149.70
E2	2	Intermediate	2	Stilt		16.25	0.98	137.00
E2	2	Intermediate	3	Knee	1			80.10
E2	2	Intermediate	3	Stilt		16.25	0.98	149.60

Site	Line	Plot	Subplot	Root type	Density m^{-2}	Number of Primary root	Highest root height (m)	Biomass ($g\ m^{-2}$)
E2	2	Landward	1	Pneumatophore	75			9.30
E2	2	Landward	1	Stilt		14.17	1.73	129.80
E2	2	Landward	2	Knee	3			211.40
E2	2	Landward	2	Pneumatophore	82			10.20
E2	2	Landward	2	Stilt		14.17	1.73	121.20
E2	2	Landward	3	Pneumatophore	38			4.80
E2	2	Landward	3	Stilt		14.17	1.73	173.00
E2	3	Seaward	1	Pneumatophore	75			18.50
E2	3	Seaward	1	Stilt		11	14.3	130.20
E2	3	Seaward	2	Knee	1			90.20
E2	3	Seaward	2	Pneumatophore	74			18.40
E2	3	Seaward	2	Stilt		11	14.3	131.10
E2	3	Seaward	3	Pneumatophore	42			10.40
E2	3	Seaward	3	Stilt		11	14.3	169.00
E2	3	Intermediate	1	Stilt		19.38	1.51	239.30
E2	3	Intermediate	2	Stilt		19.38	1.51	239.30
E2	3	Intermediate	3	Stilt		19.38	1.51	239.30

Site	Line	Plot	Subplot	Root type	Density m^{-2}	Number of Primary root	Highest root height (m)	Biomass ($g\ m^{-2}$)
E2	3	Landward	1	Pneumatophore	37			4.60
E2	3	Landward	1	Stilt		14.64	1.65	175.10
E2	3	Landward	2	Pneumatophore	40			5.00
E2	3	Landward	2	Stilt		14.64	1.65	171.00
E2	3	Landward	3	Knee	3			234.80
E2	3	Landward	3	Pneumatophore	53			6.60
E2	3	Landward	3	Stilt		14.64	1.65	155.60
E3	1	Seaward	1	Stilt		19.31	1.34	1021.44
E3	1	Seaward	2	Stilt		19.31	1.34	873.06
E3	1	Seaward	3	Stilt		19.31	1.34	822.47
E3	1	Intermediate	1	Pneumatophore	57			7.09
E3	1	Intermediate	1	Stilt		18	1.02	151.03
E3	1	Intermediate	2	Pneumatophore	40			21.31
E3	1	Intermediate	2	Stilt		18	1.02	171.18
E3	1	Intermediate	3	Pneumatophore	70			8.64
E3	1	Intermediate	3	Stilt		18	1.02	136.21
E3	2	Seaward	1	Stilt		18.3	1.09	1002.40

Site	Line	Plot	Subplot	Root type	Density m^{-2}	Number of Primary root	Highest root height (m)	Biomass ($g\ m^{-2}$)
E3	2	Seaward	2	Stilt		18.3	1.09	944.10
E3	2	Seaward	3	Stilt		18.3	1.09	903.60
E3	2	Intermediate	1	Pneumatophore	75			9.30
E3	2	Intermediate	1	Stilt		17.67	1.14	129.80
E3	2	Intermediate	2	Pneumatophore	82			10.20
E3	2	Intermediate	2	Stilt		17.67	1.14	121.20
E3	2	Intermediate	3	Pneumatophore	38			4.80
E3	2	Intermediate	3	Stilt		17.67	1.14	173.00
E3	3	Seaward	1	Stilt		17.73	0.98	811.70
E3	3	Seaward	2	Stilt		17.73	0.98	883.80
E3	3	Seaward	3	Stilt		17.73	0.98	927.40
E3	3	Intermediate	1	Pneumatophore	37			4.60
E3	3	Intermediate	1	Stilt		16.45	1.13	175.10
E3	3	Intermediate	2	Pneumatophore	40			5.00
E3	3	Intermediate	2	Stilt		16.45	1.13	171.00
E3	3	Intermediate	3	Pneumatophore	53			6.60
E3	3	Intermediate	3	Stilt		16.45	1.13	155.60

Site	Line	Plot	Subplot	Root type	Density m^{-2}	Number of Primary root	Highest root height (m)	Biomass ($g\ m^{-2}$)
E4	1	Seaward	1	Pneumatophore	109			57.67
E4	1	Seaward	1	Stilt		17.33	2.63	
E4	1	Seaward	2	Pneumatophore	61			17.99
E4	1	Seaward	2	Stilt		17.33	2.63	150.08
E4	1	Seaward	3	Pneumatophore	87			10.09
E4	1	Seaward	3	Stilt		17.33	2.63	8.38
E4	1	Intermediate	1	Pneumatophore	143			393.24
E4	1	Intermediate	2	Pneumatophore	105			212.39
E4	1	Intermediate	3	Pneumatophore	127			27.73
E4	2	Seaward	1	Pneumatophore	244			242.92
E4	2	Seaward	2	Pneumatophore	312			248.07
E4	2	Seaward	3	Pneumatophore	144			322.05
E4	2	Intermediate	1	Pneumatophore	218			187.78
E4	2	Intermediate	2	Pneumatophore	170			206.14
E4	2	Intermediate	3	Pneumatophore	168			223.01
E4	3	Seaward	1	Pneumatophore	276			258.34
E4	3	Seaward	2	Pneumatophore	243			268.44

Site	Line	Plot	Subplot	Root type	Density m^{-2}	Number of Primary root	Highest root height (m)	Biomass ($g\ m^{-2}$)
E4	3	Seaward	3	Pneumatophore	192			177.29
E4	3	Intermediate	1	Pneumatophore	136			190.31
E4	3	Intermediate	2	Pneumatophore	179			291.44
E4	3	Intermediate	3	Pneumatophore	225			234.81

Abstract

맹그로브 숲은 대표적인 해안 생태계로 열대와 아열대의 조간대 지역에 분포한다. 기근은 맹그로브의 고유한 적응 특성으로 해안의 낮은 산소 조건에서 맹그로브가 생존하도록 하고, 해안 침전물을 조절하여 해안 퇴적지의 형성과 안정화에 기여한다. 본 연구는 넓은 면적의 천연 맹그로브 숲이 남아 있는 베트남 까마우(Ca Mau) 해안 지역에서 수행되었다. 본 연구에서는 해안 작용 기간과 강도가 다른 퇴적지와 침식지에서 해안으로부터의 거리에 따라 맹그로브 임분의 구조, 맹그로브 수종의 분포와 적응 특성을 비교하였다.

본 연구는 맹그로브 보호지역 내 천연 맹그로브 임분 분포지역 중, 퇴적 또는 침식이 일어난 기간과 강도가 다른 7개 지역을 연구지로 선정하였다. 연구지 A1은 퇴적 작용이 일어난 기간이 짧고 퇴적 강도가 약한 지역이고, 연구지 A2와 A3은 퇴적이 장기간 강도로 진행된 지역이었다. 연구지 E1과 E2는 최근에 약도의 침식이 일어난 지역이고, E3는 장기간 강한 침식작용이 진행되었으며, 연구지 E4는 침식 작용이 최근에 시작되었으나 침식이 강한 지역이었다. 각 연구지에서 선조사법(line transect)을 이용하여 맹그로브 임분의 울폐가 시작되는 부분부터 육지 쪽으로 3개의 평행한 선을 100m 간격으로 설치하였다. 선을 따라 해안 방향(0~50m), 중간(50~100m) 및 육지(100~150m) 구역에 20 m x 20 m 조사구를 설치하였고, 총 57개의 조사구를 설치하였다. 하나의 선에서 조사구 간 거리는 30m였다. 조사구 내 흉고직경 6cm 이상인 임목을 대상으로 수종, 흉고직경, 수고와 각 임목의 공간 분포를 측정하였다. 각 조사지 내 대각선으로 3개의 소방형구를 설치하고 치수와 유목을 조사하기 위였다. 치수와 유목은 종과 높이를 측정하였다. 조사지 내 맹그로브 수종의 주요 기근 유형은 stilt root, pneumatophores, knee roots였다. 각 조사지 내 1 m^2 크기의 소방형구를 3개씩 설치하고 세 유형의 기근과 토양을 조사하였다. Stilt root는 소방형구 내 1차근의 수와 임목 당 가장 높은 기근의 높이를 측정하였다. Pneumatophores와 knee root의 수를 측정하였다. 소방형구 내 지상부 모든 기근을

채취하여 바이오매스를 측정하였다. 고도와 토양 pH, 염도, 용적 밀도, 수분 함량, 총 유기탄소는 뿌리 측정과 같은 소방형구에서 조사하였다. 퇴적지와 침식지, 해안으로부터의 거리에 따른 식생, 기근 분포, 토양 특성을 비교하였다.

표고, 토양 염도, 용적 밀도 및 토양 수분 함량은 퇴적지와 침식지 간에 유의한 차이가 있었다($p < 0.05$). 표고는 바다에서 육지로 갈수록 점차 증가하였고, 토양 염분 및 토양 용적 밀도와 상관관계가 있었으며, 토양 수분과는 음의 상관관계를 보였다($p < 0.05$).

교목층의 수종은 퇴적지 5종, 침식지 6종으로 1종만 차이가 났다. *Excoecaria agallocha* L.은 단단한 기질에 적응한 종으로 침식지의 표고와 토양 가비중이 높고 수분 함량이 낮은 지역에서만 나타났다. 임분 하층에서 맹그로브 수종은 퇴적지는 6종, 침식지 9종이 나타나 임분 상층보다 종 수의 차이가 컸다. 하층의 종수가 많은 곳은 침식 기간이 길고 침식 강도가 강한 E3과 E4였다. 퇴적지는 *Avicennia alba* BL., 침식지는 *Rhizophora apiculata* BL.가 우점하였고, 두 종의 분포와 적응 특성은 서로 다른 해안 작용 기간과 강도에 따른 맹그로브 임분의 발달을 보여주었다.

퇴적지는 *A. alba*가 상층을 우점하였다. A1은 *A. alba*와 *R. apiculata*가 함께 분포하였다. 반면, 장기간 강한 퇴적이 지속된 A2는 해안쪽은 *A. alba*가 우점하였으나 중간과 내륙쪽으로 갈수록 *R. apiculata*가 우점하였다. A3에서는 해안과 중간 조사구에서는 *A. alba*만 분포하고, 내륙쪽 조사구에서만 *A. alba*와 *A. officinalis* L.가 혼효하였으며, *R. apiculata*는 내륙쪽 조사구의 하층에서만 분포하였다. 모든 퇴적지에서 *A. alba*의 흉고직경은 해안쪽으로 갈수록 감소하여, 퇴적지의 확장에 따른 *A. alba*의 지속적인 침입을 보여주었다. *R. apiculata*는 *A. alba*의 하층에서 갱신하고 내륙쪽 조사구로 갈수록 중요도가 증가하며 퇴적 기간에 따른 천이를 보여주었다. 해안쪽 조사구에서 퇴적지의 pneumatophore 밀도와 바이오매스가 침식지보다 유의하게 높았으며($p < 0.01$), 이는 pneumatorphores가 퇴적지에 적응한다는 것을 나타냈다.

침식지는 *R. apiculata*가 우점하였다. 해안으로부터의 거리에 관계없이 E2와 E3에서 *R. apiculata*는 상층을 우점하였다. *A. alba*는 E1의 해안쪽 조사구, E4의 해안과 중간

조사구에서 상층을 우점하였다. 침식지에서 분지된 pneumatophore가 나타났으며 이는 침식에 대한 적응으로 보였다. 침식지에서 *A. alba*는 다른 종의 아래에서 갱신이 활발하지 않았다.

Stilt root 바이오매스는 phenumatophore 밀도와 바이오매스와 음의 상관을 보였다. *R. apciulata*는 가지 분리 지점 위에서도 stilt root를 발달시켜 고정력을 높여 침식지에서 강한 파도와 높은 조수에서 나무를 지탱하고 *R. apciulata*의 생존이 가능하도록 했다. *R. apiculata*의 stilt root는 침식지에서 우점하였다.

맹그로브 종 구성과 해안선으로부터의 거리, 퇴적 및 침식 강도와 시간에 따른 임분 구조에 대한 본 연구는 지역 특성에 따른 맹그로브 복원에 적합한 종을 선택하는 데 필요한 정보를 제공한다. *A. alba*는 퇴적 지역의 해안 보호에 적용할 수 있고, 침식 지에서 *R. Apiculata*는 맹그로브 기반 해법으로 이용할 수 있다. 울타리 및 덤불 댐과 같은 임시 조치는 파도와 조수의 영향으로부터 유목을 보호하고 맹그로브 복원에 보조적으로 사용될 수 있을 것이다.

Acknowledgements

As for the forewords, I would like to express my deepest gratitude to the Korea Forestry Promotion Institute (formerly known as Korea Green Promotion Agency) for fully sponsoring my PhD program and the R&D Program for Forest Science Technology (Project No. 2020185D10-2222-AA02) of the Korea Forestry Promotion Institute, Korea Forest Service for funding the research conduction. I would also highly appreciate my supervisor, Prof. Pil Sun Park, Department of Agriculture, Forestry, and Bioresources, College of Agriculture and Life Sciences, Seoul National University. This dissertation could not be completed without her dedicated guidance and edition.

Secondly, my acknowledgement is to the precious contributions of technical staffs in the South Western Forest Research and Experimental Center in Ca Mau province for supporting data collection in the field and my lab-mates in the Forest Ecology and Silviculture Laboratory, Department of Agriculture, Forestry, and Bioresources faculty, College of Agriculture and Life Sciences, Seoul National University for their valuables support in data analysis.

Thirdly, I am grateful for the facilitation of my working affiliation, Research Institute for Forest Ecology and Environment, Vietnamese Academy of Forest Sciences and the kind and timely support of the department assistant of Department of Agriculture, Forestry, and Bioresources, College of Agriculture and Life Sciences, Seoul National University.

Finally but most important, I would deliver a big thank to the examining committee, Prof. Hyun Seok Kim, Prof. Pil Sun Park, Prof. Sang Jun Im, Prof. Ho Sang Kang and Dr. Bora Lee to contribute for the dissertation completion.